NORWEGIAN UNIVERSITY OF SCIENCE AND TECHNOLOGY

MASTER'S THESIS

Projections of the posterior parietal cortex to the orbitofrontal cortex in the rat

Author:

Karoline Hovde

Supervisor:

Prof. Menno P. Witter

Kavli Institute for Systems Neuroscience/Centre for Neural Computation

Department of Neuroscience

Trondheim, June 2015

NTNU – Trondheim
Norwegian University of
Science and Technology

Acknowledgements

The work presented in this thesis was performed at the Kavli Institute for Systems Neuroscience/Centre for Neural Computation at the Norwegian University of Science and Technology (NTNU), under the supervision of Professor Menno P. Witter.

I would like to thank you, Menno, for giving me this possibility, for inspiration and for believing in me. Thank you so much, Grethe M. Olsen, for all the things you have taught me, for always being helpful and for your endless patience. You are a wonderful person. To the technicians Bruno Monterotti and Stefano Bradamante, thank you for great assistance and support. Your Italian humour always made the day a little brighter. Tuce, thanks for being such an energetic person, for the amazing dinners and all the good times outside the lab. Kamilla, you are truly the greatest inspiration and friend.

Further, I would like to thank my family and friends for encouraging and supporting me through all of this. Liv, I will never forget our good conversations. Thank you, Lars Petter, for the great adventures and for always knowing the right words to say even from far away. Michele, thank you for always being there for me as a friend, flatmate and classmate – your support and presence have been invaluable. Thank you for sharing this time with me, I would never have made it without you.

Abstract

The posterior parietal cortex (PPC) in the rat is a multimodal association area, implicated in spatial processing, decision-making, working memory and directed attention. PPC is commonly divided into a medial (mPPC), a lateral (lPPC) and a posterior (PtP) region, all reciprocally connected to specific parts of the thalamus. The orbitofrontal cortex (OFC) is part of the ventral prefrontal cortex and is commonly divided into the medial orbital (MO), ventral orbital (VO), ventrolateral orbital (VLO), lateral orbital (LO) and dorsolateral orbital (DLO) cortices. The subregions of OFC have distinct connectivity patterns and are functionally different regarding spatial information processing, value-based decision-making and behavioural flexibility.

Reciprocal connections between PPC and OFC have previously been described, but variations in delineation of both cortical regions and difficulties in distinguishing PPC from the secondary visual cortex (V2) hampered a clear understanding of the connections. Moreover, no study has addressed PPC-OFC projections, differentiating the origins in the three posterior parietal subdivisions.

The aim of this study was therefore to describe the projections of PPC to the subregions of OFC, with a special focus on the differences in projection patterns arising from the three subregions of PPC. To this end, we injected the anterograde tracers 10 KD biotinylated dextran amine (BDA) and *phaseolus vulgaris*-leucoagglutinin (PHA-L) into the subregions of PPC. The retrograde tracers Fast Blue (FB) and Fluorogold (FG) were injected into VO and VLO to study the layers of origin of these projections. The brains were cut in the coronal plane and cortical areas were delineated based on Nissl stains with Cresyl Violet. Anterograde tracers were visualised using either 3.3'-diaminobenzidin tetrahydrochloride (DAB) or AlexaFluor® dyes, and their distribution, as well as that of the retrograde fluorescent tracers was analysed with conventional microscopical techniques.

Anterograde tracing showed that the projections from PPC to OFC are not strong, which is supported by the retrograde tracer cases that showed an overall low number of labelled neurons in layers V and VI of PPC. mPPC projects mainly to lateral VO and medial VLO, with some sparse projections to MO. Projections from lPPC terminate in medial VLO, while the most lateral part of PPC, PtP, projects to central to lateral VLO. The results indicate that projections from PPC target OFC, showing a subtle topographical pattern within MO, VO and VLO, with a clear preference for VO and VLO and excluding LO and DLO.

Contents

Abbreviations

ACC	Anterior cingulate cortex
AI	Agranular insular cortex
AOD	Anterior olfactory nucleus, dorsal part
AuD	Auditory cortex
BDA	Biotinylated dextran amine
Cl	Claustrum, anterior part
d	Dorsal
DAB	3.3'-Diaminobenzidin tetrahydrochloride
DLO	Dorsolateral orbitofrontal cortex
dm	Dorsomedial
DMSO	Dimethyl sulfoxide
FB	Fast Blue
FG	Fluorogold
IL	Infralimbic cortex
l	Lateral
LD	Laterodorsal nucleus of the thalamus
LGN	Lateral geniculate nucleus
LO	Lateral orbitofrontal cortex
LP	Lateral posterior nucleus of the thalamus
lPPC	Lateral posterior parietal cortex
M2	Secondary motor cortex (AGm, Fr2)
MD	Mediodorsal nucleus of the thalamus
MEC	Medial entorhinal cortex
MO	Medial orbitofrontal cortex
mPFC	Medial prefrontal cortex
mPPC	Medial posterior parietal cortex
mr	Mediorostral
OFC	Orbitofrontal cortex
PAG	Periaqueductal gray
PB	Phosphate buffer

PFA	Paraformaldehyde
PFC	Prefrontal cortex
PHA-L	*Phaseolus vulgaris*-leucoagglutinin
PL	Prelimbic cortex
Po	Posterior nucleus of the thalamus
POR	Postrhinal cortex
PPC	Posterior parietal cortex
PrS	Presubiculum
PtP	Posterior parietal cortex, posterior area
RSC	Retrosplenial cortex
S1	Primary somatosensory cortex
TBS-Tx	Tris-buffered saline with triton X-100
Tris	Tris(hydroxymethyl)aminomethane
v	Ventral
V1	Primary visual cortex
V2	Secondary visual cortex
V2L	Lateral secondary visual cortex
V2M	Medial secondary visual cortex
VB	Ventrobasal complex of the thalamus
vl	Ventrolateral
VLO	Ventrolateral orbitofrontal cortex
VO	Ventral orbitofrontal cortex
VP	Ventral posterior nucleus of the thalamus

Chapter 1

Introduction

'Planning of movements requires information about the intended act and also information about actions, including the goal and value of reward related to that action' (Kandel et al., 2012: p. 866).

The posterior parietal cortex (PPC) is a multimodal association area involved in several cognitive functions such as movement planning, visual attention, decision-making and working memory (Whitlock, 2014). The literature about PPC in primates and rodents is divergent, in which primate studies have focused on cognitive functions, while rodent studies mainly have focused on spatial navigation. Recently, development of new tasks to isolate cognitive functions also in rodents has extended the knowledge about PPC. In the rat, one proposed role of PPC in movement planning is the synthesis of goal-directed sequences, and neurons in PPC have been shown to be active 250 ms in advance of a movement, also called 'readiness potential' (Whitlock, 2014). However, to be able to plan movements, one needs information not only about the intended act that PPC may provide, but also information about the goal of the act and the value of reward related to that particular action (Kandel et al., 2012: p. 866). This is a suggested role of the orbitofrontal cortex (OFC), an area in the ventral prefrontal cortex involved in reward processing and value-based decision-making (Rolls, 2000; Wallis, 2012).

Previous studies have shown that PPC is reciprocally connected with OFC and the secondary motor cortex (M2), connections suggested to constitute a neural circuit for directed attention (Chandler et al., 1992). Further, lesion studies have implicated that both PPC and OFC are involved in spatial processing (King and Corwin, 1992; Corwin et al., 1994). Although there is convincing neuroanatomical evidence on reciprocal connections between PPC and OFC in the rat, the delineation of PPC has varied among studies, leaving the precise circuitry still undefined. Moreover, details on which part of the functionally heterogeneous OFC are connected with PPC are also lacking. This implies that the functional circuitry cannot yet be fully appreciated.

Topographic organisation of connections is considered necessary and a hallmark of higher order brain functions, and is observed in several brain areas including OFC (Thivierge and Marcus, 2007; Kondo and Witter, 2014). Therefore, it will be relevant to assess whether there are noticeable topographical differences in the projection pattern of the subregions of PPC to the subregions of OFC. The present study aims to provide data contributing to a broader knowledge about the cortico-cortical projections from PPC to OFC by use of traditional anterograde and retrograde tracers.

1.1 The posterior parietal cortex

The parietal cortex is considered the area underlying the parietal bone and can be divided into two subregions; the anterior part called the somatosensory cortex (S1) and a posterior multimodal association area called the posterior parietal cortex (PPC; Krieg, 1946). Based on cytoarchitecture, myeloarchitecture, expression pattern of neurotransmitters, thalamic and cortical connections as well as physiological studies, PPC can be described in almost any species (Whitlock et al., 2008). In humans, PPC consists of Brodmann areas 5 and 7 (Brodmann, 1909), and corresponding areas 5 and 7 have been described in the rhesus monkey (Cavada and Goldman-Rakic, 1989; Cappe et al., 2007). Krieg (1946) was the first to define an area 7 in the rat brain, which was described as 'parietal region' based on its anatomical position between the somatosensory and visual cortices as shown in primates. Later studies have shown that Krieg's area 7 likely has similar functions in the rat as in primates (Kolb and Walkey, 1987), and today area 7 is better known as PPC. However, the existence of PPC in the rat was for a long time questioned, which lead to a variety of delineations. The biggest difference among studies was the border between the secondary visual cortex (V2) and PPC (Figure 1; Whitlock et al., 2008).

Today, the rat PPC is commonly divided into three subregions based on thalamic and cortico-cortical connections. In this thesis, the terms medial posterior parietal cortex (mPPC) and lateral posterior parietal cortex (lPPC) correspond to the medial parietal association cortex (MPtA) and lateral parietal association cortex (LPtA), respectively, as described by Paxinos and Watson (2007). Ventrolateral to these areas is the posterior part of posterior parietal cortex (PtP). The anterior, posterior and dorsal subdivisions of PtP, described by Paxinos and Watson (2007), are here considered one region.

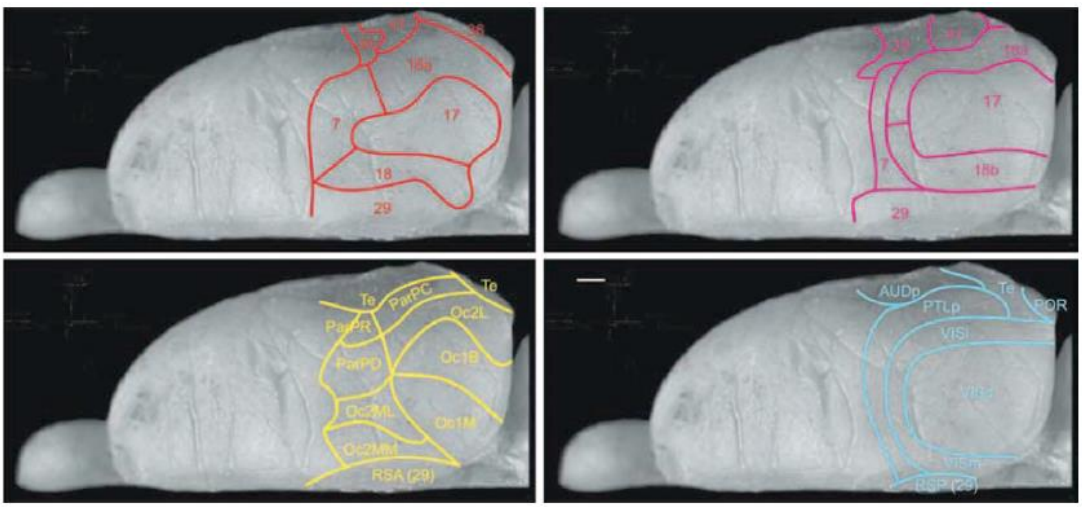

Figure 1. The right hemisphere of a rat brain seen from the dorsal side illustrating the different delineations of the parietal cortex reported by Krieg (1946) in red, Miller and Vogt (1984) in magenta, Palomero-Gallagher and Zilles (2004) in yellow and Burwell and Amaral (1998) in blue. Reproduced from Whitlock et al. (2008). Scale bar, 1 mm.

1.1.1 Delineation and cytoarchitecture of PPC in the rat

PPC in the rat has previously been described based on cyto- and myeloarchitecture (Krieg, 1946; Kolb and Walkey, 1987; Reep et al., 1994). However, the delineation of PPC has been extensively debated. In the present study, delineation criteria resulting from an anatomical tracer study by Olsen and Witter (pers. com.) will be used, in which cytoarchitecture of the subregions of parietal and occipital domains and their thalamic connection patterns were taken into account. The main difference of the latter study from the Rat Brain Atlas (Paxinos and Watson, 2007) and other studies (Chandler et al., 1992; Reep et al., 1994; Wilber et al., 2015) is the existence of the medial secondary visual cortex (V2M) between the retrosplenial cortex (RSC) and mPPC in posterior portions of PPC. Thereby, V2M replaces some of the cortex that in other studies is considered mPPC.

In the following account, I will describe cytoarchitectonic features and borders of PPC and its neighbouring cortical areas, as seen in coronal sections. As stated above, this account is based on the work of Olsen and Witter (pers. com.). In a coronal section, taken through the most anterior level of PPC, mPPC borders medially with M2 and laterally with the primary somatosensory cortex (S1; not illustrated). Moving posteriorly, V2M replaces M2 and lPPC comes in on the lateral side of mPPC (Figure 2, A). PtP appears on the lateral side of lPPC and borders S1 laterally (Figure 2, B-C). Posteriorly, V2M extends more laterally, and together with the primary visual cortex (V1), replaces mPPC and lPPC. The lateral secondary visual cortex (V2L) comes in on the lateral side of V1 and PtP is shifted to a more lateral position (Figure 2, D-E). Here, PtP borders auditory cortex (AuD). Through the whole extent of PPC, the corpus callosum defines its ventral border.

Cytoarchitectonically, PPC is less laminated than the surrounding areas. S1 has a well differentiated, granular layer IV that is easy to distinguish from the more homogenous PPC. Further, layers II and III are wide, and layer V has a cell-sparse zone deeply and superficially. V1 also has a granular layer IV that makes it easy to distinguish V1 from PPC, with a cell-sparse zone deeply and superficially in layer V as in S1. In anterior sections, mPPC borders M2. Layer V of M2 is densely packed, whereas layer III is weakly stained and superficial layers are narrow, which makes it possible to distinguish M2 from the adjacent, more homogenous PPC. lPPC shows a more distinct lamination than mPPC, although the density of cells in layer V is lower than in mPPC. Especially layer II of lPPC is denser and easier to distinguish from layer III compared to mPPC. Cells in PtP are less densely packed than in the rest of PPC, with a weakly stained layer III and a less densely packed layer V than the surrounding areas. In posterior sections, V2M can be distinguished from mPPC by having a more densely packed layer V and narrower layers II/III. Similar to V2M, V2L has a homogenous appearance with a diffuse transition between layers V and VI, and is difficult to distinguish from PPC.

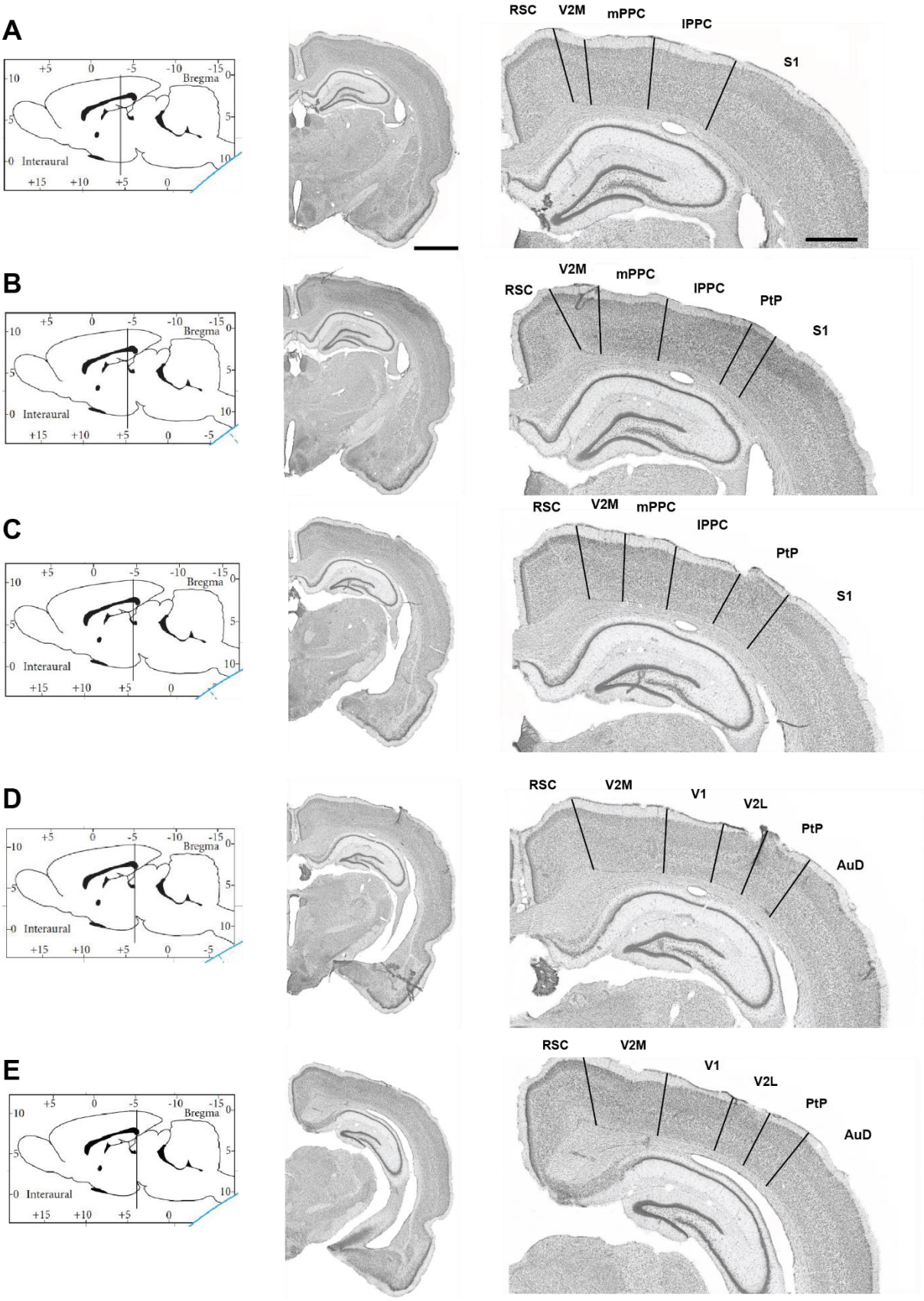

Figure 2. Delineation of the parietal cortex illustrated in coronal sections of the right hemisphere from anterior to posterior (A-E). In the most anterior sections, mPPC and lPPC are present (A). At intermediate anterior-posterior levels, all three subregions of PPC are present (B-C), while only PtP extends posteriorly together with the visual domains (D-E). Scale bars 2000µm (left) and 1000µm (right). For abbreviations, see list of abbreviations.

1.1.2 Connections of PPC in the rat

Together with cytoarchitecture, the use of topography of thalamic connections when defining cortical areas is widely accepted. In a retrograde tracer study, Chandler et al. (1992) described thalamic and cortical connections of PPC. They found retrogradely labelled cells in the lateral posterior nucleus (LP), lateral dorsal nucleus (LD) and posterior nucleus (Po) of the thalamus. No labelling was seen in the lateral geniculate nucleus (LGN) or the ventrobasal complex (VB), nuclei connected with V1 and S1, respectively. A recent, unpublished study aimed to map thalamic connectivity of the subregions of PPC and the visual cortices (Olsen and Witter, pers. com.). Their results showed that mPPC preferentially connected with LP, in particular the mediorostal component (mr) with weaker connections with Po, while lPPC had the opposite preferences (Figure 3). PtP projected mainly to Po, and all PPC areas had few projections to LD. Further, they found that V2M was reciprocally connected with LP and LD, and V2L projected to LP. Strong labelling in the lateral part of LP (LPl) was seen for cases of anterograde tracer injections in both V2M and V2L.

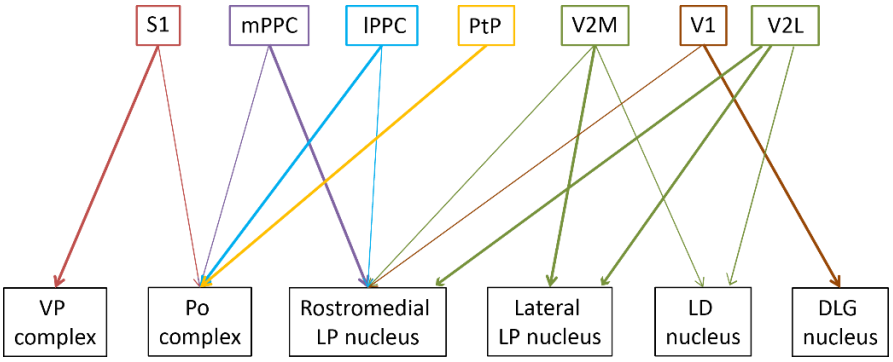

Figure 3. Thalamic projections of the subregions of PPC and adjacent areas. The thickness of the arrow illustrate the strength of projections. Modified from Olsen and Witter (pers. com.). For abbreviations, see list of abbreviations.

PPC is regarded to be a multimodal associative area based on its extensive connectivity with subcortical and other cortical areas (Figure 4; Save and Poucet, 2009). Note that additional connections have been reported and the most relevant for this thesis have been added to Figure 4. PPC receives input from multiple sensory cortices such as S1 and AuD as well as from visual areas V1 and V2. Input from the cerebellum and vestibular input via the thalamus suggests involvement with the motor system (Giannetti and Molinari, 2002; Smith et al., 2005). The anterior cingulate cortex (ACC) and M2, as well as the ventrolateral orbitofrontal cortex (VLO) are reciprocally connected with PPC and have been proposed to constitute a neural network implicated in directed attention (Kolb and Walkey, 1987; Chandler et al., 1992; Conte et al., 2008). Involvement in directed attention is based on the findings that lesions to either of M2, PPC or VLO, or the connection between M2 and PPC typically lead to a dysfunctional state, contralateral neglect (King et al., 1989; Chandler et al., 1992; Burcham et al., 1997). Further, PCC has a minor

connections with the medial entorhinal cortex (MEC), while indirect connections with MEC via RSC and the postrhinal cortex (POR) are likely stronger (Burwell and Amaral, 1998; Agster and Burwell, 2009).

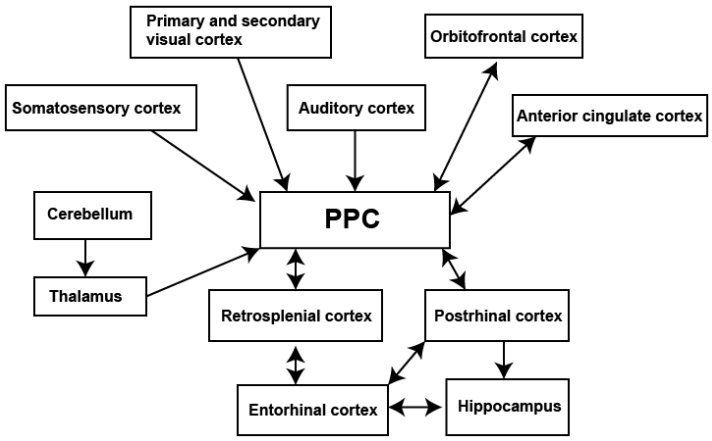

Figure 4. A simplified illustration of the main cortical and subcortical connections of the rat PPC. Modified from Save and Poucet (2009). Additional, relevant connections are added from Agster and Burwell (2009) and Burwell and Amaral (1998).

Kolb and Walkey (1987) were the first to report input to PPC from M2, which was confirmed by Chandler et al. (1992), additionally showing that these inputs were reciprocated. The latter authors used retrograde tracers injected into M2, VLO and PPC and found that all three areas are reciprocally connected with each other. PPC receives input from the whole extent of M2, whereas projections targeting V2M originate only in the posterior portions of M2 (Reep et al., 1990). Another retrograde tracer study showed input to PPC from the medial orbitofrontal cortex (MO), VLO, M2, RSC, S1, V2 and auditory areas (Reep et al., 1994). Studies investigating potential connectional differences between the subregions of PPC are sparse. A recent study (Wilber et al., 2015) reported that input to PPC from cortical and subcortical regions is topographically organised along the mediolateral axis, but not along the anterior-posterior axis, suggesting that connectivity patterns of medial and lateral PPC resemble those of medial and lateral V2M, respectively. Another, anterograde tracing study reported differences in the connection pattern of mPPC and lPPC, with mPPC projecting to more medial portions of dorsocentral striatum than lPPC (Reep et al., 2003). The same authors showed that V2M projected to more dorsal parts of the striatum than both mPPC and lPPC. Since Wilber et al. (2015) suggest that V2M and PPC have similar connectivity pattern, while dissimilar projections to the striatum as well as thalamus dispute this notion, it is relevant to investigate whether V2M as well as V2L projection patterns to OFC differ from those of PPC.

1.1.3 Functions of PPC in the rat

Most functional studies on PPC carried out in monkeys typically focused on cognitive functions such as decision-making and movement planning, in which the animal typically is head-restrained,

solving tasks via precise movements of the arm, hand or eyes (Whitlock, 2014). Rats, on the other hand, are usually completing navigational tasks without any restraint. Therefore, the literature for primates and rats is diverse and may be difficult to compare directly because of differences between species. However, recent studies have tried to overcome the differences by designing tasks that isolate cognitive functions in rodents such as motor planning (Erlich et al., 2011), visual attention (Broussard et al., 2006), decision-making (Raposo et al., 2012; Brunton et al., 2013) and working memory (Harvey et al., 2012). The majority of studies in rats have largely focused on spatial navigation and Whitlock (2014) recently suggested that one of PPC's roles is 'the synthesis of goal-directed behavioural sequences'. In another study (McNaughton et al., 1994), 30-50% of neurons in PPC was found to conjointly encode specific types of movements together with particular spatial trajectories, such as straight running followed by a right or left turn, also called two-part movement motifs. In a later study, PPC neurons were found to have the ability to map single and multiple navigational epochs according to their order in a route (Nitz, 2006). Importantly, the mapping was found to be independent from the direction of motion or spatial position, and equally functional in darkness, suggesting an involvement in path integration. Further, it has been shown that PPC is more linked to the reference frame of the animal's route instead of a world-based frame, based on the observation that PPC neurons, in contrast to hippocampal place cells, scaled to match the maze segment if it was shortened or lengthened (Nitz, 2006).

In a recent review (Whitlock, 2014), the role of neurons in PPC with respect to the so-called 'readiness potential' was described. In both humans and primates, a group of PPC neurons as well as frontal motor area neurons have been shown to be active prior to movements. This 'readiness potential' has also been described in the rat, in which neurons on average showed tuning 250 ms in advance of a movement. This ability to predict movement may imply that PPC is involved in planning of movements, which is supported by a human study where stimulation of PPC resulted in intention to move (Desmurget et al., 2009). Another proposed function of PPC neurons is goal action modulation, which is well described in primates as different levels of activation depending on whether the monkey was 'grasping to eat' or 'grasping to place' (Whitlock, 2014). In Whitlock et al. (2012), a similar phenomenon in rats was described, in which neurons showed different tuning depending on whether the rat was foraging in an open area, or if they were moving in a goal-directed manner through a hairpin maze. A recent study using two-photon calcium imaging, showed that PPC neurons in rodents are involved in all phases of a virtual T-maze task (Harvey et al., 2012). This suggests that the rat PPC also is involved in decision-making and sensory processing similarly to the primate PPC. Taken together, it seems clear that PPC plays a role in movement planning and goal-directed behaviour.

1.2 The orbitofrontal cortex

The orbitofrontal cortex (OFC) comprises a large and heterogeneous cortical region located on the ventral surface of the frontal lobe and is considered part of the prefrontal cortex (PFC; Figure 5; Price, 2007). Brodmann (1909) delineated the human PFC into areas 10, 11, 24, 25 and 32 (Price, 2007). He did not study OFC in detail, but included most of it in his area 11. Further he did not use the word 'prefrontal cortex' but he considered the areas anterior to motor areas as 'frontal cortex'. Later, Walker (1940) aimed to map this region in the macaque monkey, and recognised areas 10 and 11 anteriorly, 12 laterally, 13 centrally and 14 medially, which made the basis of what is known in primates today (Price, 2007). In primates, including humans, PFC varies in a distinct pattern along the anterior-posterior axis; near the frontal pole, the cortex is granular, changing to dysgranular cortex in the central region, while the posterior part close to the insular cortex is agranular (Figure 5; Wallis, 2012). In rodents, however, PFC consists exclusively of agranular cortex, and for that reason, it was for a long time questioned if rodents have a PFC. This question was revised after a study by Rose and Woolsey (1948), who suggested that PFC could be defined based on connections with the mediodorsal (MD) nucleus of thalamus. OFC in rodents is situated in the ventral prefrontal domain, which together with the medial prefrontal cortex (mPFC) and anterior insular regions, makes up PFC (Price, 2007).

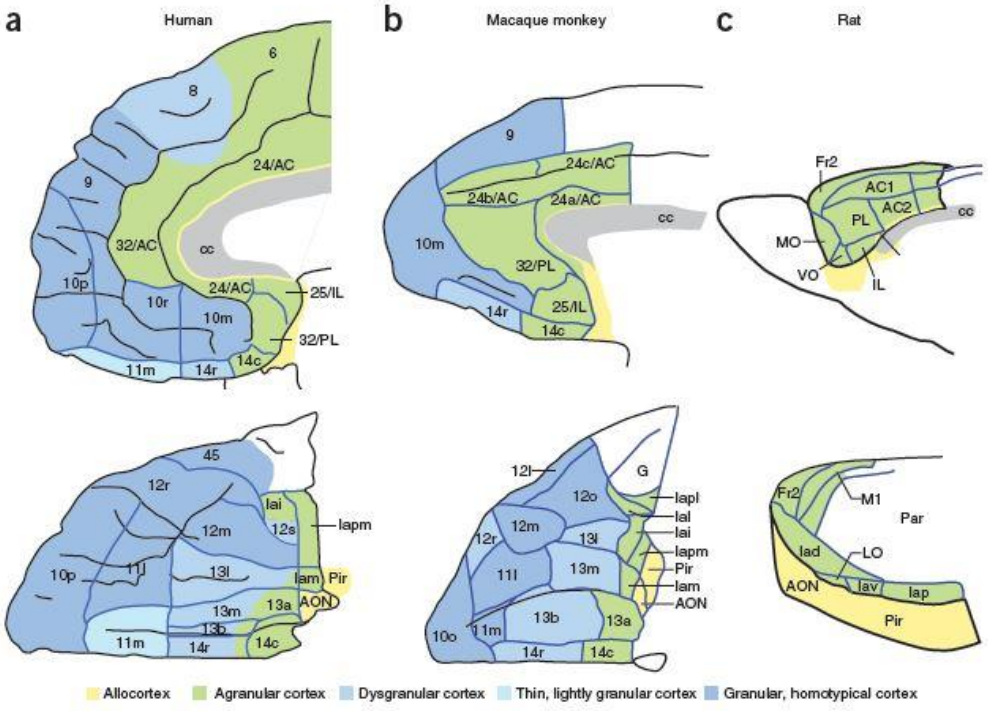

Figure 5. Comparison of PFC in the human (a), the macaque monkey (b) and the rat (c). Adapted from Wallis (2012).

1.2.1 Architecture of OFC in the rat

OFC in the rat is commonly divided into the medial orbitofrontal (MO), the ventral orbitofrontal (VO), the ventrolateral orbitofrontal (VLO), the lateral orbitofrontal (LO) and the dorsolateral orbitofrontal (DLO) cortices (Krettek and Price, 1977; Ray and Price, 1992; Price, 2007; Van De Werd and Uylings, 2008). It is noteworthy that the delineations of the subregions vary among studies. Van De Werd and Uylings (2008) used Nissl, parvalbumin, dopamine, calbindin and SMI-32 stains to describe the cytoarchitecture of OFC in detail. They included MO through the anterior-posterior extent of OFC, while other mentioned studies did not. Another discrepancy in the same study is the presence of agranular insular cortex (AI) between VLO and LO, which has not been described in any other study and was not found in the mouse (Van De Werd et al., 2010). There is an ongoing debate whether DLO belongs to OFC or not. DLO can be described as the area lateral to LO, on the lip of the anterior rhinal fissure, and was found to extend posteriorly until the merger of the dorsal part of the anterior olfactory nucleus (AOD) with OFC (Van De Werd and Uylings, 2008). Kondo and Witter (2014) suggested that DLO extends more posteriorly, but they decided not to include it in their study since the chemoarchitecture (SMI-32 stain) looks more similar to that seen for AI. Since the delineation and cytoarchitectural features of OFC have varied among papers, the cytoarchitectonical criteria used in this thesis will be described in the results.

1.2.2 Connections of OFC in the rat

The different subregions of OFC have been found to have different projection patterns both when it comes to thalamic connections and cortico-cortical connections (Reep et al., 1996). By use of retrograde tracers these authors showed that OFC receives afferents from MD and the submedial nuclei of the thalamus, and that each subregion of OFC is connected to a different part of MD. Further, they showed that MO is connected to the cingulate cortex, secondary motor cortex and PPC (Figure 6). VO receives projections from the anterior cingulate cortex, secondary motor cortex, agranular insular cortex, secondary somatosensory cortex, PPC and secondary visual areas. VLO receives cortical input from secondary motor cortex, agranular insular cortex, primary and secondary somatosensory cortices, PPC and secondary visual cortices, while the origins of projections to LO are limited to agranular insular and the secondary somatosensory cortices. The same study reported that VO and VLO have more extensive cortico-cortical connections than LO and MO.

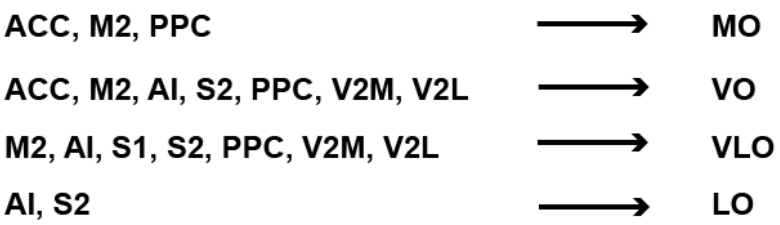

Figure 6. Cortico-cortical projections to the different subregions of OFC. AAC: anterior cingulate cortex; M2: secondary motor cortex; AI: anterior insular cortex; S2: secondary somatosensory cortex; V2M: medial secondary visual cortex; V2L: lateral secondary visual cortex; S1: primary somatosensory cortex. For other abbreviations, see list of abbreviations. Abbreviations are modified from Reep et al. (1996).

Another study used anterograde and retrograde tracers and described the connections of MO and VO in more detail (Hoover and Vertes, 2011). The authors showed that cortical targets of MO projections are the prelimbic (PL) and infralimbic (IL) cortices, AI, the piriform cortex, the lateral agranular RSC, the parahippocampal and the temporal association cortices. VO has strong projections to M2, ACC, sensorimotor cortices, PPC, the lateral agranular RSC, the temporal association cortices and the perirhinal and lateral entorhinal cortices.

A recent study by Kondo and Witter (2014) investigated the projections of the different subregions of OFC to the subregions of the parahippocampal region by using anterograde tracers. They described that all subregions of OFC studied (MO, VO, VLO, LO) were connected with parts of perirhinal and the lateral entorhinal cortex, while projections to POR, the presubiculum (PrS) and MEC mainly originated in VO.

1.2.3 The medial and orbital prefrontal networks

PFC can be divided into two functional networks called the medial and orbital prefrontal networks in humans, primates and rats, which do not fully overlap with the medial and orbital prefrontal cortices (Price, 2007). That is, parts of OFC belong to the medial prefrontal network and not to the orbital prefrontal network. The networks are originally based on studies in primates in which the medial prefrontal network projects to the brainstem and hypothalamus (visceromotor information), and is connected with the superior temporal sulcus, RSC and the cingulate cortex, the entorhinal cortex, the posterior parahippocampal cortex and dorsomedial prefrontal cortex (dmPFC; Price, 2007). The orbital prefrontal network receives input from the olfactory, somatic association and taste cortices and is connected with the perirhinal and the ventrolateral prefrontal cortex (vlPFC; Price, 2007). In rats, the networks are based on connectivity studies with the periaqueductal gray (PAG) and hypothalamus (Floyd et al., 2000; Floyd et al., 2001). The medial prefrontal network consists of PL, IL, ventral and dorsal part of the anterior cingulate cortex (ACCv/d), the dorsal part of agranular insular cortex (AId) and DLO, while the orbital prefrontal network comprises the ventral agranular insular cortex (AIv), VLO and LO. MO and VO are thought to function in both networks, similar to the areas on the gyrus rectus in the primate (Price, 2007).

1.2.4 Functions of OFC

OFC has been studied extensively with respect to behavioural flexibility, value-based and goal-directed decision-making, reversal learning, odour processing and reward (Schoenbaum et al., 1998; Rolls, 2000; Feierstein et al., 2006; Wallis, 2012). Because of its extensive connections with sensory cortices, it is regarded a multisensory receiving area, thought to be linking sensory cues with outcomes (reward; Schoenbaum et al., 2007). mPFC on the other hand, is thought to associate responses with outcomes (Ostlund and Balleine, 2007), and integration of information from the two areas is necessary for successful goal-directed behaviour. Goal-directed behaviour requires that a decision about the final goal is made, and OFC has been shown to encode for many variables necessary for decision-making, in which OFC's core function is to value many alternatives in order to determine the best choice (Wallis, 2012). OFC has been extensively studied the last decades, yet it is not clear what the precise role of OFC is (Stalnaker et al., 2015). Although many lesion studies include big areas of lateral OFC or the whole OFC (Schoenbaum et al., 2002; Schoenbaum et al., 2003; Boulougouris et al., 2007), others have shown that subregions of OFC have distinct functions. More specifically, lesions to VLO resulted in allocentric deficits while lesions to LO did not (Corwin et al., 1994).

1.3 Aim

The delineation of PPC has been under debate for the last decades and many functional studies do not subdivide this area at all. However, it is possible to delineate and subdivide PPC based on cytoarchitectonic criteria and patterns of thalamic projections. To be able to understand higher brain functions, such as goal-directed behaviour and directed attention, it is necessary to know the connectivity of the brain areas possibly involved. Even though previous studies have investigated projections of PPC to OFC, no one has to my knowledge looked at the projections arising from the three different subregions of PPC separately. Furthermore, previous studies have not been able to distinguish V2 from PPC cytoarchitectonically, and the delineation of OFC has also varied among studies making the results difficult to interpret.

The aim of this study was to describe the projections of the three subregions of PPC (mPPC, lPPC and PtP) to the subregions of OFC (MO, VO, VLO, LO, DLO) by use of anterograde tracers. Retrograde tracers have been used to support the findings and to analyse the cells of origin of the projections from PPC to OFC.

Chapter 2

Materials and methods

A list of chemicals and antibodies is included in Appendix A. Recipes for solutions are included in Appendix B. A detailed surgical procedure is included in Appendix C. Full histology protocols are found in Appendix D. Delineations of injection sites, table of anterograde labelling and an example of how the representative anterograde labelling figures are made are included in Appendix E. Additional retrograde labelling figures are included in Appendix F. Finally, a comparison of delineations of OFC is available in Appendix G.

2.1 Animals

The experiments included in this study were performed at the Kavli Institute for Systems Neuroscience/Centre for Neural Computation, at the Norwegian University of Science and Technology (NTNU). All animals were housed and treated according to the regulations of the Norwegian Animal Research Authority (Forsøksdyrutvalget), with a 12-hours day-night cycle, stabilised room temperature (21°C ± 2°C) and humidity level (60% ± 5%) and with free access to food and water. All surgeries and perfusions were performed using established procedures approved by the Animal Welfare Committee at NTNU.

Injections from 21 female Sprague Dawley rats (Charles River, Germany, weighing 180-250g at the time of surgery) from a previous study were analysed (Olsen and Witter, pers. com.). An additional number of 18 female Sprague Dawley rats (Charles River, Germany, 203-237g) were prepared for this study. Among these, 10 yielded useful results, meaning that the injections were in PPC or OFC and had good transport of the tracer. These injections were added to the analysed material.

2.2 Tracers

Neuroanatomical tracing is a method to study the anatomical wiring of neuronal populations by use of intrinsic cellular transport systems for macromolecules in live neurons (Lanciego and Wouterlood, 2011). In this way, it is possible to identify the route and termination of axons and the cell bodies from which they originate. Transport of molecules away from the soma to the periphery is called anterograde transport, while transport in the opposite direction is called retrograde transport. Anterograde tracers are taken up by the soma and are transported towards the axons terminals, revealing labelled axons. Retrograde tracers are taken up by axons and are

transported back to the some revealing cell bodies. Retrograde tracing can be used to establish the layer of origin of projections seen with anterograde tracers (Lanciego and Wouterlood, 2011).

In this study two anterograde tracers and two retrograde tracers were used. The anterograde tracers were 10 KD biotinylated dextran amine (BDA; Vector laboratories, Inc., Burlingame, USA), 5% solution in 0.125M phosphate buffer (PB), and *phaseolus vulgaris*-leucoagglutinin (PHA-L; Vector laboratories, Inc., Burlingame, USA), 2.5% solution in 10mM PB. Retrograde tracers used were Fast Blue (FB; EMS-grivory), 2% solution in 0.125M PB, and Fluorogold (FG; Fluorochrome) 2.5% diluted in H_2O. Both tracers were fluorescent so no further processing was necessary for visualising the injections site and labelling under a fluorescence microscope. FB binds to adenine-thymine rich nucleic acids and makes their cytoplasm appear blue, while FG accumulates in tiny punctate structures in the neuronal cell bodies (Lanciego and Wouterlood, 2011). Because of the challenge of photo bleaching of these tracers (Shaner et al., 2005), the tissue was hidden from light as much as possible and stored in a freezer at -23°C when not in use.

2.3 Stereotaxic surgeries

A stereotaxic surgery is a procedure to precisely target a specific region of the brain by fixing the animal's head into a three-dimensional coordinate system (Carter and Shieh, 2010). Calculated coordinates obtained from the Rat Brain Atlas (Paxinos and Watson, 2007) were adapted to each animal (depending on size and age). Bregma, the intersection between the sagittal and coronal sutures of the skull (Carter and Shieh, 2010), was used as a reference to position injections in the anterior-posterior axis (Figure 7). The height of the skull was measured at the level of bregma and lambda, which is the intersection between lines of best fit thought the lambdoid and sagittal sutures, in order to assure that those two points were similarly positioned in the horizontal plane. The sagittal sinus (not illustrated) was used as a reference to position injections along the mediolateral axis.

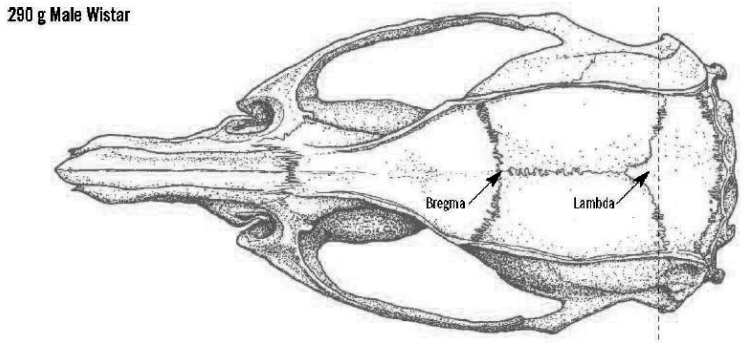

Figure 7. The positions of bregma and lambda are illustrated on the skull of a male Wister rat. Adapted from Paxinos and Watson (2007).

2.3.1 Anaesthesia and analgesia

The animals were anaesthetist in a pre-filled chamber with oxygen and isoflurane (5%) with an airflow at 1L/min. Throughout the surgery, the isoflurane concentration was slowly reduced starting from 3% when the animal was moved to the stereotaxic apparatus, to 2% after approximately 25 min and eventually 1.5% after 45 min, all in accordance to the breathing of the animal. The local anaesthetic Marcain (Bupivacaine, 2.5mg/mL, 1mg/kg) was injected subcutaneously on the head 10 min prior to making the incision. The analgesics Temgesic (Buprenorphine, 0.03mg/mL, 0.05-0.1mg/kg), Metacam (Meloxicam, 2mg/mL, 1mg/kg) were injected subcutaneously to ensure that anaesthesia was fully reached and no pain was experienced. To prevent dehydration, a saline solution was given subcutaneously (5mL on each side) every second hour. The day post-surgery, oral Metacam (1.5 mg/mL, 1 mg/kg) was given.

2.3.2 Surgical procedure

All animals were weighed prior to surgery. The surgery table was cleaned with soap and disinfected with ethanol (70%) and surgical equipment were placed in a bowl containing ethanol (70%) on sterile paper. The induction chamber was pre-filled with oxygen (air flow 1L/min) and isoflurane (5%) and the animal was placed in the chamber. When the animal anesthetised, it was moved to the surgery table where isoflurane (3%) was given via a surgical mask. A heating pad at 37◦C prevented the animal from hypothermia during the surgery. The toe-pinch reflexes were regularly checked to ensure that the animal was sufficiently anaesthetised before and during the surgery. Ear bars were used to fix the skull in the stereotaxic frame (David Kopf Instruments, USA) and Simplex (Tubilux Pharma S.p.A., Italy) was applied to avoid the rat's eyes from drying out. After injecting analgesics, the head was shaved and disinfected with ethanol (70%) and iodine. By use of a scalpel, an incision was made along the midline and the periost was scraped to the sides revealing bregma and lambda (Figure 7), and the height at each position was measured and adjusted to the same level. To reveal the sagittal sinus, a rectangular window was drilled in between bregma and lambda, perpendicular to the midline. Bregma and the sagittal sinus were used as reference points for the coordinates of injections, and a circular hole was drilled to reveal the brain. A glass capillary (Borosilicate Glass Capillaries) was filled with tracer, the dura was removed by use of a bent needle and the horizontal level of the cortical surface was measured. After lowering the capillary to a given depth, BDA or PHA-L were iontophoretically injected by applying pulses of positive DC-current (6s on/off alterations, 6μA for BDA and 7μA for PHA-L) for 10 min. Retrograde tracers were injected by use of pressure on a capillary with a plunger (approx. 150nl FB or 100nl FG) in two sessions, and the capillary was left to rest for 10 min to avoid diffusion of the tracer. The capillary was carefully removed from the brain and the skull and skin were cleaned with sterile saline before suturing the wound. To avoid infections, iodine was

applied to the skin and the animal was placed in a heating chamber to recover. The animal was moved back to its cage when awake and active, and it was checked after one hour to ensure that it was doing well. The animal's health was monitored and registered the following days to ensure that the weight was re-gained and the animal was healthy.

2.4 Tissue collection and preparation

2.4.1 Perfusion

After surgery, the animal survived for seven to nine days before perfusion. The animal was weighed and deeply anaesthetised by use of a pre-filled chamber with oxygen (1L/min) and isoflurane (5%) and given an overdose of pentobarbital (0.2mL/100g) intraperitoneally. Both toe-pinch reflexes and breathing level (deep and slow) were monitored before proceeding to ensure that the animal was unconscious and not experiencing any pain. The animal was moved to a table were oxygen was administered through a mask before the animal was transcardially perfused using a Peri-Star Pro 4-channel low rate pump (World Precision Instruments Inc., USA). The skin was opened along the abdomen and ribs, the diaphragm was removed, and a needle (25 gauge) with running ringer solution was placed into the left ventricle at the same time as the right atrium was cut. After removing the blood, a solution of freshly depolymerised paraformaldehyde (PFA, 4% in 125mM PB) was used to fixate the tissue. The brain was carefully removed from the skull and kept in a container with PFA for post-fixating overnight. Subsequently, the brain was stored in a cryoprotective solution containing 2% dimethyl sulfoxide (DMSO) in the fridge for at least 24 hours before sectioning.

2.4.2 Sectioning

The brain was fixed onto a freezing microtome (Microm HM430, Thermo Scientific, Waltham, USA) with a sucrose solution (30%). Dry ice was applied around the brain to keep it sufficiently frozen (approximately at -40°C) throughout the sectioning. The brain was cut coronally in 50µm sections in six alternating series, where the first series was mounted directly onto Superfrost Plus microscope slides (Gerhard Menzel GmbH, Braunschweig, Germany) using a Tris-(hydroxymethyl)aminomethane buffer solution (Tris; Merck KGaA, Darmstadt, Germany) adjusted to pH 7.6 with HCl, and the slides were left on a heating pad to dry overnight. The following day, the first series was either stained with Cresyl Violet (Sigma-Aldrich, St. Louis, USA) and coverslipped for anterograde tracer cases, or coverslipped and analysed with a fluorescence microscope (Axio Imager M2, Carl Zeiss MicroImaging, Jena, Germany) for retrograde tracer cases. The remaining series were put into tubes with cryoprotective solution and stored in a freezer at -23°C.

2.5 Histology

2.5.1 Cresyl Violet

Cresyl Violet (Sigma-Aldrich, St. Louis, USA) is a staining method that visualises Nissl bodies in the cytoplasm of neurons and is used to accurately delineate cytoarchitectonical borders. Cresyl Violet is often referred to as Nissl staining. Shortly, the sections were dehydrated in ethanol with increasing percentage and cleared in xylene (VWR International, Fontenay-sous-Bois, France) for 2 min, before rehydration and staining with Cresyl Violet (0.1%) on a shaker. Duration of staining varied from 3-5 min depending on the desired darkness of the sections and the age of the solution. The sections were differentiated in a solution of ethanol and acetic acid (VWR International, Fontenay-sous-Bois, France) and in water to remove excess colour, dehydrated and cleared in xylene before coverslipping with entellan and xylene (Merck KGaA, Darmstadt, Germany). A detailed protocol is included in Appendix D.

2.5.2 BDA

For brains injected with BDA, the first series of sections was stained with 3.3'-Diaminobenzidine tetrahydrochloride (DAB; Sigma-Aldrich, St. Louis, USA). Briefly, the sections were incubated with a Vector ABC kit (Vector laboratories, Inc., Burlingame, USA) for 90 min at room temperature, reacted with DAB until desired staining level was reached (15-20 min), and mounted onto non-frost microscope slides (Menzel glass slides, Gerhard Menzel GmbH, Braunschweig, Germany) with a 0.2% gelatine solution. After drying overnight, the slides were coverslipped with entellan and xylene.

Another series was incubated with streptavidin 546 or 488 (1:200; Invitrogen, Ltd., Paisley, UK) in TBS-Tx for 90 min at room temperature. The sections were mounted onto non-frost microscope slides using a 0.2% gelatine solution and coverslipped with entellan and toluene (Merck KGaA, Darmstadt, Germany) the following day. Detailed protocols for both staining methods are included in Appendix D.

2.5.3 PHA-L

For brains injected with PHA-L, the first series of sections was stained with DAB by incubating with goat anti-PHA-L (1:1000; Invitrogen, Ltd., Paisley, UK) for 24 hours before incubating with unconjugated donkey anti-goat (1:100; Invitrogen, Ltd., Paisley, UK) on a shaker for 2 hours. Further, the sections were incubated with goat PAP (1:200; Invitrogen, Ltd., Paisley, UK) for 2 hours and DAB until desired staining level, all at room temperature. The sections were mounted onto Superfrost Plus microscope slides with a Tris-HCl solution and coverslipped with entellan and xylene.

Another series was incubated with goat anti-PHA-L (1:1000; Invitrogen, Ltd., Paisley, UK) in Tris-buffered saline with triton X-100 (TBS-Tx; Merck KGaA, Darmstadt, Germany) for 24 hours, before incubating with Alexa 488 or 546 anti-goat (1:400) for 2 hours, all at room temperature. The sections were mounted onto non-frost microscope slides with a 0.2% gelatine solution and coverslipped with entellan with toluene. For brains with injections of both BDA and PHA-L, a double fluorescent staining was performed. Detailed procedures for all staining methods are found in Appendix D.

2.5.4 FB and FG

No staining method was necessary for visualising the injection site and labelled cell bodies for brains with injections of FB or FG since the tracers were fluorescent. After digitalising the slides, coverslips were removed in a bath with toluene (VWR International, Fontenay-sous-Bois, France) and the slides were stained with Cresyl Violet to accurately delineate the cytoarchitectonic borders of areas of interest.

2.6 Data analysis

All slides stained with Cresyl Violet or DAB were digitalised with a brightfield scanner (Zeiss Mirax Midi, Merlin Camera F-146 IERF MEDICAL, Vision Technologies Medial) for further analyses. Pannoramic Viewer software (1.15.3 RTM, 3DHHISTECH) was used to look at the slides and relevant sections were exported for use in Adobe Photoshop CS6 (Adobe Systems Inc.) and Adobe illustrator CS6 (Adobe Systems Inc.) for further processing. For brains with injections of retrograde tracers, or injections of anterograde tracer made fluorescent, a fluorescence microscope (Zeiss Axioimager M2) was used to look at the injection site and labelling before the slides were scanned with a fluorescence scanner (Zeiss Midi, with HXP 120 illuminator and AxioCam Mrm Rev. 3 Camera). FB and FG labelled cells were visualised with the BP 365/12 filter, while fibres stained with AX488 or AX546 were visualised with BP450-490 and BP546/12 filters, respectively.

For anterograde tracer cases, the first series was stained with Cresyl Violet and used for delineation. An adjacent series was stained either with DAB or with a fluorophore. Overlays of the digitised images of the two series were made in Adobe Photoshop CS6, which made it possible to precisely decide the positions of the injection sites. For the representative cases, figures were made in Adobe Illustrator CS6 to illustrate the distribution of anterograde labelling. The fibres were drawn onto a DAB or fluorescent stained series and subsequently overlayed with the corresponding Nissl stained sections (see Appendix E). For retrograde tracer cases, the first series was used for analysis and later stained with Cresyl Violet for delineation purposes.

2.6.1 Injection sites

Anterograde tracer injections were made into the right hemisphere with the exception of cases 20546B and 12551P. To reduce the number of animals used, two or more tracer injections were performed in each brain when possible.

The site and size of the injections of anterograde tracers in this study varies from big injections, covering all layers of an area, to tiny injections in a single or two layers (for delineations, see Appendix E). The exact spread of the injection is often difficult to establish, but the core of the injection, i.e. the section with the densest deposit of tracer, is referred to as the 'injection site'. When deciding the injection site, all sections with deposit of tracer were delineated and evaluated so that possible leakage into other areas could be included in the analyses. For retrograde tracer cases, the injection extended over a few sections. The core, however, was considered the section where the needle tract was visible and the deposit the densest.

2.6.2 Neurolucida

Neurolucida (MBF Bioscience, MicroBrightfield Inc.) was used to make a 3D overview figure of anterograde tracer injections (Figure 9). I used a neurolucida file containing an outlined and delineated rat brain with previously mapped injections (adapted from Olsen and Witter (pers. com.)) to add the injections performed in the present study. I made a 3D-construction and edited the file before exporting pictures viewed in a desired rotation. The picture was overlayed with a real image of a rat brain in Adobe Illustrator CS6 and the delineation of areas and the injections were mapped onto the brain image.

2.6.3 Analysis of labelling

When analysing the anterograde tracer cases, it is important to distinguish between passing axons and terminating axons. Passing axons generally have a smooth and fairly straight appearance while terminating axons show labelling thickenings called varicosities, are generally thin, somewhat tortuous and branching. Passing axons or fibres are smooth and straight, and can easily be distinguished from terminating fibres, which are branching and have large varicosities (terminal boutons). However, the plane of cutting can make fibres look different, depending on if they are in the plane or are cut. Retrogradely labelled neurons show a clearly cell shaped soma with a blue colour for FB and yellow colour for FG.

Chapter 3

Results

3.1 Delineation of OFC

The delineations of both OFC and PPC have varied over the last years, and for PPC, delineation criteria from Olsen and Witter (pers. com.) were agreed on and presented in the introduction. For OFC, we have delineated the subregions slightly different from previous studies based on cytoarchitectonical features that will be presented below. The differences between the present study and among previous studies are mainly found in posterior sections (see Appendix G). OFC is commonly subdivided into MO, VO, VLO, LO and DLO from medial to lateral.

MO

MO makes up the medioventral part OFC and borders VO laterally and medially to PL in anterior sections and IL in posterior sections (Figure 8). MO fades away at the level where OFC merges with AOD (Figure 8, E-F). This is different from Van De Werd and Uylings (2008) where MO extended through the whole extent of OFC, but similar to what is described by Linley et al. (2013). Cytoarchitectonically, MO can be distinguished from PL by layers I, II and III. Cells in PL layer III are sparsely packed appearing like a "light band" ending at the border to MO. Layer II of PL is homogenously packed and looks denser compared to MO layer II, which is more loosely packed with 'patches' of cells. Layer II of MO also has a more diffuse transition into layer III. MO layer III has bigger cells compared to VO. Area IL appears as the least differentiated of all areas, making the distinction between layers II and III almost impossible, which is in agreement with Kondo and Witter (2014).

VO

VO is situated on the dorsal bank of the anterior rhinal fissure and borders MO medially and VLO laterally (Figure 8, A-E). VO fades away at the level where OFC merges with AOD (Figure 8, E), while in Linley et al. (2013), VO extended more posteriorly (Figure 8, F). Cytoarchitectonically, layer II of VO is wider with smaller, more densely packed than in MO. VO layer III is more sparsely packed with smaller, rounder cells compared to MO. Layers II and III of VO are more heterogeneous than in MO.

VLO

VLO is situated around the 'notch' of the anterior rhinal fissure, which was described by Van De Werd and Uylings (2008) as 'the dorsally directed indentation in the orbital cortical surface, which occurs in the middle of the line between the medial and lateral side of the frontal lobe'. VLO borders VO medially and LO laterally (Figure 8), having a balloon-formed shape. In anterior sections, the frontal association cortex and secondary motor cortex make up its dorsal border (Figure 8, A-C; Paxinos and Watson, 2007). In posterior sections, where the forceps minor of the corpus callosum comes in, a thin stripe of the anterior blade of the claustrum (Cl) defines VLO's dorsal border (Figure 8, E-H). The anterior rhinal fissure defines its ventral border and as one moves more posteriorly, VLO follows the fissure maintaining its balloon-formed shaped. Compared to Kondo and Witter (2014), VLO is a bit broader in both the medial and lateral extent. The main characteristic of VLO is in the layer II cells, which lie in vertical columns towards the pial surface, as previous described by Van De Werd and Uylings (2008). Layer II of VLO is thicker compared to that in VO, and the border between layers II and III is less sharp. Layer III and V cells in VLO are less densely packed than in VO. In posterior sections, cells of Cl are small and densely packed, making a clear contrast to deep layers of VLO.

LO

LO is situated laterally on the dorsal bank of the anterior rhinal fissure and borders VLO medially. In anterior sections, LO borders laterally to DLO. Posteriorly to the appearance of the forceps minor of the corpus callosum, DLO is replaced by AI (Figure 8, E). This is commonly agreed on among authors expect of in Van De Werd and Uylings (2008), in which AI appears between VLO and LO. Cytoarchitectonically, layer II of LO is narrow with dark, clustered cells, making a visible border to the columnar arranged cells in VLO. Layers II and III are somewhat easier to separate compared to VLO and DLO.

DLO

DLO makes up the most lateral part of the ventral bank of the anterior rhinal fissure, and borders LO medially and AI laterally (Figure 8, A-D). At the level where the forceps minor of the corpus callosum appears, DLO is replaced by AI, which is similar to what Van De Werd and Uylings (2008) described. In contrast, in Kondo and Witter (2014), DLO extends more posteriorly. Cytoarchitectonically, layers II and III of DLO are more difficult to distinguish compared to in LO. Cells in layer III of DLO are larger compared to in LO, and layer V of DLO has large, loosely packed cells. Compared to DLO, AI has clearer lamination.

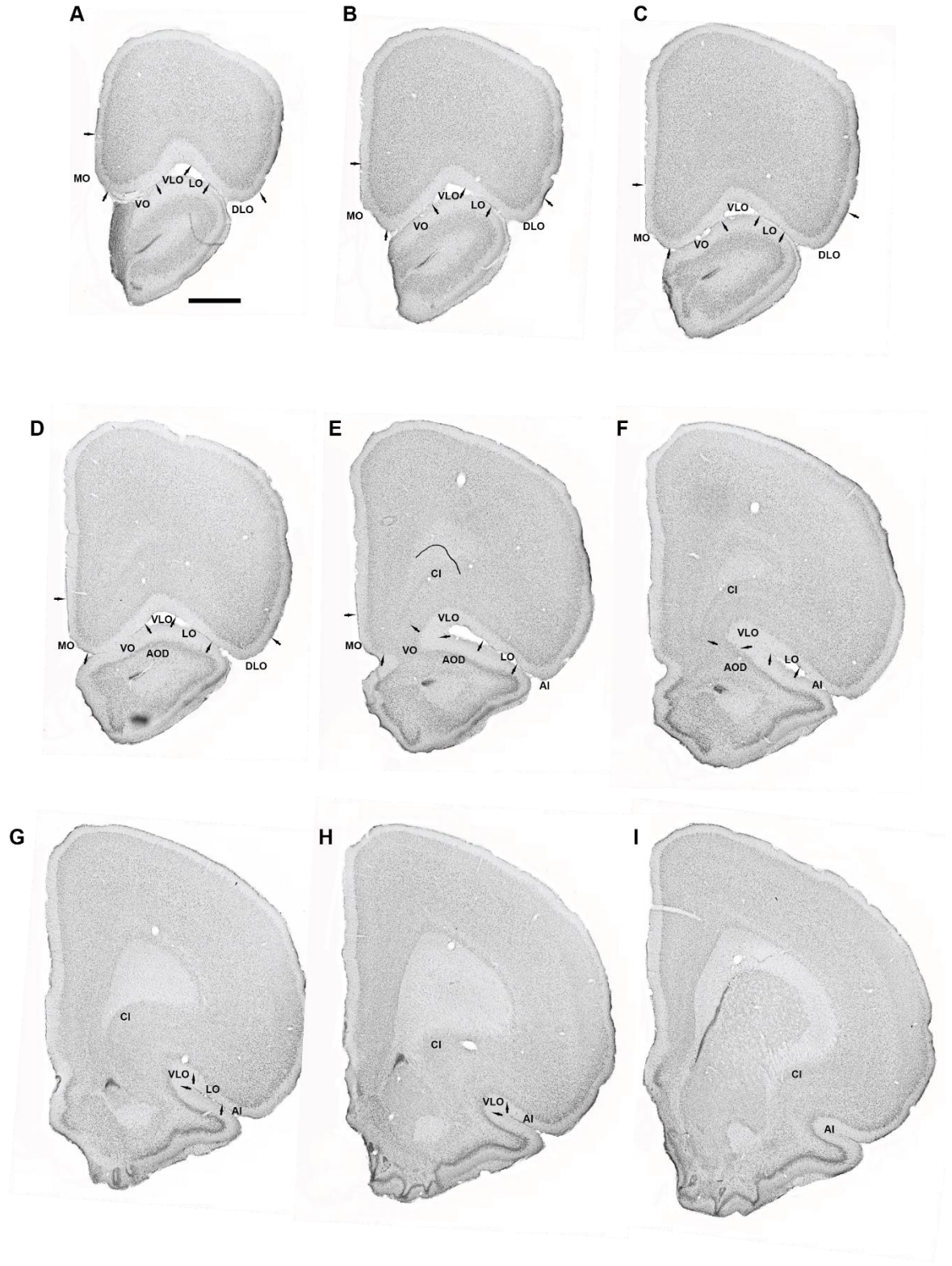

Figure 8. Delineation of the whole anterior-posterior extent of OFC in coronal sections including only the right hemisphere (A-I). Scale bar 1000 µm. For abbreviations, see list of abbreviations.

3.2 Injection sites of anterograde tracers

26 animals with a total number of 31 anterograde tracer injections were analysed. Based on cytoarchitecture and thalamic patterns, six injections were into mPPC (purple), eight into lPPC (blue) and six into PtP (yellow; Figure 9). In addition, control injections were made into the neighbouring areas to illustrate possible projections to OFC. Three injections were into V2M (green), one into V1 (brown), one into V2L (green) and five into S1 (orange). The figure below illustrates the core of the injections. That means that the halo may extend into adjacent areas, which is addressed when describing the injections in detail. All injections were made into the right hemisphere, except of 20546B and 12551P, which were mirrored to be analysed together with the other cases. All injection sites of anterograde tracers into PPC were delineated, which together with a table of labelling, are included in Appendix E.

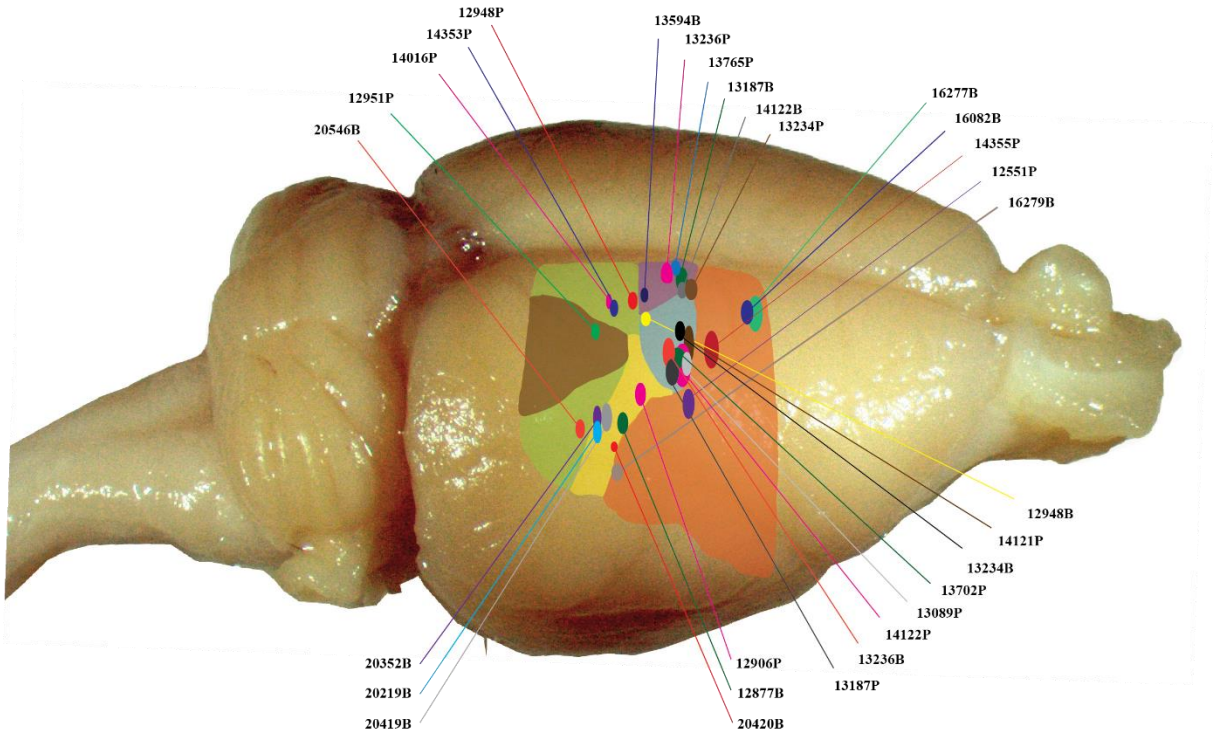

Figure 9. The distribution of anterograde tracer injection sites of BDA and PHA-L into mPPC (purple), lPPC (blue), PtP (yellow), V2M (green, medially), V1 (brown), V2L (green, laterally) and S1 (orange). Each elipsoid illustrates the core of the injection, implying that the halo may extend into adjacent areas. Modified from Olsen and Witter (pers. com.).

The results from three representative cases with injections of anterograde tracers, one for each subregion of PPC, will be presented to illustrate the projection patterns to OFC. In addition, two additional injections for each subregion will be presented at two different anterior-posterior levels to compare the labelling resulting from different injection sites.

3.3 Injection sites of retrograde tracers

In eight animals, I obtained 10 injections of retrograde tracers in OFC. Out of those, five injections resulted in sufficient uptake and transport and were analysed in order to establish the layer of origin of the cells projecting in the anterograde tracer cases (Figure 10). The injections varied in size, extended over three to four sections and included VLO and the lateral part of VO. One injection was chosen as the representative case based on location and good uptake and transport of the tracer (20461FB). One section from each of the other cases, illustrating the retrograde labelling in PPC, is included in Appendix F.

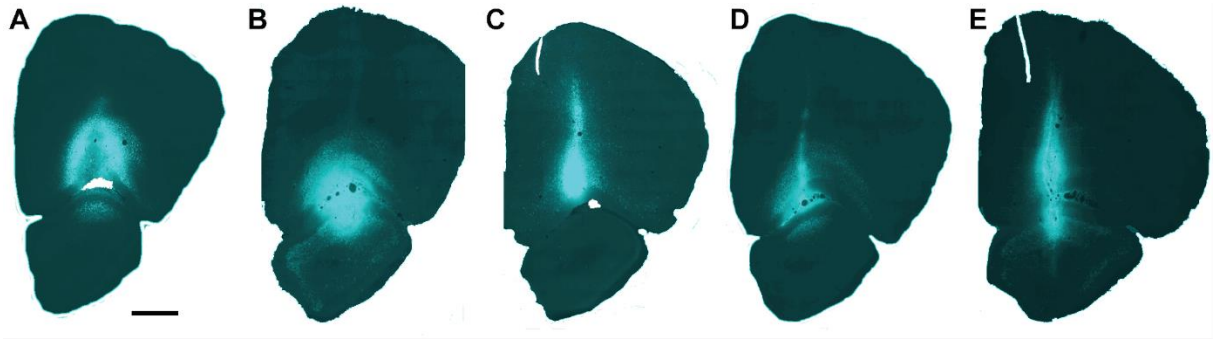

Figure 10. Microphotographs of the injection sites of retrograde tracers into OFC from anterior to posterior for case 20705FG (A), case 20545FB (B), case 20560FB (C), case 20705FB (D) and case 20461FB (E). The injections in A, C and E are mirrored along the vertical axis. Scale bar 1000µm.

3.4 Description of distribution in OFC

In order to describe anterograde labelling within subregions of OFC, a mediolateral axis was used (Figure 11, A). Unless specified otherwise, central refers to the mediolateral axis and indicates labelling in the mid part of VLO or VO. The notch, dorsal and ventral bank of the anterior rhinal fissure were used to locate labelling in posterior sections of OFC (Figure 11, B).

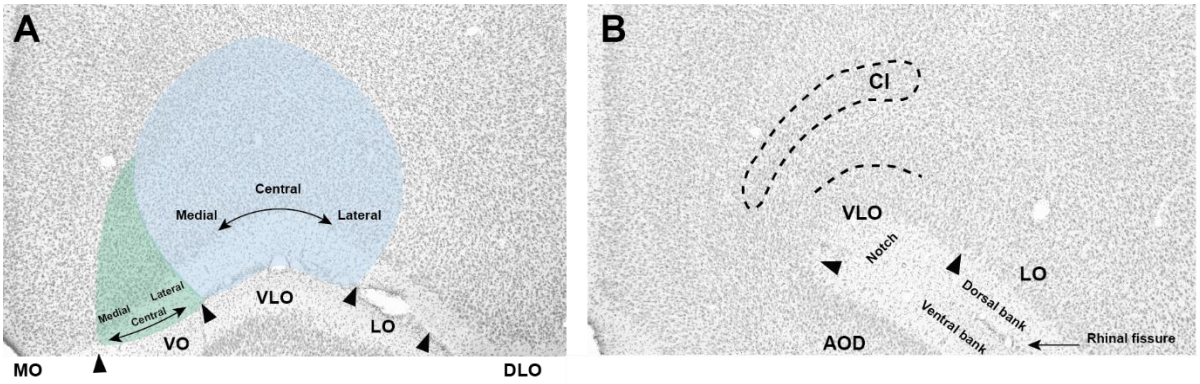

Figure 11. Mediolateral axis used to describe labelling in anterior sections within the subregions of VO and VLO (A). Location of the notch of the anterior rhinal fissure, ventral bank and dorsal bank used to describe labelling in posterior sections of OFC (B). The dashed lines indicate the approximate border between superficial and deep layers and the contour of Cl. For abbreviations, see list of abbreviations.

3.5 Anterograde tracer injections into mPPC

Injections into mPPC generally resulted in labelling in MO, VO and VLO (see Appendix E). One representative case will be presented illustrating the pattern of labelling over the entire extent of OFC (Figure 12, A). Two supporting cases (Figure 12, B and C), with injection sites located at different anterior-posterior levels, will be presented at one intermediate and one posterior level to compare the pattern of labelling.

A case representative for injections into mPPC had a PHA-L injection in anterolateral mPPC, mainly within one section, covering all layers with its core in layer V and VI (13234P; Figure 12, A). I observed a few retrogradely labelled cells in mPPC in the directly adjacent sections. Since anterograde thalamic labelling was not only found in LPmr and Po, but also in VP, S1 might have been weakly involved by way of retrograde transport (Olsen and Witter, pers. com.). In anterior sections, sparse labelling was seen in MO and VO, mainly in superficial layers (Figure 13, A-C). At a more posterior level, fibres were seen in superficial layers of VO, extending into medial VLO. Fibres were also seen in deep layers, extending from lateral VO to central VLO (Figure 13, D). At the level right anterior to the merging of OFC with AOD (Figure 13, E), dense labelling was seen in superficial layers of medial VLO at the border to VO. Labelling extended into deep layers from medial to central VLO (Figure 13, E). Sparse labelling was also seen in deep layers of VO. Further posteriorly, dense labelling was seen in deep layers of VLO extending into Cl, focused medially, while labelling in superficial layers gradually faded off (Figure 13, F-H).

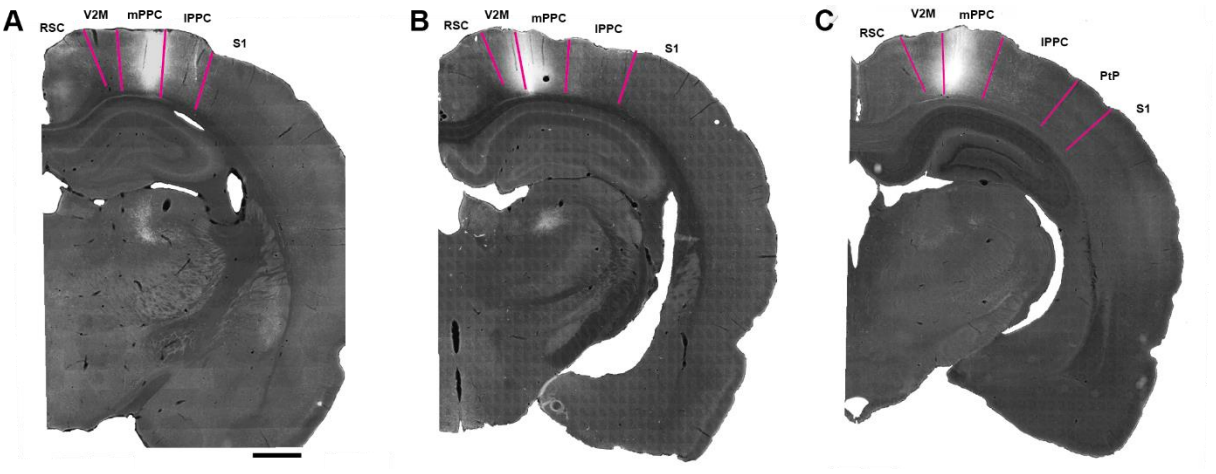

Figure 12. Injection sites of three injections into mPPC arranged from anterior to posterior. A) The representative case, 13234P, having a PHA-L injection positioned anterolaterally in mPPC. B) One additional case, 13765P, showing an injection of PHA-L injection at an intermediate anterior-posterior level, medially in mPPC. C) The second additional case, 13594B, a BDA injection positioned medially in a posterior section of mPPC. Scale bar 1000µm. For abbreviations, see list of abbreviations.

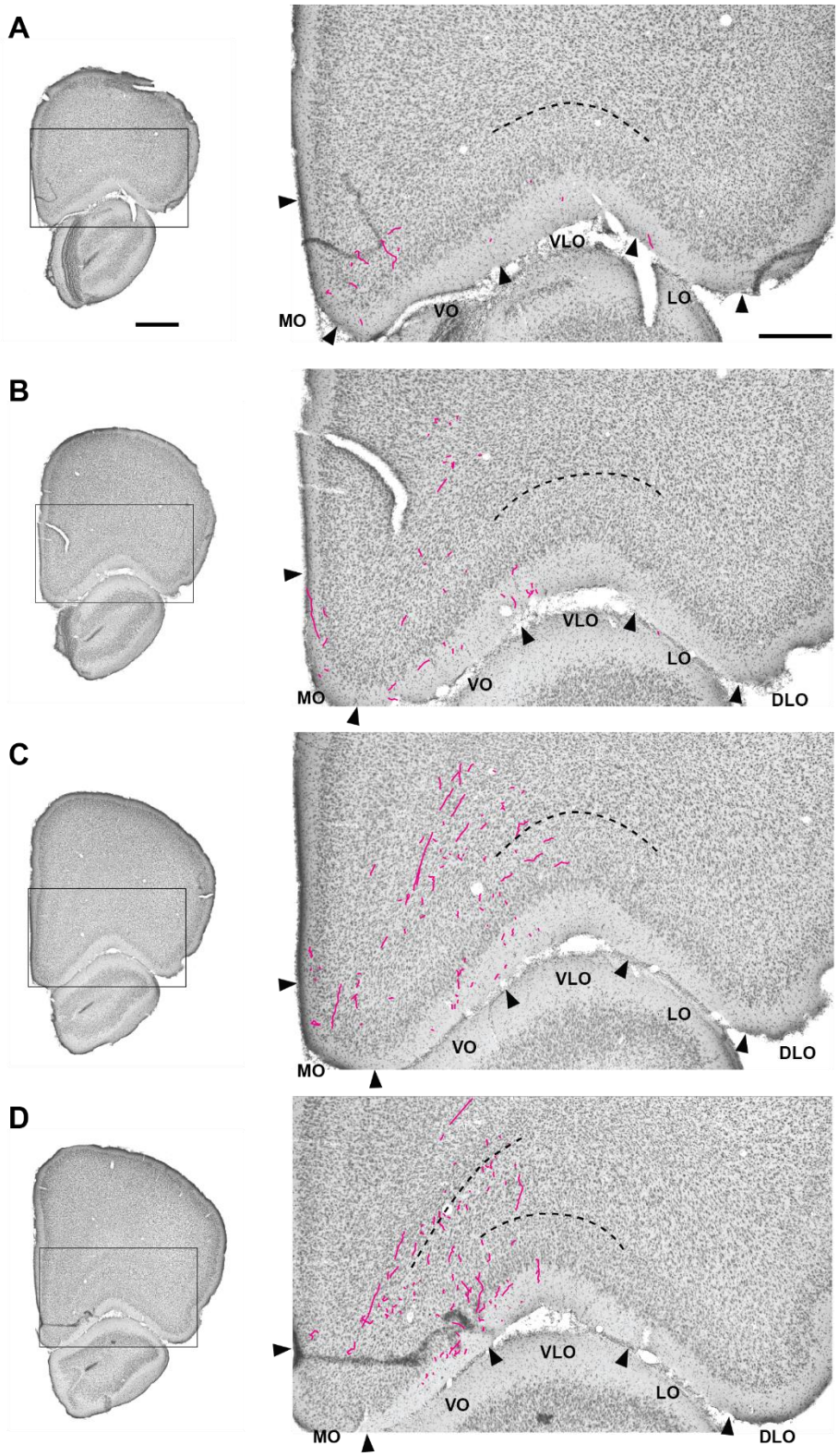
A
VLO
LO
VO
MO
B
VLO
LO
VO
MO
DLO
C
VLO
LO
VO
MO
DLO
D
VLO
LO
VO
MO
DLO

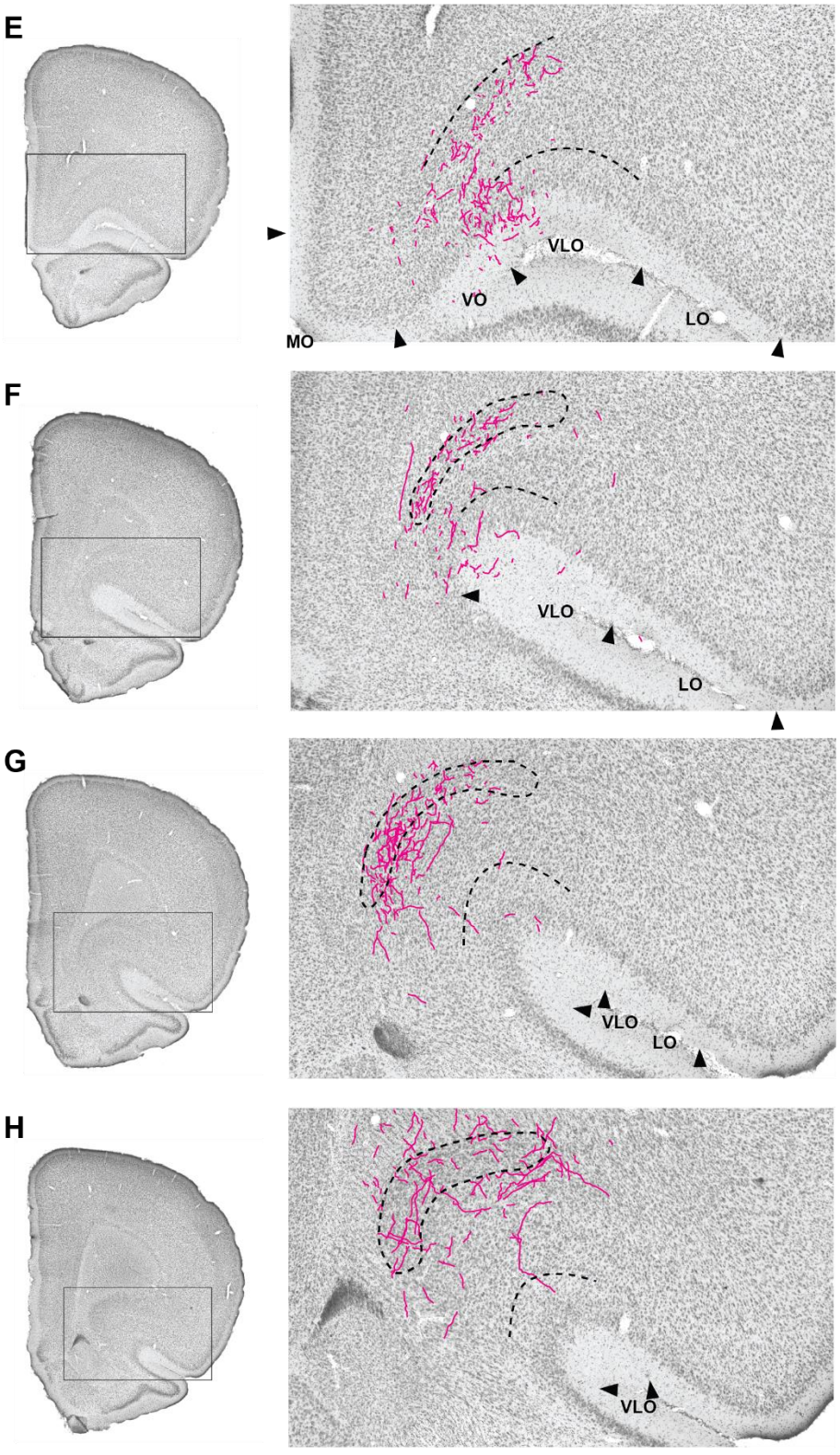

Figure 13. Labelling in the anterior-posterior extent (A-H) of OFC resulting from a representative injection into mPPC with PHA-L (13234P). The boxed areas in the left panels illustrate precisely the areas shown with higher magnification to the right. The dashed lines indicate the approximate border between superficial and deep layers and the contour of Cl. Scale bars 1000µm (left) and 500µm (right). For abbreviations, see list of abbreviations.

Another case had a PHA-L injection positioned at an intermediate anterior-posterior level in mPPC, in particular more medially than the representative case, close to the border to V2M (13765P; Figure 12, B). The injection had its core in the deep layers and was mainly confined to one section with only a few labelled cells in the adjacent anterior section. Thalamic labelling was strongest in LPmr but also involved Po (Olsen and Witter, pers. com.). Similarly to the representative case, labelling in OFC was found in MO, VO and VLO. A few fibres were seen in superficial MO in anterior sections, while the strongest labelling was seen in superficial layers in lateral VO and medial VLO (Figure 14, A, a), extending more laterally in the next sections. Some fibres were seen in deep layers. In posterior sections, some fibres were seen medially in VLO, on the ventral bank of the notch of the anterior rhinal fissure, with some extending into deep layers and medially into Cl (Figure 14, B, a). Labelling in superficial layers of VLO gradually faded off more posteriorly, where only a couple of labelled fibres were observed. In deep layers of VLO and Cl, weak labelling was observed.

A third injection of BDA, positioned more posteriorly in mPPC, showed a slight extension into V2M (13594B; Figure 12, C). The injection extended over two section and covered all layers but had a core layer V. Thalamic labelling was seen in LPmr with some fibres in LDl. Labelling was also present in Po, but not in VP (Olsen and Witter, pers. com.). The labelling in OFC was similar to the latter case (13765P), having the strongest labelling in superficial layers from central VO and to medial VLO (Figure 14, A, b). However, in contrast to the previous case, very few fibres were seen in deep layers. Comparably, fibres were seen medially in VLO, on the ventral bank of the notch of the anterior rhinal fissure with some involvement of deep layers of VLO and medial Cl (Figure 14, B, b). Labelling in superficial layers of VLO and in deep layers of VLO and Cl gradually faded off more posteriorly.

In addition to the injections already mentioned, three other injections into mPPC (14122B, 13187B, 13765P) resulted in similar labelling as the representative case. The strength of labelling was weak or very weak. A fourth case showed stronger labelling in MO than the other cases and it also had fibres in LO (13236P). This case had overall extensive cortical labelling not comparable to other cases.

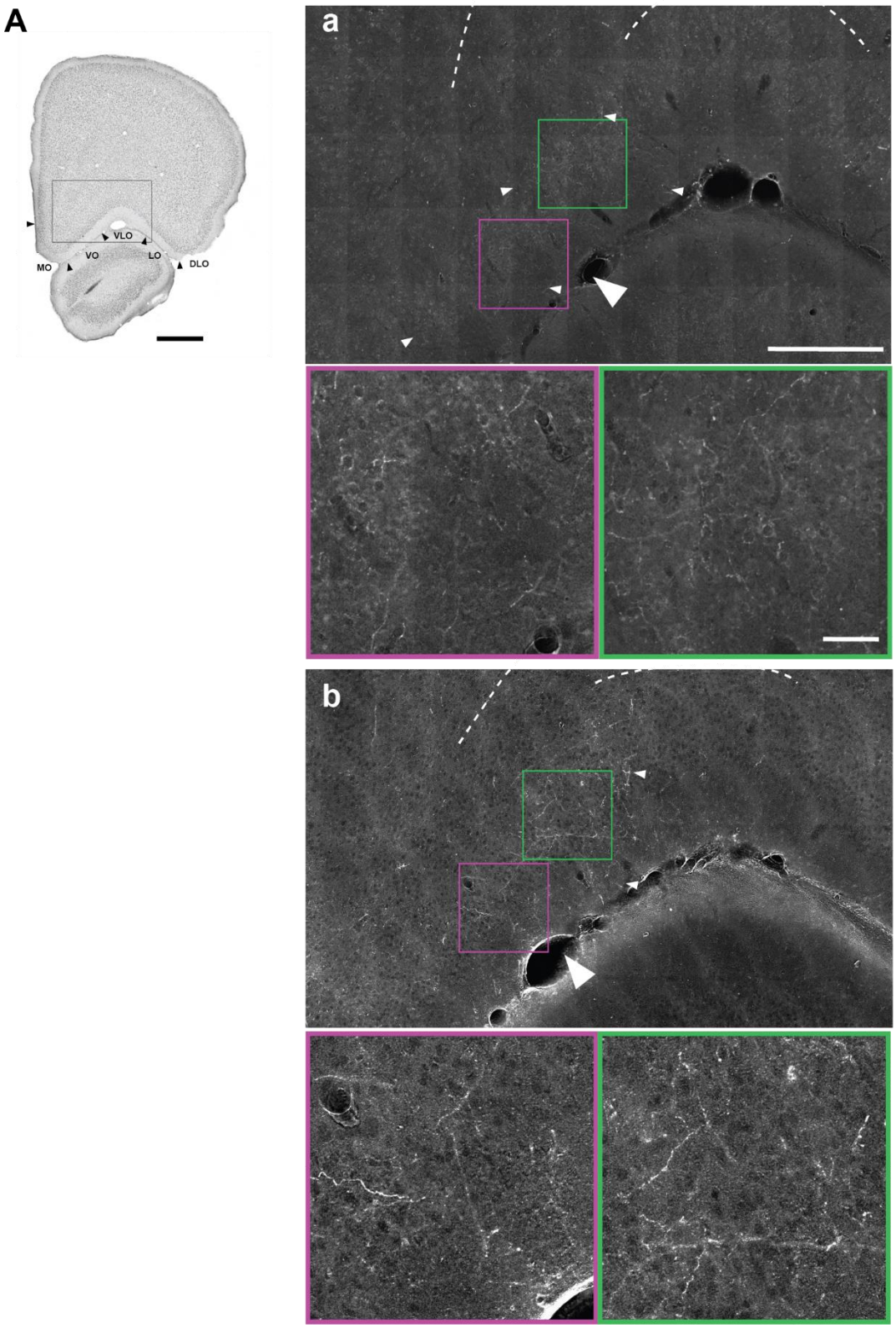
A
VLO
VO
LO
DLO
MO
a
b

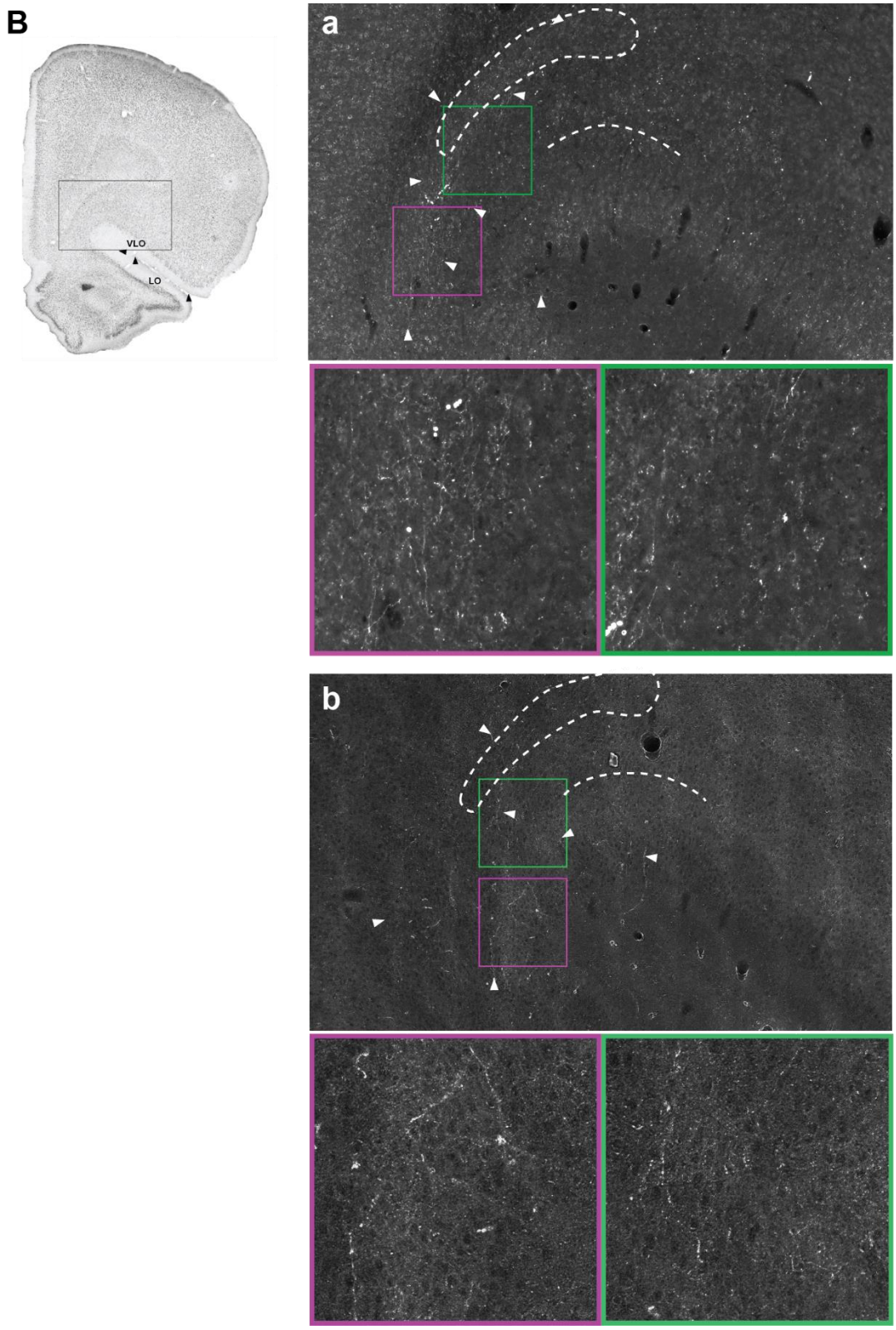

Figure 14. Labelling at one anterior and one more posterior level of OFC resulting from two additional injections into mPPC. The boxed areas to the left indicate the approximate size and position of the areas shown with higher magnification to the right. Pictures a in A and B illustrate labelling from case 13765P, while pictures b are from case 13594B. Pink and green boxes shows higher magnification of the labelling in the corresponding areas. Small arrows indicates the position of fibres and the big arrow the border between VO and VLO. The dashed lines indicate the approximate border between superficial and deep layers and the contour of Cl. Scale bars 1000µm (left), 500µm (right), 100µm (pink, green). For abbreviations, see list of abbreviations.

3.6 Anterograde tracer injections into lPPC

Injections into lPPC mainly resulted in labelling in VLO, with some occasional fibres in VO. A representative case had a PHA-L focused in layers V and VI of lPPC (13187P; Figure 15, B). The core of the injection was mainly confined to lPPC and extended over two sections. However, there were a few retrogradely labelled cells in mPPC and S1. The injection resulted in strong thalamic labelling dorsolaterally in Po, spanning several sections. Minor labelling was seen in LPmr in addition to sparse fibres in VP (Olsen and Witter, pers. com.). In OFC, moderate labelling was observed mainly in VLO showing a central position throughout most of the anterior-posterior extent of VLO and Cl, with some occasional fibres in VO (Figure 16). In anterior sections, labelling was focused in superficial layers of central VLO, with some labelling in deeper layers extending from medial to central VLO (Figure 16, A-D). Right anterior to the merger of OFC with AOD (Figure 16, E), labelling was seen in superficial layers of VLO, from medial to lateral. The labelling extended into deep layers, covering the same mediolateral extent. Also, a few short fibres were seen in lateral VO, in both superficial and deep layers. Further posteriorly, labelling was seen in VLO on the notch of the anterior rhinal fissure, mainly in superficial layers (Figure 16, F). Fibres were also seen in deep layers of VLO, extending medial to lateral and also into Cl. Labelling in superficial layers faded off in the most posterior sections (Figure 16, G-H), while labelling in deep layers of VLO and Cl was still present, showing a clear central position.

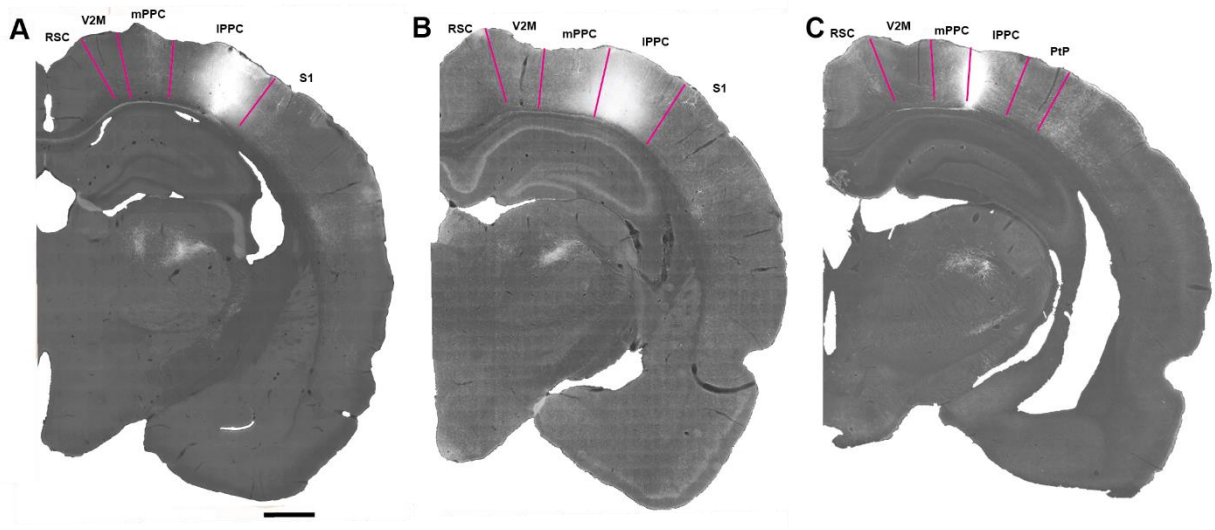

Figure 15. Injection sites for three injections into lPPC arranged from anterior to posterior. A) One injection, 14122P, positioned anterolateral in lPPC. B) The representative case, 13187P, positioned at an intermediate anterior-posterior level, medially in lPPC. C) A third case, 12948B, positioned medially in a posterior level of lPPC. Scale bar 1000µm. For abbreviations, see list of abbreviations.

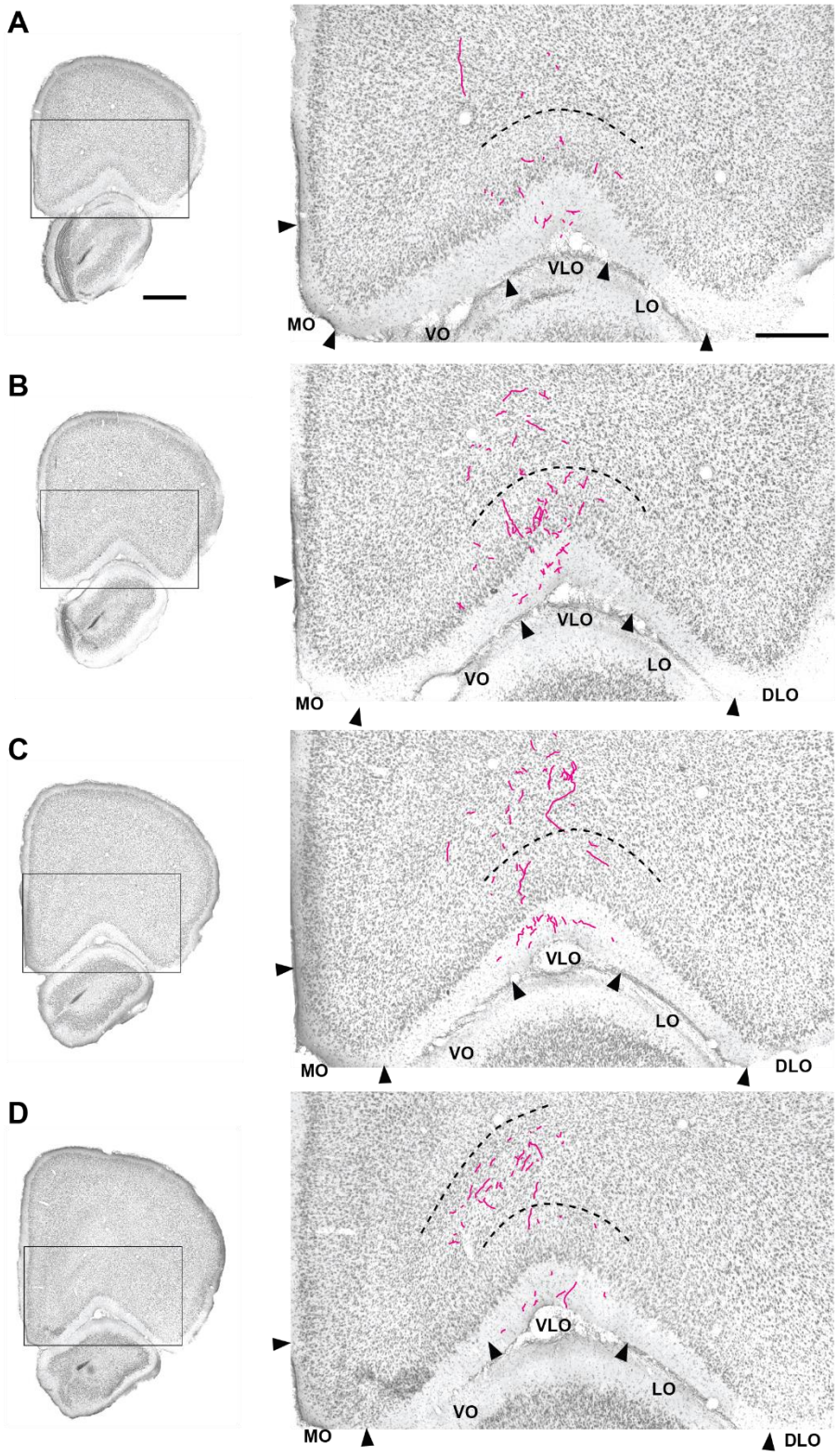
A
VLO
LO
MO
VO
B
VLO
LO
VO
MO
DLO
C
VLO
LO
VO
MO
DLO
D
VLO
LO
VO
MO
DLO

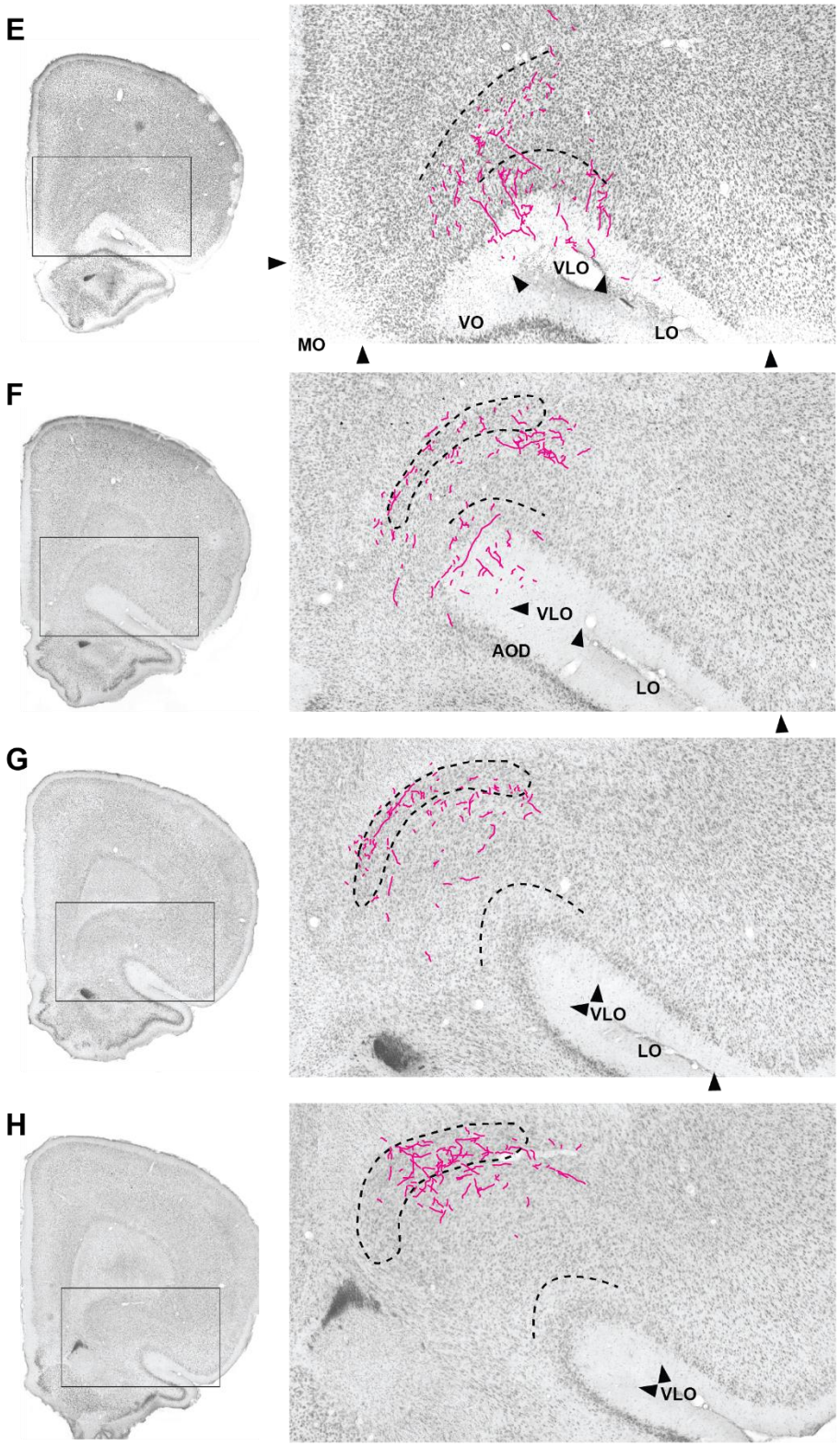

Figure 16. Labelling in OFC along the anterior-posterior extent (A-H) resulting from a representative injection into lPPC with PHA-L (13187P). The boxed areas in the left panels indicate the areas shown with higher magnification to the right. The dashed lines indicate the approximate border between superficial and deep layers and the contour of Cl. Scale bars 1000µm (left) and 500µm (right). For abbreviations, see list of abbreviations.

Another case had a PHA-L injection positioned more anteriorly in lPPC than the representative case, mainly confined within one section, with a few labelled cells in the two adjacent sections (14122P; Figure 15, A). The injection covered all layers, having its core in deep layers. Strongest thalamic labelling was found in Po in addition to moderate labelling in LPmr and LDm (Olsen and Witter, pers. com.). Overall, the injection resulted in strong OFC labelling with a distribution pattern similar to the representative case, with the strongest labelling in VLO in addition to some labelled fibres in VO. In anterior sections, strong labelling was seen in superficial layers of medial VLO, extending into deep layers from lateral VO to central VLO (Figure 17, A, a). In posterior sections, labelling was seen in superficial layers around the notch of the anterior rhinal fissure. It extended from the ventral bank, including AOD, to the dorsal bank, moving laterally towards LO (Figure 17, B, a). Moderate labelling was also seen in deep layers, extending from medial to central VLO and Cl. In the most posterior sections, labelling in deep layers of VLO and Cl was still present, having a slightly more lateral position than in more anterior sections. Like the representative case, labelling in the superficial layers ceased at the most posterior levels of VLO.

A BDA injection was positioned in the posterior part of lPPC, with possibly a slight extension into mPPC (12948B; Figure 15, C). The injection extended over two sections, and its core covered all layers. Strongest thalamic labelling was seen in Po, while LPmr and LDm had very sparse labelling (Olsen and Witter, pers. com.). In general, the labelling in OFC followed the same pattern as for the representative case, though the labelling was weaker. Intermediate labelling was seen in superficial layers of medial VLO in anterior sections (Figure 17, A, b). Some fibres were seen in deep layers, extending from lateral VO to central VLO. At the level of merging of OFC with AOD, dense labelling was focused centrally on the notch, continuing more posteriorly. Different from case 14122P, labelling did not extend laterally on the dorsal bank (Figure 17, B, b). Similar to the representative case, labelling in superficial layers faded off posteriorly, while deep layers of VLO and Cl still had labelled fibres.

Five additional injections into lPPC were analysed (13702P, 13234B, 13236B, 13089P and 14121P) and all of them showed a labelling pattern similar to that described for the representative case. However, labelling in OFC was weak for all cases. In summary for all lPPC cases, labelling was present mainly in VLO and Cl, and compared to cases with injections into mPPC, labelling showed a shift to a more lateral position.

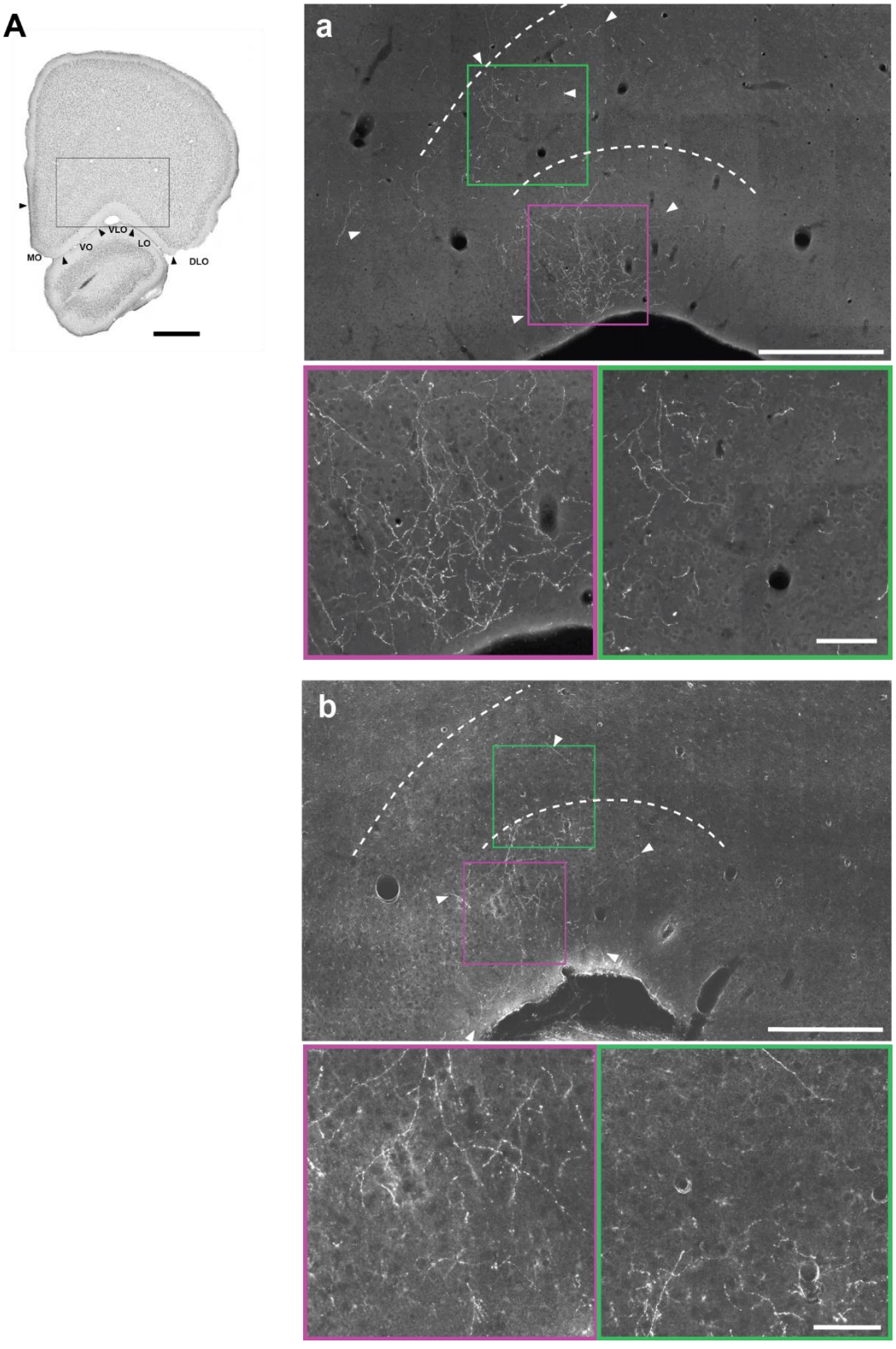
A
VLO
VO
LO
MO
DLO
a
b

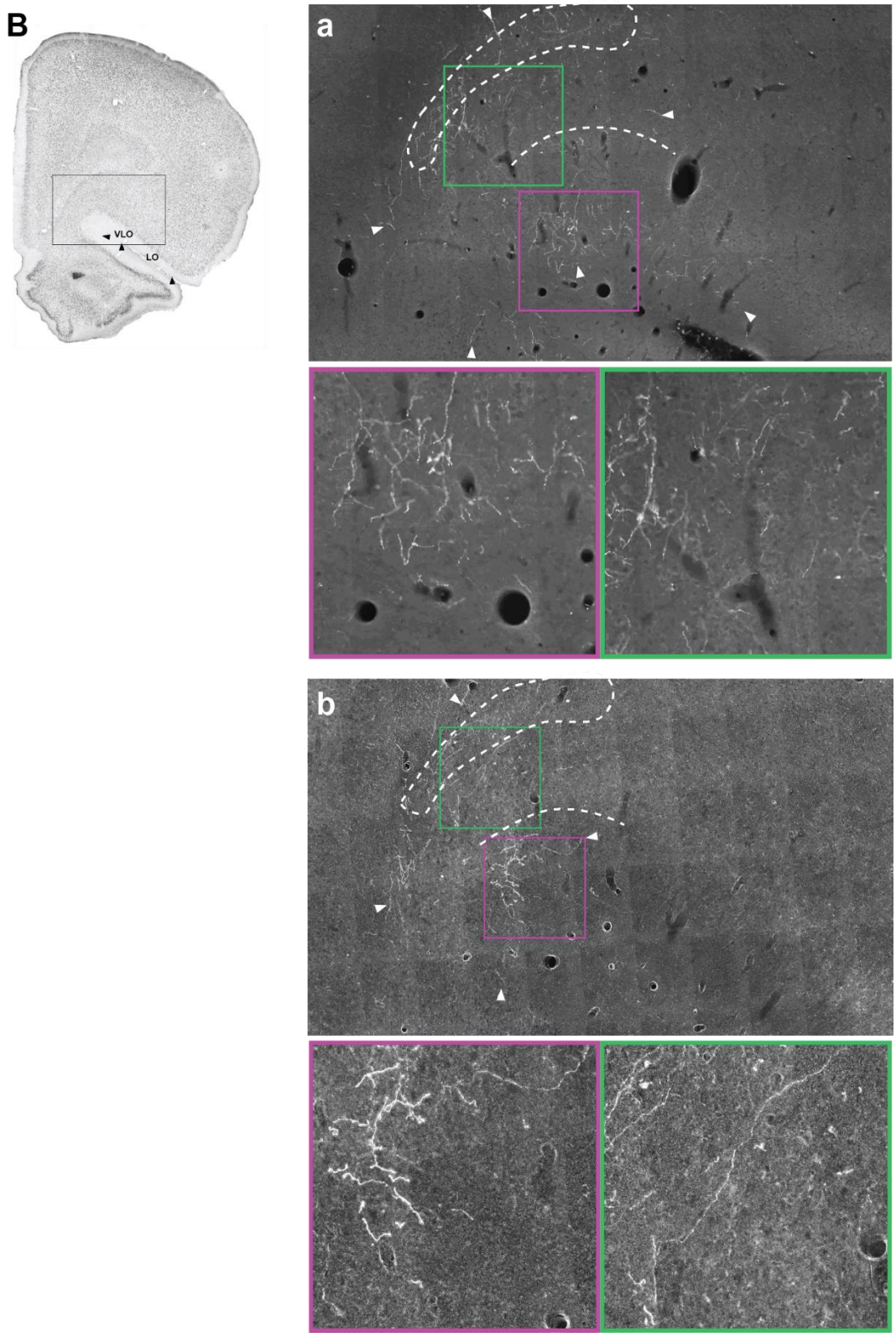

Figure 17. Labelling at one anterior and one more posterior level of OFC resulting from two additional injections into lPPC. The boxed areas to the left indicate the approximate size and position of the areas shown with higher magnification to the right. Pictures a in A and B illustrate labelling from case 14122P, while pictures b are from case 12948B. Pink and green boxes shows higher magnification of the labelling in the corresponding areas. Small arrows indicates the position of fibres. The dashed lines indicate the approximate border between superficial and deep layers and the contour of Cl. Scale bars 1000µm (left), 500µm (right), 100µm (pink, green). For abbreviations, see list of abbreviations.

3.7 Anterograde tracer injections into PtP

Injections into PtP generally resulted in labelling in VLO, and compared to injections into lPPC, the labelling had a slightly more lateral position in VLO. A representative case had a PHA-L injection into PtP at an intermediate anterior-posterior level, positioned next to the border to V2L. The injection covered all layers with its core focused in layers V and VI (12906P; Figure 18, B). Only a few stained cells were seen in the directly adjacent sections. The strongest thalamic labelling was seen dorsolaterally in Po. Noteworthy is also some labelling ventrally in LPl (Olsen and Witter, pers. com.). In anterior sections, labelling was focused in central VLO, mainly in superficial layers (Figure 19, A-C), with a few labelled short fibres in superficial LO. More posteriorly (Figure 19, D), sparse labelling was seen in superficial and deep layers of central VLO, in which the labelling in deep layers extended more medially. Slightly posterior to the level of merging of OFC with AOD, labelling was seen in VLO around the notch of the anterior rhinal fissure, extending from the ventral bank including AOD to the dorsal bank, moving laterally into LO, focused in layers I and II (Figure 19, F). Moderate labelling was seen in deep layers of VLO and Cl, being most prominent laterally in VLO. In the most posterior sections, a couple of labelled fibres were seen in VLO layers I-III, in addition to a few short fibres in deeper layers and in Cl (Figure 19, G). Labelling in superficial layers faded off posteriorly, while sparse labelling was still present in deep layers of VLO and Cl (Figure 19, H).

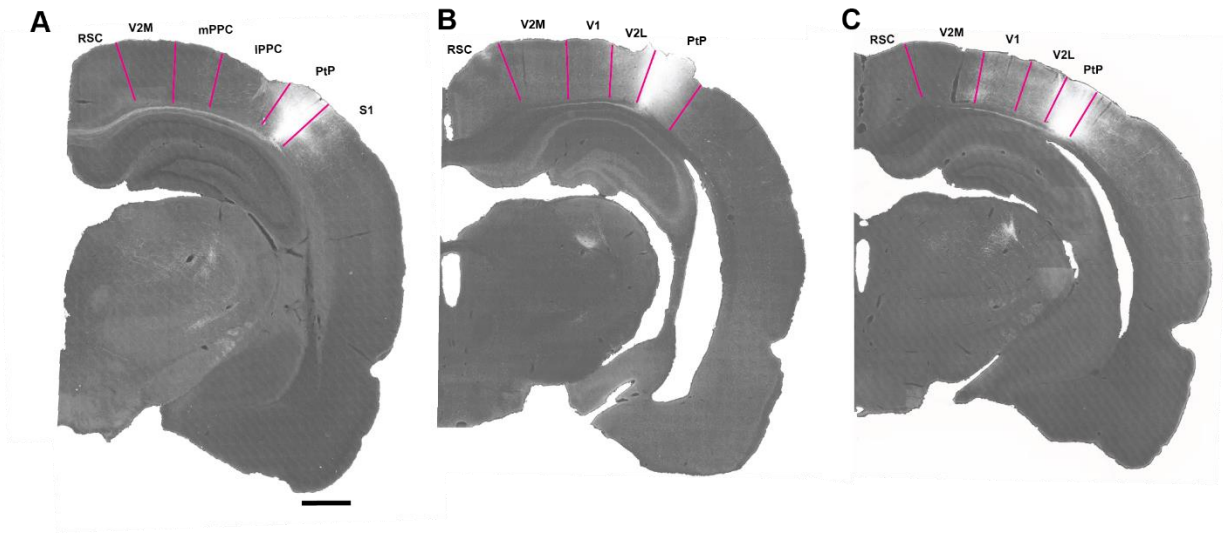

Figure 18. Injection sites for three injections into PtP arranged from anterior to posterior. A) A BDA injection, positioned anterolaterally in PtP (12877B). B) The representative case (12906P), a PHA-L injection positioned at an intermediate anterior-posterior level, medially in PtP. C) A more posteriorly positioned BDA injection (20219B). Scale bar 1000µm. For abbreviations, see list of abbreviations.

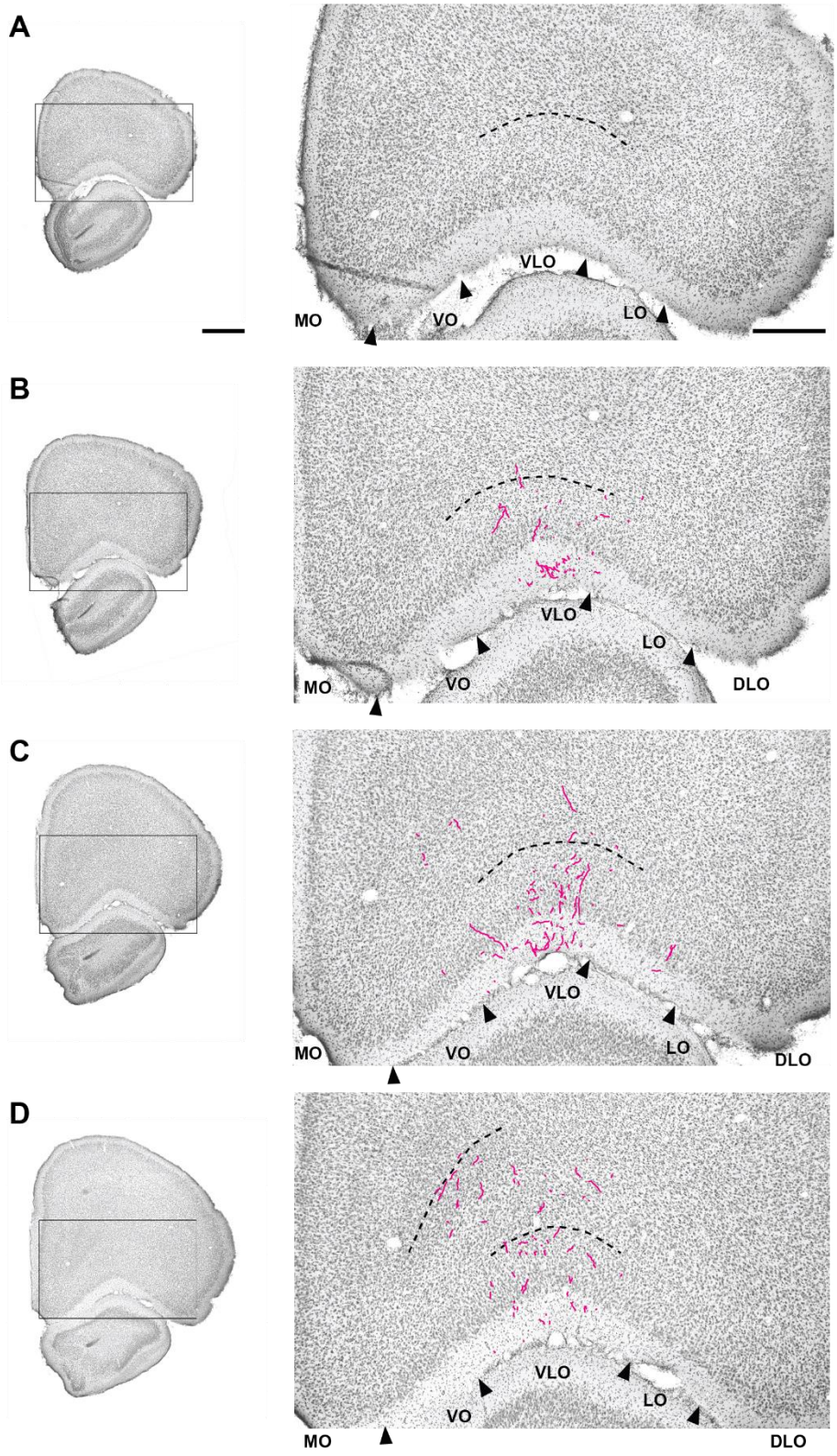
A
VLO
VO
LO
MO
B
VLO
LO
VO
DLO
MO
C
VLO
MO
VO
LO
DLO
D
VLO
VO
LO
MO
DLO

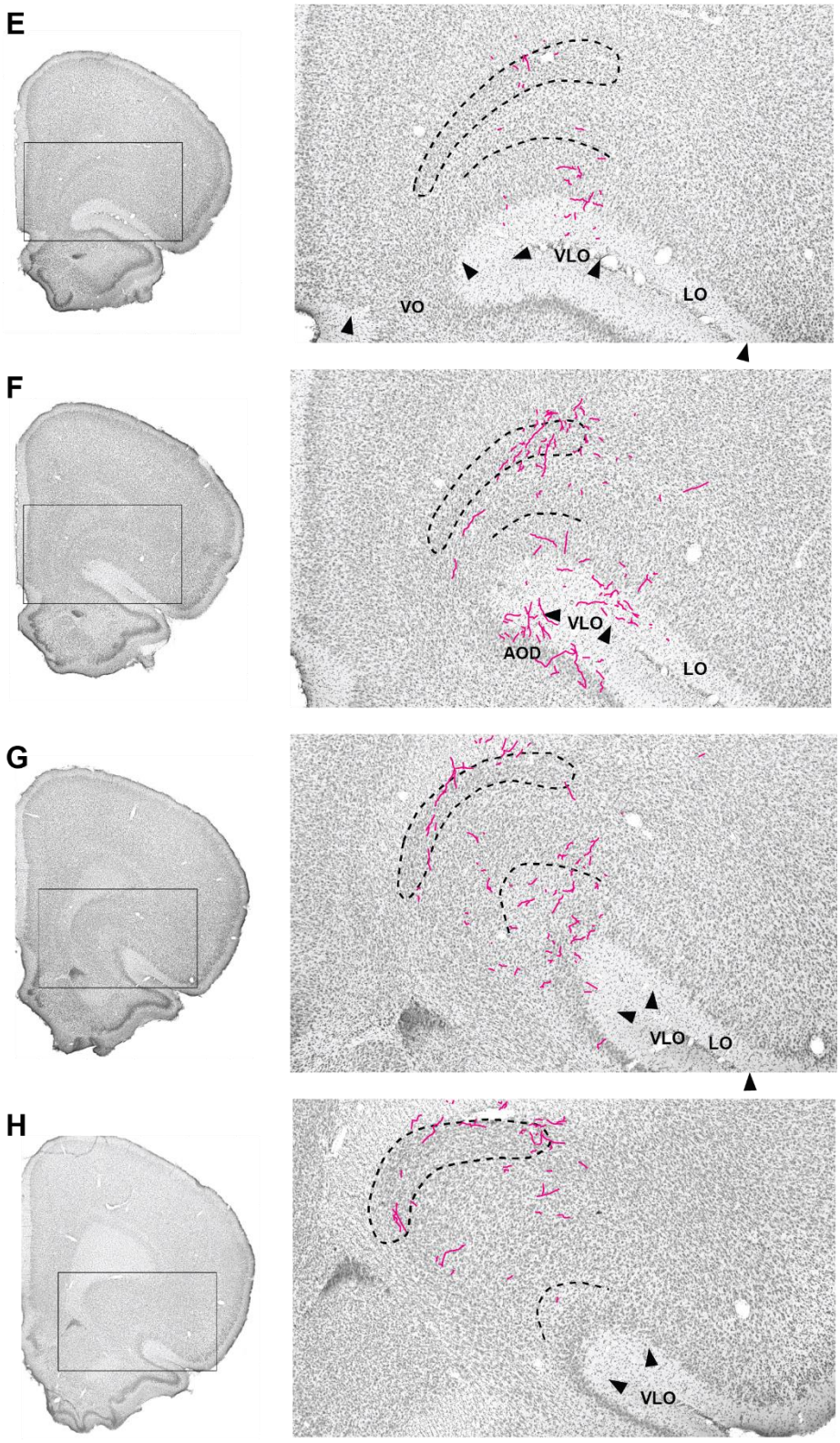

Figure 19. Distribution of anterograde labelling along the anterior-posterior extent (A-H) of OFC resulting from a representative injection into PtP with PHA-L (12906P). The boxed areas in the left panels indicate the areas shown with higher magnification to the right. The dashed lines indicate the approximate border between superficial and deep layers and the contour of Cl. Scale bars 1000µm (left) and 500µm (right). For abbreviations, see list of abbreviations.

A second injection of BDA was positioned anteriorly in PtP, covered all layers having its core in layer V (12877B; Figure 18, A). A few cells were labelled in the two directly adjacent sections. In this case, thalamic labelling was strongest in Po. A tiny cluster of fibres was present in VPm (Olsen and Witter, pers. com.). At anterior levels of OFC, fibres were seen in superficial layers of central VLO, some extending laterally (Figure 20, A, a). Weak labelling was seen in deep layers from medial to central VLO, extending posteriorly. At the level posterior to the merging of OFC with AOD, differently from the representative case, labelling was focused intermediately on the notch (Figure 20, B, a). Labelling in deep layers extended from medial to lateral VLO, including Cl. Labelling in posterior sections was similar to the representative case but weaker.

The third case was selected because it had an involvement of V2L in the section posterior to the injection site (20219B; See Appendix E for delineation). The core of the injection was in deep layers of posterior PtP (Figure 18, C). Thalamic labelling was dense in Po across several sections, posteriorly in thalamus a plexus of labelled fibres was also seen laterally in LPl (Olsen and Witter, pers. com.). The injection further resulted in moderate labelling in OFC with labelling slightly more medially positioned, though overall comparable pattern to what was described for the representative case. At anterior levels, very little labelling was seen, with some fibres in superficial layers of the medial to lateral extent VLO and a couple of short, straight fibres in VO and LO (not illustrated). Sparse labelling in deep layers of VLO continued and increased in density slightly more posteriorly. At an intermediate anterior-posterior OFC level, fibres were mainly seen in superficial layers of medial to central VLO with an extension into deep layers (Figure 20, A, b). A few short fibres were also labelled in lateral VO. Labelling in both superficial and deep layers of VLO got denser posteriorly with the strongest labelling in layer I at a medial portion, while the strongest labelling in layers II and III was positioned more laterally (not illustrated). At the level posterior to the merging between OFC and AOD, the most prominent labelling was found in superficial layers on the central part of the notch, extending into deep layers and Cl, from central to lateral positions (Figure 20, B, b). A couple of short fibres were seen in superficial layers on the dorsal bank of the anterior rhinal fissure. As for the other cases, labelling in deep layers and Cl continued posteriorly, while superficial labelling disappeared.

Two additional injections into PtP, a small injection covering layers V-VI only (20420B) and a big injection covering all layers (20352B), both had a small involvement of S1 and resulted in labelling similar to the representative case. A third additional case (20419B), which had a bigger S1 component, showed more extensive labelling in Cl than the other injections into PtP.

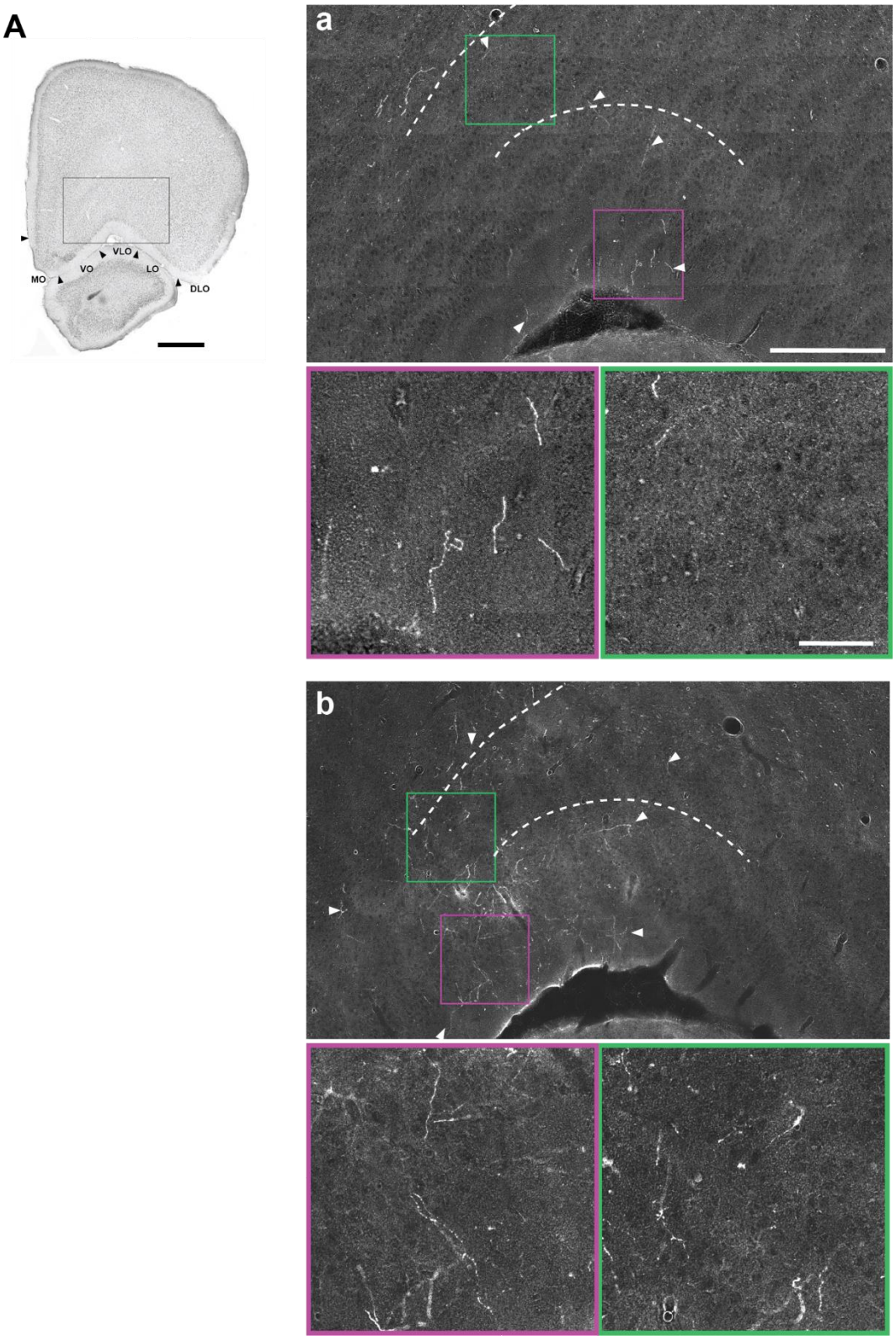
A
VLO
VO
LO
MO
DLO
a
b

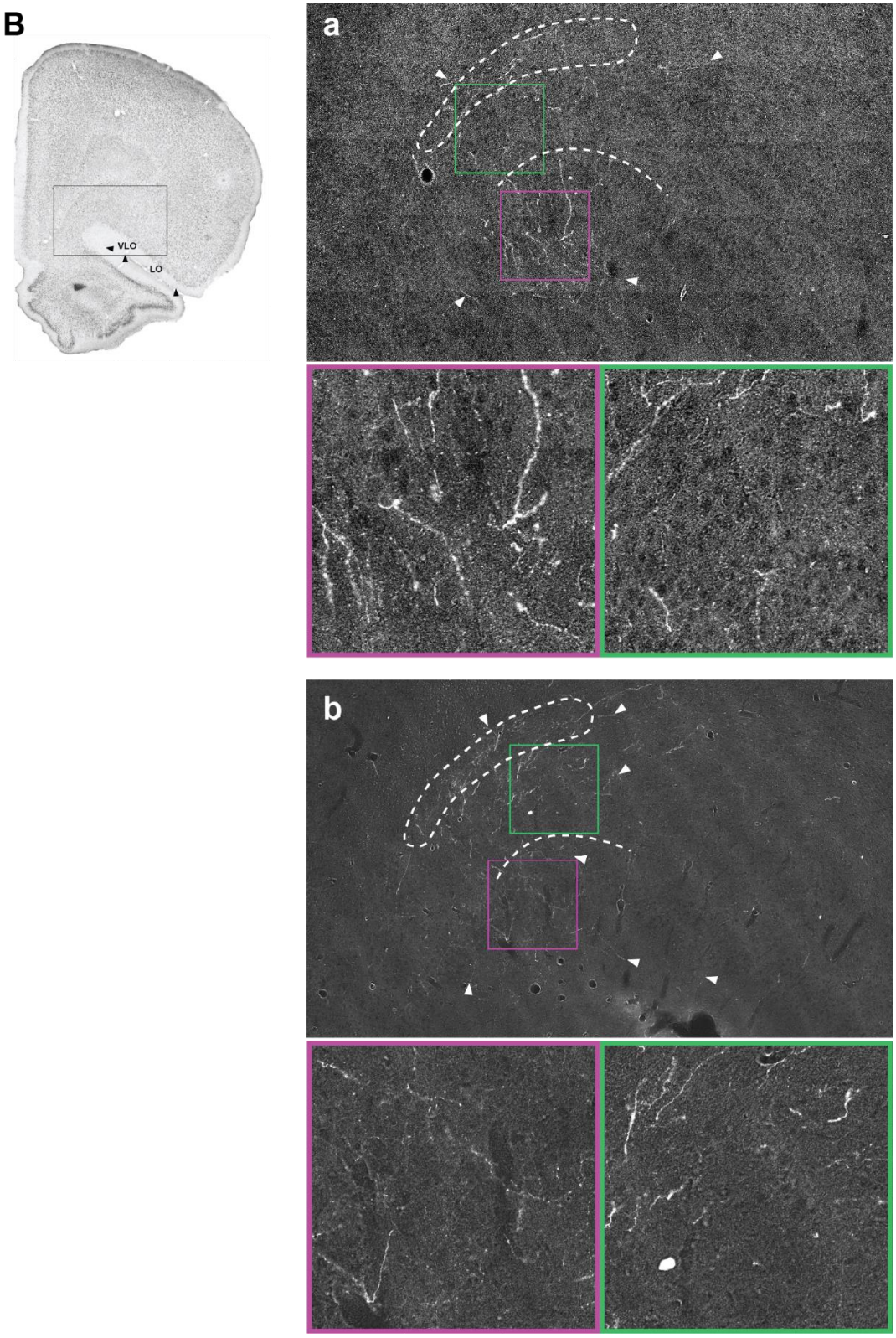

Figure 20. Anterograde labelling at one anterior (A) and one more posterior level of OFC (B) resulting from two additional injections into PtP. The boxed areas to the left indicate the approximate size and position of the areas shown with higher magnification to the right. Pictures a in A and B illustrate labelling from case 12877B, while pictures b are from case 20219B. Pink and green boxes shows higher magnification of the labelling in the corresponding areas. Small arrows indicates the position of fibres. The dashed lines indicate the approximate border between superficial and deep layers and the contour of Cl. Scale bars 1000µm (left), 500µm (right), 100µm (pink, green). For abbreviations, see list of abbreviations .

3.8 Control cases with anterograde tracers into S1, V1, V2M and V2L

Anterograde tracer injections were placed into neighbouring areas of PPC in order to check if leakage of tracers into these areas might have contributed to the anterograde labelling in OFC, when injecting in PPC. Injections into V2M and V2L resulted in labelling in OFC and will be presented at one anterior and one posterior level for comparison with labelling resulting from injections into PPC. Anterograde tracer injections into S1 did not result in any labelling in OFC, but some fibres were observed in Cl in for all cases (12551P, 16082B and 16277B). An exception was an injection that was positioned more posteriorly in S1 on the border to PPC (14355P). The latter case had a few labelled fibres in VLO in addition to a plexus in Cl. An injection into V1 did not result in labelling in OFC and will therefore not be discussed further (12951P).

A representative case for V2M had a PHA-L injection positioned at an intermediate anterior-posterior level on the border to V1, extending over two sections (14016P; Figure 21). The injection covered all layers but had its core in layer I-III. Thalamic labelling was moderate in LD and strong in LPm and LPl (Olsen and Witter, pers. com.). This injection resulted in very dense labelling in layer I from central VO to medial VLO in anterior sections (Figure 22, A). Labelling was also strong in layer III, while there were few labelled fibres in deep layers of VLO. A few short fibres were also seen in MO. The pattern was similar to injections into mPPC, except that injections into mPPC may result in more labelling in deep layers and less dense labelling in layer I. Strong superficial labelling continued more posteriorly, moving slightly more lateral towards medial VLO, but faded off at the level of merging of OFC with AOD. At this level, less dense labelling was seen in superficial layers, extending from AOD to VLO (Figure 22, B). Compared to the amount of labelling in anterior sections, few fibres were seen in deep layers of VLO and in Cl. Differently, injections into mPPC had more labelling in deep layers that extended into Cl. Two other injections into V2M showed similar projection patterns (12948P, 14353P; not illustrated).

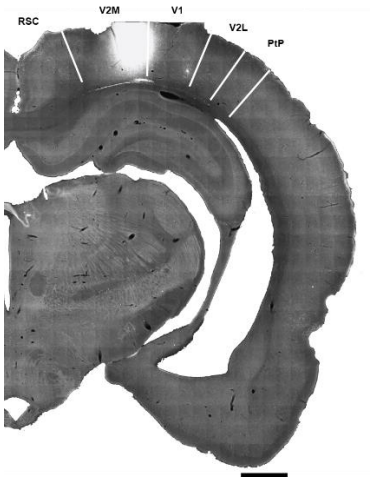

Figure 21. A representative PHA-L injection into anterior V2M (14016P). Scale bar 1000µm. For abbreviations, see list of abbreviations.

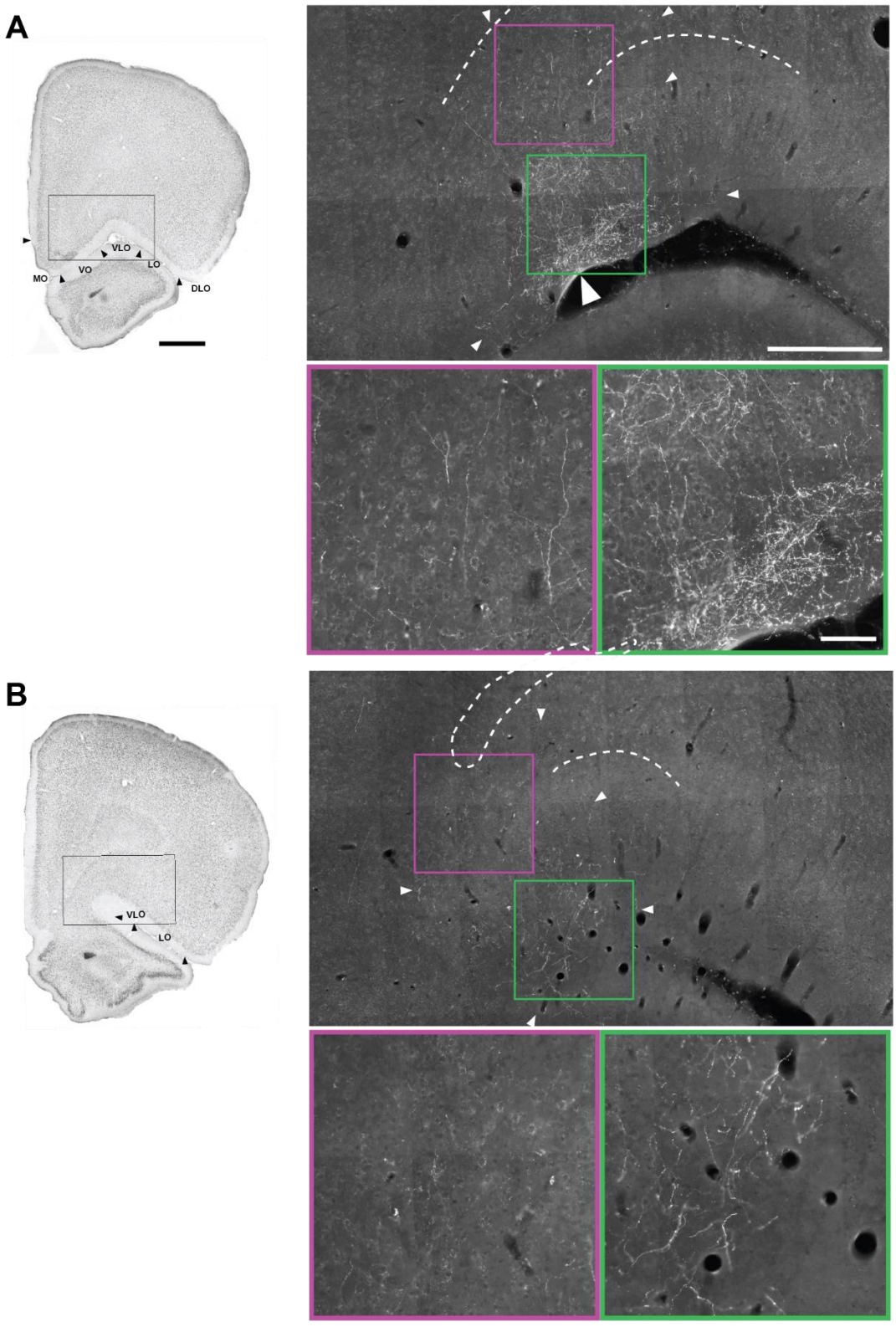

Figure 22. Labelling at one anterior (A) and one more posterior level of OFC (B) resulting from a PHA-L injection into V2M (14016P). The boxed areas to the left indicate the approximate size and position of the areas shown with higher magnification to the right. Pink and green boxes shows higher magnification of the labelling in the corresponding areas. Small arrows indicates the position of fibres. The dashed lines indicate the approximate border between superficial and deep layers and the contour of Cl. Scale bars 1000µm (left), 500µm (right), 100µm (pink, green). For abbreviations, see list of abbreviations.

One injection of BDA was made into anterior V2L covering mainly deep layers, having its core in layer V (Figure 23). Thalamic labelling was moderate in LD and strong in LPmr and LPl (Olsen and Witter, pers. com.). At anterior levels of OFC, sparse labelling was seen in superficial layers of medial to central VLO. At the level anterior to the merger of OFC with AOD, labelling in superficial layers was dense, while deep layers of VLO showed sparse labelling (Figure 24, A). Posteriorly, branching fibres were seen in layer I from extending from AOD around the notch of the anterior rhinal fissure, with a couple of short fibres labelled in medial LO (Figure 24, B). Strong labelling was also seen in Cl with a possible extension into medial to central portions of deep VLO. The pattern was similar to that resulting from the representative injection into PtP, except that in the V2L case, more labelling was seen in medial VLO.

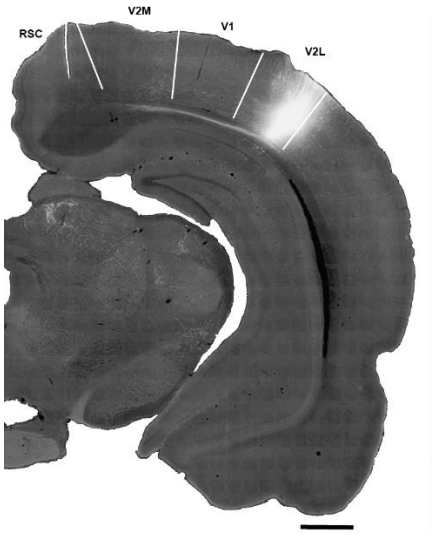

Figure 23. A BDA injection made into anterior V2L (20546B). The section is mirrored. Scale bar 1000µm. For abbreviations, see list of abbreviations.

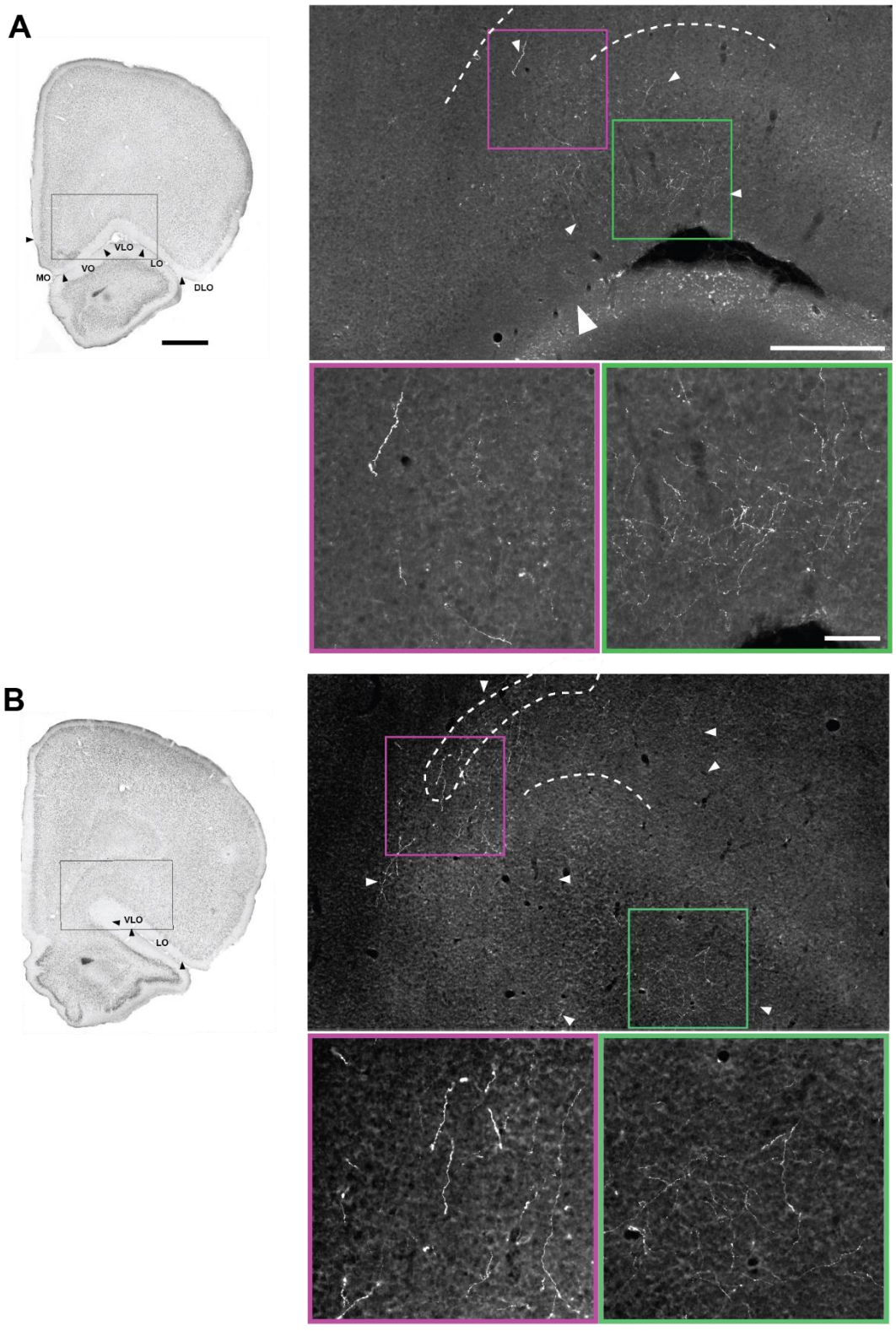

Figure 24. Labelling at one anterior (A) and one more posterior level of OFC (B) resulting from a BDA injection into V2L (20546B). The boxed areas to the left indicate the approximate size and position of the areas shown with higher magnification to the right. Pink and green boxes shows higher magnification of the labelling in the corresponding areas. Small arrows indicates the position of fibres. The dashed lines indicate the approximate border between superficial and deep layers and the contour of Cl. Scale bars 1000µm (left), 500µm (right), 100µm (pink, green). For abbreviations, see list of abbreviations.

3.9 Retrograde tracer injections into VLO and VO

In order to assess the distribution of PPC neurons projecting to OFC, I injected retrograde tracers into OFC. A representative injection was positioned at an intermediate anterior-posterior level, medially close to the border of VO, continuing ventrally into AOD (20461FB; Figure 10, E). The injection site was ellipsoid and extended over approximately 900µm anterior-posteriorly, 300-660µm mediolaterally and 540-1300µm in the dorsal-ventral axis. The injection site might have had a tiny Cl component (See Appendix E for Nissl stained section). Retrogradely labelled cells were mainly seen in layers V and VI of mPPC, lPPC and PtP (Figure 25). Some labelled cells were observed in superficial layers of mPPC and lPPC. The adjacent areas V2M and V2L had more, or approximately the same amount of labelled neurons as PPC, respectively. Only a few labelled cells were observed in S1.

The remaining retrograde tracer injections into more anterior levels of VO and VLO also showed labelling in layers V and VI of all subregions of PPC. Labelling was for three of the cases very sparse, while the last one had a higher density of labelled neurons (20545FB). Pictures of labelling for one section from each of the additional retrograde tracer injections are presented in Appendix F. Notably, only a couple or no cells were seen in S1 when the injections were positioned into anterior parts of OFC.

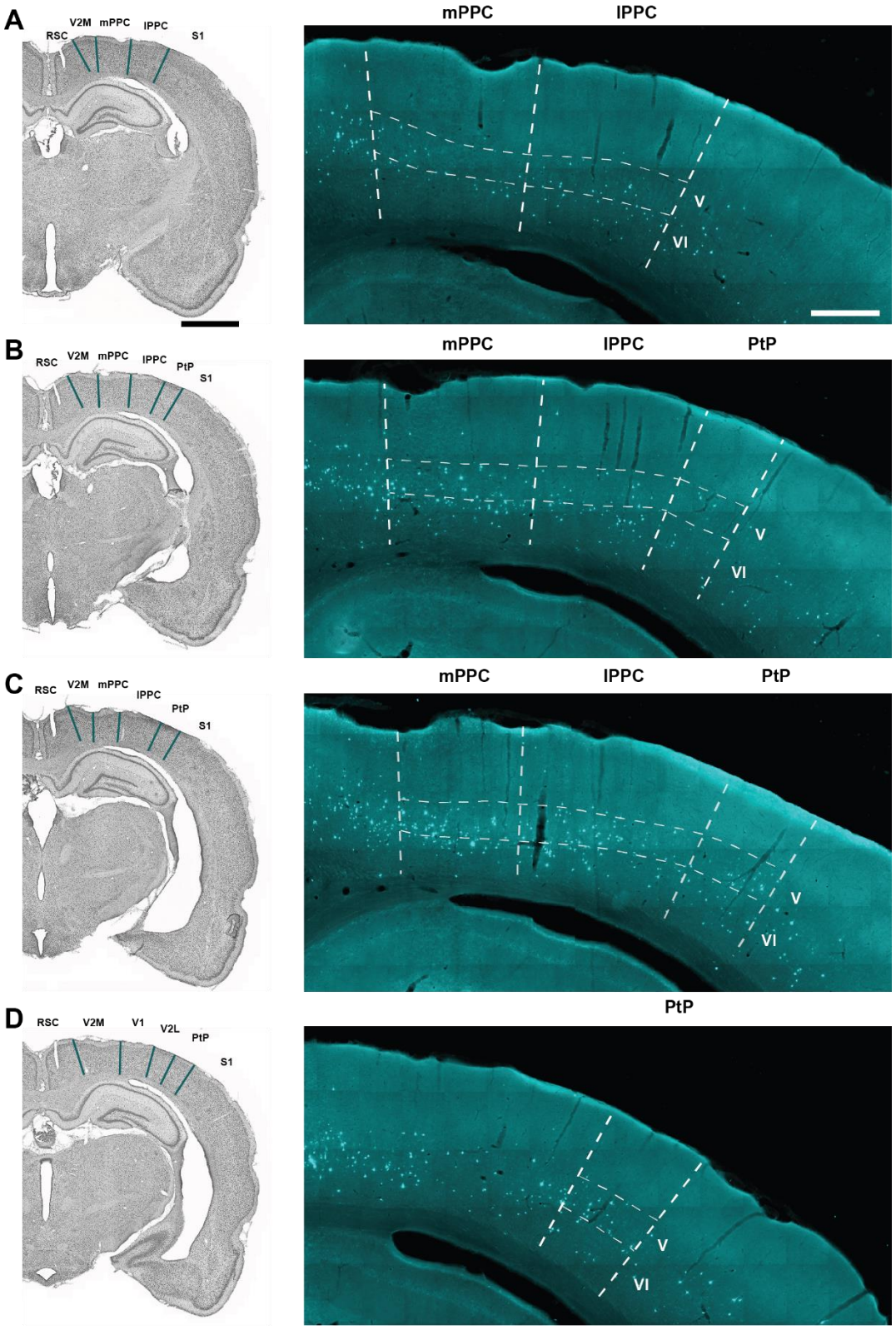

Figure 25. Retrograde labelling in PPC at four different anterior-posterior levels resulting from a FB injection into medial VLO (20461FB). Scale bars 2000µm (left) and 500µm (right). For abbreviations see list of abbreviations.

Chapter 4

Discussion

4.1 Summary of the main findings

This study aimed to describe the projections of three subregions of PPC, mPPC, lPPC and PtP to the five subregions of OFC, MO, VO, VLO, LO and DLO in the rat (Figure 26). My anterograde tracer data showed that the projections from PPC to OFC are not strong. This notion is supported by the retrograde tracer cases that showed overall low numbers of retrogradely labelled neurons in layers V and VI of PPC. The results further indicate that projections from PPC target exclusively MO, VO and VLO. I did not observe projections to LO nor to DLO. The projections showed a subtle topographical organisation within MO, VO and VLO, such that mPPC preferentially projects to lateral VO and medial VLO, with only a weak involvement of MO. Projections from lPPC reach medial VLO, while those originating in the most lateral part of PPC, PtP, reach central and lateral VLO.

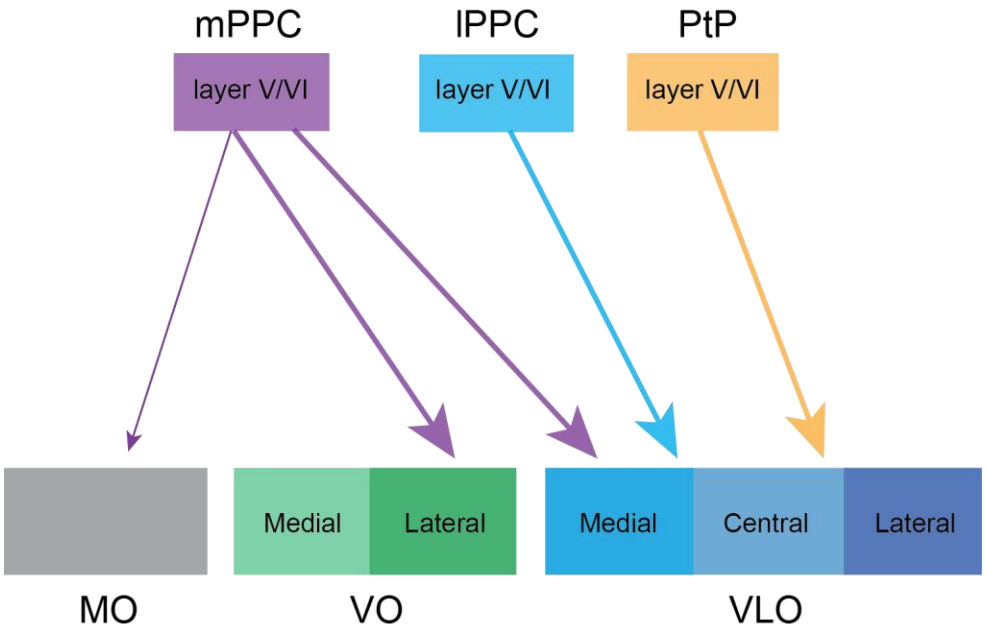

Figure 26. Summary of the projections from the different subregions of PPC to the subregions of OFC. Thickness of the arrows indicate the approximate strength of projections.

4.2 Methodological considerations

4.2.1 Tracers

In the present study, traditional neuroanatomical tracer techniques were used. 10 KD BDA is one of the most used and preferred anterograde tracers because it is reliable, efficient for combination with other tracing methods and it is easily visualised with a two-step histochemical staining procedure (Lanciego and Wouterlood, 2011). However, retrograde uptake of the tracer by cells that project to the area of injection may occur, and this could lead to 'indirect' anterograde labelling. In cases where retrogradely labelled cells were seen in superficial layers of adjacent areas next to the injection sites (V2M, V2L), no precaution was needed since retrograde tracer cases showed that superficial layers do not project to OFC. Retrogradely labelled cells that occurred in layers V and VI, on the other hand, were taken into account when analysing the cases by comparing the resulting labelling to cases without retrogradely labelled cells. Fortunately, retrograde labelling was only seen in a few cases and was minor compared to the injection site. Therefore, I am confident that it did not contribute to the anterograde labelling to any extent. Visualisation of the other anterograde tracer used, PHA-L, required more extensive immunohistochemical procedures, and in many cases the procedure resulted in high background DAB labelling, which in some cases could be overcome by analysing with higher magnification (30x). Staining different series from the same case using different visualisation methods (DAB versus fluorescent dyes) to reveal labelled fibres sometimes resulted in varying amounts of labelling. This could be a result of the incubation or blocking time, age of solution and incubation temperature. In all cases, labelling was seen in the same areas independent of visualisation method, although very sparse labelling seen in one series could be absent in another series from the same case. However, by comparing the anterograde labelling resulting from several injections for each subregions of PPC, each having a different injection size, tracer type and involved layers, I am confident that the labelling presented in the results is representative.

The retrograde tracers FB and FG were used in the present study to confirm the anterograde tracer results and yielded labelling in layers V and VI of all subregions of PPC. The injection sites of the retrograde tracers in OFC tended to be bigger than for anterograde tracer injections in PPC. However, the core of the retrograde tracer injections were mostly within VO and VLO and leakage of tracer did not seem to influence the retrograde labelling pattern to any extent; the labelling looked very similar for all cases and was in general weak. One disadvantage of retrograde tracers is possible uptake by passing fibres (Lanciego and Wouterlood, 2011). However, there are likely very few passing fibres through OFC that continue to the olfactory domains (olfactory bulb and anterior AOD), as supported by the present study. No labelled fibres were seen in these areas (not illustrated). In any case, projections from PPC to these areas would be a lot weaker or absent,

concluding that the labelled cells in layer V, and to a lesser degree layer VI of PPC project to OFC. Another disadvantage of retrograde tracers is that they are vulnerable to photo bleaching, but as described in the methods, precautions were taken to protect the sections from extensive exposure to light.

4.2.2 Control cases and retrograde tracer cases

I compared the projection patterns of PPC to those that originate from the directly adjacent areas, including S1, V1, V2M and V2L, in order to investigate if leakage of tracer into these regions could contribute to the anterograde labelling in OFC. In summary the results indicated that S1 and V1 do not project to OFC at all, while V2M and V2L project to the same subregions of OFC as PPC, however, there are laminar differences of the termination patterns.

In more detail, S1 borders medially with all three subregions of PPC at different anterior-posterior levels and can be subdivided into different areas processing information related to different body parts. Control injections were made into S1, more specifically into the trunk area and the barrel cortex (Paxinos and Watson, 2007). Injections into either of the two subregions of S1 did not result in any labelling in OFC, which is partially in agreement with Zakiewicz et al. (2014) who reported on the barrel part of S1. In contrast, Reep et al. (1996) reported labelling S1 (their Par1) after retrograde tracer injections in OFC. Notably, their Par1 comprises a very big part of cortex and is not directly comparable with delineations made in this study (Paxinos and Watson, 2007). Also, one may argue that leakage of tracer into Cl could be the explanation for retrograde labelling in S1 since the barrel cortex has been found to have weak projections to the anterior part of claustrum (Zakiewicz et al., 2014). This is supported by the present study, and may explain why case 20419B, which had a S1 component, had more extensive Cl labelling than the other injections into PtP. Zakiewicz et al. (2014) also described projections from PPC layers V and VI to Cl, which is supported by the present study. Leakage of tracer into Cl may also be the explanation for why retrogradely labelled cells where observed in S1 in the representative retrograde tracer case in the present study (20461FB; Figure 25). The other retrograde tracer cases were situated more anteriorly, where Cl is not present, and did not show any or only a few labelled cells in S1. The involvement of Cl might also explain why this injection (20461FB) resulted in stronger labelling than that in the other cases. However, the overall labelling pattern was similar even when considering this possibility. Involvement of AOD in some of the injection sites of retrograde tracers, situated in anterior sections of OFC, did likely not contribute to retrograde labelling in PPC since no anterograde tracer injections into PPC yielded labelling in AOD in anterior sections.

Two other adjacent areas of PPC are V2M, which borders mPPC, and V2L that borders PtP. The results of the control cases with anterograde tracer injections into V2M indicated the presence of substantial projections to central-lateral VO and medial VLO, in addition to sparse projections to

MO. The single injection into V2L also showed projections to OFC, specifically VO and VLO. Connections between V2 and OFC have previously been reported (Vogt and Miller, 1983; Miller and Vogt, 1984; Reep et al., 1994; Reep et al., 1996). However, the laminar distribution was not considered in these studies and, as mentioned before, the delineations were different from the present study. Although V2M and V2L project to OFC, cases that had a small involvement of either of the areas did not show any prominent difference in projection pattern to OFC when comparing them to injections confined to PPC.

AuD is another neighbouring area of PtP, which was not included in the control injections in this study. The reason for this is that no injections were directly available for analysis and also that only one of the injections into PtP was close to AuD (20219B). The representative retrograde tracer case showed some labelled cells in deep layers of AuD, in line with a previous report (Reep et al., 1996). However, the latter study reported that retrograde labelling in auditory areas was inconsistent among cases with injections into OFC (Reep et al., 1996), which is in line with my results. Another study injected PHA-L into auditory areas (Te1, Te2, Te3) and found labelling in deep portions of VLO (Mascagni et al., 1993). However, no illustrations of the labelling was shown in the article, making it impossible to asses which part of OFC they were describing. In conclusion, possible leakage of tracer into AuD did not contribute to the PPC projection pattern to OFC to any extent.

4.2.3 Data analysis

When making the figures for the representative anterograde tracer cases, too much background staining made it impossible to show pictures directly. Therefore, DAB or fluorescent stained series were overlaid with Nissl stained series and fibres were drawn onto the Nissl-images to better visualise the distribution of fibres. Since two different series were used, they did not overlap perfectly, which might have resulted in some small differences from the 'real' labelling. However, the series were often adjacent (e.g. series one and two) and much effort was put into overlaying the images as precisely as possible. The figures show the distribution and density of labelling in the representative case. However, the amount of labelling varied between cases that may be due to the type of tracer, volume of tracer injected, which layers the injection covered, and how good the uptake and transport of the tracer were (Lanciego and Wouterlood, 2011). Important to mention is that the projections from PPC to OFC are generally not strong, which means that 'strong labelling' described in the results of this study is relative to this study and is not comparable to other studies.

4.3 Discussion of the main findings

4.3.1 Connectivity of PPC with OFC

The present study showed that mPPC projects to MO, VO and VLO, while lPPC and PtP project to VLO. Reciprocal connections between PPC and VLO have been reported by Chandler et al. (1992), however, they did not consider the other regions of OFC in their study. Reep et al. (1994) and Reep et al. (1996) injected retrograde tracers into the subregions of PPC and OFC, respectively. The two studies taken together showed that PPC has reciprocal cortical connections with areas corresponding to MO, VO and VLO in the present study. The results from the present study are in line with these previously published results and provide additional details in that only mPPC projects to MO, and these projections are sparser than to VO and VLO. It is of interest to note that the projections from MO and VO apparently show a similar preference, that is, the projections to PPC originating in MO are sparser than those originating in VO (Hoover and Vertes, 2011). I did not observe projections originating from different parts of mPPC having different terminal patterns in OFC. In line with this, even though head-directional cells only have been observed for cells in the anterior part of mPPC (Chen et al., 1994), two other recording studies did not see any functional topography within mPPC (Nitz, 2012; Whitlock et al., 2012). Further, I did not observe projections from PPC to LO or DLO, which is in agreement with previous studies (Chandler et al., 1992; Reep et al., 1996).

The observation that projections from PPC to OCF arise mainly from neurons in layers V and VI, and that OFC projections from V2M originate in the same layers, is in line with what was reported by Reep et al. (1996). Noteworthy, neither of the last three papers discussed above distinguished between the different subregions of PPC. In addition, when observing their delineations, parts of what they call PPC are considered V2M in the present study. Difficulties in distinguishing V2M from PPC based on cytoarchitecture was reported by the authors themselves. Reep et al. (1994) also pointed out that no effort was made to distinguish VO from MO and VLO, which implies that their projections to MO and VLO also include VO, as discussed above.

The present study showed that PPC projections have a subtle topographical pattern within MO, VO and VLO. That is, mPPC projects to lateral VO and medial VLO, lPPC projects to medial VLO, while PtP projects to central to lateral VLO. A comparable medial-to-lateral topographical organisation of projections have been reported for projections from mPPC and lPPC to the dorsocentral striatum, that is, mPPC projects to more medial parts than lPPC does (Reep et al., 2003). A similar topographic relationship has also been observed for projections from OFC to the striatum (Berendse et al., 1992; Reep and Corwin, 2009). Particularly, projections originating in

medial to lateral parts of OFC showed a (dorso)medial to ventro(lateral) gradient within the dorsocentral striatum.

The delineation of PPC has varied among studies, in which the border between PPC and V2 has been particularly unclear. Based on a proposed functional similarity between V2M and PPC in the rat (Wilber et al., 2014), a recent tracer study considered V2M together with PPC as one region defined 'parietal cortex' (Wilber et al., 2015). However, the results of the present study supports the division between PPC and V2M because of differences in projection pattern with OFC. PPC and V2M project to the same subregions of OFC, however, they target different layers. In particular, mPPC, which borders V2M, projects more strongly to deeper layers of VLO and Cl than V2M, which preferentially targets superficial layers. Therefore, the present study shows that it is useful to distinguish V2M and PPC based on anterograde projection patterns, which is also supported by distinct projections to the thalamus (Figure 3; Olsen and Witter, pers. com.). The distinction is further supported by the retrograde tracer cases in the present study, which showed that there were clearly more OFC-projecting cells in V2M than in PPC, supporting the cytoarchitectonical border (see Appendix F). Whether V2M and PPC are similar in terms of function in the rat is yet to be discovered.

4.3.2 The orbital and medial prefrontal networks

OFC and mPFC have been divided into two functional networks called the medial prefrontal and orbital networks, which are considered to process visceromotor and multisensory information, respectively. In the rat, the medial network consists of PL, IL, ACCv/d and AId and DLO, while the orbital network consists of AIv, VLO and LO (Price, 2007). MO and VO were regarded to function in both networks by the latter author, however, Hoover and Vertes (2011) proposed them to function predominately in the medial network based on their results that showed strong connections with the limbic system. Irrespective of which definition one follows, the projections from PPC to OFC described in the present study lead to the conclusion that lPPC and PtP would function in the orbital network, while mPPC would be more strongly, though not exclusively, connected with the medial network. There are some questionable aspects of the Price (2007) article. When it comes to the networks in the rat, drawing the conclusion that there are two networks based on connections with only the hypothalamus and PAG might be a bit simplified. To further complicate matters, Price (2007) did not report the results from Floyd et al. (2001) correctly. In fact, the latter authors did not examine connections of the orbital network with hypothalamus, as is claimed by Price (2007). Further, in Floyd et al. (2000), the medial part of VLO is included in the medial network based on connections with PAG. The latter would make more sense regarding mPPC projections that also involve medial parts of VLO in addition to MO and VO. However, lPPC would be connected to both networks and PtP to the orbital network. To conclude,

if there are two functionally distinct networks in the prefrontal cortex, PPC is connectionally related to both by way of its projections to OFC.

4.4 Functional implications

PPC and OFC are both association cortices, indicating that their functions are likely complex. Functional studies on PPC in rats have mainly focused on spatial navigation, including goal-directed action (McNaughton et al., 1994; Nitz, 2006; Whitlock et al., 2012), while OFC has been implicated in many cognitive functions such as behavioural flexibility and value-based decision-making (Rolls, 2000; Wallis, 2012). Functional interpretations are strongly dependent on the context in which both OFC and PPC are analysed. Common to both areas are the observations that lesions result in contralateral neglect, a deficit in directing attention in the hemifield contralateral to the lesion (Husain, 2008). For this reason, they are thought to be involved in directed attention, that is a voluntary allocation of attention to a spatial location relevant for a specific task (Prinzmetal et al., 2009). Additionally, both areas are thought to be involved in goal-directed behaviour, which can be described as when a subject 'desires the goal and believes that the behaviour in question will achieve the goal' (de Wit and Dickinson, 2009). Therefore, connections between PPC and OFC will be discussed further in relation to their possible involvement in directed attention and goal-directed behaviour including spatial navigation.

4.4.1 Directed attention

In humans, the inferior parietal lobule, cingulate cortex and the frontal eye fields have been suggested to constitute a network mediating directed attention because lesions to the areas involved typically lead to a dysfunctional state, contralateral neglect (Mesulam, 1999). A similar cortical network in rodents was first thought to be formed by reciprocal connections between PPC, VLO and M2 (Chandler et al., 1992). The hypothesis is based on findings that lesions to either of PPC, VLO or M2, or the connections between PPC and M2, produce severe neglect of auditory, visual and tactile stimulation in rats similar to human neglect (King et al., 1989; Chandler et al., 1992; Burcham et al., 1997). Recently, other areas have been implemented in the circuit including LPmr nucleus of the thalamus and the dorsocentral striatum (Cheatwood et al., 2003; Reep et al., 2003; Kamishina et al., 2009). Projections from PPC, VLO and M2 have been shown to converge in the dorsocentral striatum (Reep et al., 2003). Adding VLO to the directed attention illustration of Kamishina et al. (2009) would therefore yield a more complete picture of the circuitry implicated in directed attention (Figure 27). The results from the present study showed that all subregions of PPC project to VLO, suggesting that all subregions may be involved in directed attention.

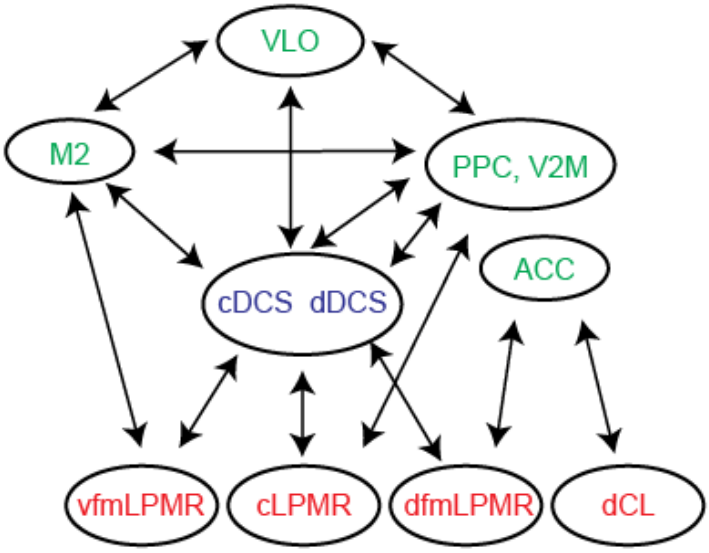

Figure 27. A proposed circuit for directed attention in the rat. Connections with VLO have been added to the circuit. Areas in purple: central and dorsal part of the dorsocentral striatum (DCS). Areas in red: specific parts of the mediorostral lateral posterior (LPMR) and the central lateral (CL) nuclei of the thalamus. For other abbreviations, see list of abbreviations. Modified from Kamishina et al. (2009).

4.4.2 Spatial navigation and goal-directed behaviour

Both PPC and OFC have been implicated in goal-directed action. Goal-directed action requires that one is able to navigate in the environment and involve approach, orientation and other locomotion behaviour to reach a specific goal, actions often referred to as 'spatial navigation' (Feierstein et al., 2006). VLO is anatomically situated in a network that processes spatiomotor information together with M2 and PPC. Functionally, this has been illustrated by lesion studies. Bilateral lesions of areas of OFC described in the present study as VO and VLO, resulted in deficits in an allocentric 'cheese board task' but not in the egocentric 'adjacent arm maze task' (Corwin et al., 1994). Lesions to LO, on the other hand, did not result in impairments in the same tasks, indicating that the subregions of OFC are functionally different. Similarly to lesions to VO and VLO, bilateral lesions to PPC resulted in severe deficits in the same allocentric task (King and Corwin, 1992), as well as egocentric tasks (Kolb et al., 1983; Rogers and Kesner, 2006). PPC is involved in movement planning, as it encodes two-part movement motifs like straight running followed by a right turn (McNaughton et al., 1994) and it tracks progress of the movement along routes (Nitz, 2006). A recent study by Whitlock et al. (2012) reported that PPC neurons showed tuning to movements 250 ms in advance, and that tuning of neurons was different according to whether the states happened during structured, goal-directed movement sequences or random foraging. Similar indications of involvement in movement planning have been shown in humans where stimulation of PPC triggered a strong intention and desire to move (Desmurget et al., 2009). The hippocampal-parahippocampal region has proved important in spatial processing; creating an allocentric

cognitive map of the environment (O'Keefe and Dostrovsky, 1971; Fyhn et al., 2004; Hafting et al., 2005). However, in order to navigate in space, the animal must convert these allocentric coordinates into egocentric coordinates necessary for route planning. PPC has been proposed to be an essential node for this translation and has, with its connections with the motor cortices, a suitable anatomical position for guiding execution of movement (Whitlock et al., 2008). Direct connections between MEC and PPC are, however, very weak. The prefrontal cortex (including OFC), together with RSC and POR, have been suggested to be alternative connectional pathways between MEC and PPC (Whitlock et al., 2008). Kondo and Witter (2014) showed that projections of OFC with MEC, PrS and POR arise mainly from VO and this is likely a reciprocal pathway (Delatour and Witter, 2002; Agster and Burwell, 2009). The results from Kondo and Witter (2014) thus strongly supports VO's involvement in spatial processing. As presented in the present study, PPC projects to MO, VO and VLO, and these connections have also been proven to be reciprocal with return projections arising from layers II and III of OFC (Sakshaug, 2015). The latter study also corroborates that connections between MO and PPC are very weak and only with mPPC.

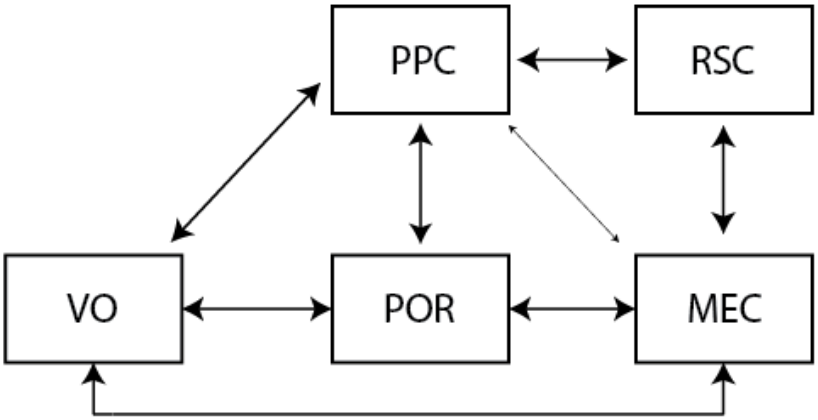

Figure 28. Schematic representation of the relevant connections between PPC and MEC via VO, RSC and POR. The illustration is based on Kondo and Witter (2014), Burwell and Amaral (1998), Agster and Burwell (2009), Sakshaug (2015) and the present study. Sakshaug (2015) and the present study showed that connections between VO and PPC are mainly with mPPC. For abbreviations, see list of abbreviations.

As previously mentioned, OFC is thought to be involved in value-based decision-making, choosing the goal that gives the best reward, and it has further been proposed that OFC monitors goal-directed choices rather than executing them (Feierstein et al., 2006). By use of a two-alternative choice discrimination task with odour, the latter authors showed that OFC not only assigns the economic value of the options, but also encodes the spatiomotor variables necessary to obtain them. Reciprocal connections between OFC and PPC could be a possible link in the circuit for goal-directed behaviour, in which OFC decides on the most suitable goal and signals it to PPC, which in turn has strong connections with the motor cortices for guiding and execution of movements (Whitlock et al., 2008). Taken together, it is likely that the reciprocal connections between VO/VLO and PPC are involved in goal-directed behaviour.

The projections from layers V and VI of PPC to superficial and deep layers of OFC, found in the present study, may be considered as feedback projections according to 'the classic view' (Kandel et al., 2012: p. 348)[1], contributing a copy of PPC signals as input to OFC. Processed spatial information could be sent back to the hippocampal-parahippocampal region via VO where it is integrated and used to update position information on the cognitive map (Chen et al., 1994; McNaughton et al., 1994; Goodrich-Hunsaker et al., 2005). Since PPC is also involved in decision-making regarding movement planning, it is possible that PPC projections to OFC contribute to modulation of the decision-making in OFC and influence how rewarding different choices are.

4.5 Future directions

The results presented in this study as well as the thalamic projection pattern of PPC (Olsen and Witter, pers. com.) indicate that there are functional differences between the subregions of PPC. This has been shown in primates where different parts of PPC have been suggested to be involved in different functions, such as control of eye-movements and planning of reaching (Andersen and Cui, 2009). However, recording studies in PPC have been confined to mPPC (Chen et al., 1994; Nitz, 2006; Nitz, 2012; Whitlock et al., 2012) and lesion studies specific to the subregions of PPC are lacking (Kolb and Walkey, 1987; DiMattia and Kesner, 1988; Save and Moghaddam, 1996; Save and Poucet, 2000). More research is needed in order to derive valid conclusions about the functional differentiation in the rat PPC and how this might compare to that in primates.

One way to study the functional aspects of the connections of PPC with OFC would be to do dual recordings during a task to see if they are active in the same part of a given task, or if one is activated before the other. Another option could be to optogenetically inhibit one of the areas and record from the other. This would allow to see if changes in neuronal responses occur that could be correlated to changes in behaviour.

[1] In the 'classic view', feedforward projections originate in superficial layers (II and III) and terminate in layer IV, while feedback projections originate in deep layers (V and VI) and terminate in layers I, II and VI (Kandel et al., 2012: p. 348). This was establish in the primate visual cortex, and lateral projections have also been described in higher order visual areas as projections originating in agranular layers terminating in all layers (David et al., 2005). According to the latter statement, the PPC-OFC projections could also be considered lateral projections, since both PPC and OFC are high up in the hierarchy. However, since the concept of hierarchical organisation of projections have been based on studies of the primate visual cortex, it is not directly comparable to the rat and other cortical areas. Therefore, it will not be further discussed in this thesis.

Chapter 5

Conclusion

The aim of this thesis was to investigate the projections of the three subregions of PPC to the subregions of OFC. The projections from PPC to OFC are not strong and arise from neurons in layers V and VI. The projections from PPC target only MO, VO and VLO, avoiding LO and DLO. More specifically, the projections to OFC show a subtle topographical pattern within MO, VO and VLO, in which mPPC projects to MO, VO and medial VLO with a preference for the latter two. lPPC projects to medial VLO, while PtP projects to central to lateral VLO. Based on previous functional studies, one may suggest that the projections form part of cortico-cortical networks involved in spatial processing and directed attention, yet, the definitive functions remain to be discovered.

Bibliography

Agster K. L. and Burwell R. D. (2009) Cortical efferents of the perirhinal, postrhinal, and entorhinal cortices of the rat. *Hippocampus* 19: 1159-1186.

Andersen R. A. and Cui H. (2009) Intention, Action Planning, and Decision Making in Parietal-Frontal Circuits. *Neuron* 63: 568-583.

Berendse H. W., Graaf Y. G.-D. and Groenewegen H. J. (1992) Topographical organization and relationship with ventral striatal compartments of prefrontal corticostriatal projections in the rat. *The journal of comparative neurology* 316: 314-347.

Boulougouris V., Dalley J. W. and Robbins T. W. (2007) Effects of orbitofrontal, infralimbic and prelimbic cortical lesions on serial spatial reversal learning in the rat. *Behavioural brain research* 179: 219-228.

Brodmann K. (1909) *Vergleichende Lokalisationslehre der Grosshirnrinde,* Leipzig: Barth.

Broussard J., Sarter M. and Givens B. (2006) Neuronal correlates of signal detection in the posterior parietal cortex of rats performing a sustained attention task. *Neuroscience* 143: 407-417.

Brunton B. W., Botvinick M. M. and Brody C. D. (2013) Rats and Humans Can Optimally Accumulate Evidence for Decision-Making. *Science (New York, N.Y.)* 340: 95-98.

Burcham K. J., Corwin J. V., Stoll M. L., et al. (1997) Disconnection of medial agranular and posterior parietal cortex produces multimodal neglect in rats. *Behavioural brain research* 86: 41-47.

Burwell R. D. and Amaral D. G. (1998) Cortical afferents of the perirhinal, postrhinal, and entorhinal cortices of the rat. *The journal of comparative neurology* 398: 179-205.

Cappe C., Morel A. and Rouiller E. M. (2007) Thalamocortical and the dual pattern of corticothalamic projections of the posterior parietal cortex in macaque monkeys. *Neuroscience* 146: 1371-1387.

Carter M. and Shieh J. C. (2010) Chapter 3 - Stereotaxic Surgeries and In Vivo Techniques. In: Shieh MCC (ed) *Guide to research techniques in neuroscience.* New York: Academic Press, 73-90.

Cavada C. and Goldman-Rakic P. S. (1989) Posterior parietal cortex in rhesus monkey: II. Evidence for segregated corticocortical networks linking sensory and limbic areas with the frontal lobe. *The journal of comparative neurology* 287: 422-445.

Chandler H. C., King V., Corwin J. V., et al. (1992) Thalamocortical connections of rat posterior parietal cortex. *Neuroscience letters* 143: 237-242.

Cheatwood J. L., Reep R. L. and Corwin J. V. (2003) The associative striatum: cortical and thalamic projections to the dorsocentral striatum in rats. *Brain research* 968: 1-14.

Chen L. L., Lin L. H., Green E. J., et al. (1994) Head-direction cells in the rat posterior cortex. I. Anatomical distribution and behavioral modulation. *Experimental brain research* 101: 8-23.

Conte W. L., Kamishina H., Corwin J. V., et al. (2008) Topography in the projections of lateral posterior thalamus with cingulate and medial agranular cortex in relation to circuitry for directed attention and neglect. *Brain research* 1240: 87-95.

Corwin J. V., Fussinger M., Meyer R. C., et al. (1994) Bilateral destruction of the ventrolateral orbital cortex produces allocentric but not egocentric spatial deficits in rats. *Behavioural brain research* 61: 79-86.

David O., Harrison L. and Friston K. J. (2005) Modelling event-related responses in the brain. *NeuroImage* 25: 756-770.

De Wit S. and Dickinson A. (2009) Associative theories of goal-directed behaviour: a case for animal–human translational models. *Psychological Research* 73: 463-476.

Delatour B. and Witter M. P. (2002) Projections from the parahippocampal region to the prefrontal cortex in the rat: evidence of multiple pathways. *The european journal of neuroscience* 15: 1400-1407.

Desmurget M., Reilly K. T., Richard N., et al. (2009) Movement intention after parietal cortex stimulation in humans. *Science (New York, N.Y.)* 324: 811-813.

Dimattia B. V. and Kesner R. P. (1988) Spatial cognitive maps: Differential role of parietal cortex and hippocampal formation. *Behavioral neuroscience* 102: 471-480.
Erlich J. C., Bialek M. and Brody C. D. (2011) A Cortical Substrate for Memory-Guided Orienting in the Rat. *Neuron* 72: 330-343.
Feierstein C. E., Quirk M. C., Uchida N., et al. (2006) Representation of spatial goals in rat orbitofrontal cortex. *Neuron* 51: 495-507.
Floyd N. S., Price J. L., Ferry A. T., et al. (2000) Orbitomedial prefrontal cortical projections to distinct longitudinal columns of the periaqueductal gray in the rat. *The journal of comparative neurology* 422: 556-578.
Floyd N. S., Price J. L., Ferry A. T., et al. (2001) Orbitomedial prefrontal cortical projections to hypothalamus in the rat. *The journal of comparative neurology* 432: 307-328.
Fyhn M., Molden S., Witter M. P., et al. (2004) Spatial Representation in the Entorhinal Cortex. *Science (New York, N.Y.)* 305: 1258-1264.
Giannetti S. and Molinari M. (2002) Cerebellar input to the posterior parietal cortex in the rat. *Brain research bulletin* 58: 481-489.
Goodrich-Hunsaker N. J., Hunsaker M. R. and Kesner R. P. (2005) Dissociating the role of the parietal cortex and dorsal hippocampus for spatial information processing. *Behavioral neuroscience* 119: 1307-1315.
Hafting T., Fyhn M., Molden S., et al. (2005) Microstructure of a spatial map in the entorhinal cortex. *Nature* 436: 801-806.
Harvey C. D., Coen P. and Tank D. W. (2012) Choice-specific sequences in parietal cortex during a virtual-navigation decision task. *Nature* 484: 62-68.
Hoover W. B. and Vertes R. P. (2011) Projections of the medial orbital and ventral orbital cortex in the rat. *The journal of comparative neurology* 519: 3766-3801.
Husain M. (2008) Hemineglect. *Scholarpedia* 3.
Kamishina H., Conte W. L., Patel S. S., et al. (2009) Cortical connections of the rat lateral posterior thalamic nucleus. *Brain research* 1264: 39-56.
Kandel E. R., Schwartz J. H., Jessel T. M., et al. (2012) *Principles of Neural Science*. 5th ed. New York: The McGraw-Hills Companies, Inc.
King V., Corwin J. V. and Reep R. L. (1989) Production and characterization of neglect in rats with unilateral lesions of ventrolateral orbital cortex. *Experimental neurology* 105: 287-299.
King V. R. and Corwin J. V. (1992) Spatial deficits and hemispheric asymmetries in the rat following unilateral and bilateral lesions of posterior parietal or medial agranular cortex. *Behavioural brain research* 50: 53-68.
Kolb B., Sutherland R. J. and Whishaw I. Q. (1983) A comparison of the contributions of the frontal and parietal association cortex to spatial localization in rats. *Behavioral neuroscience* 97: 13-27.
Kolb B. and Walkey J. (1987) Behavioural and anatomical studies of the posterior parietal cortex in the rat. *Behavioural brain research* 23: 127-145.
Kondo H. and Witter M. P. (2014) Topographic organization of orbitofrontal projections to the parahippocampal region in rats. *The journal of comparative neurology* 522: 772-793.
Krettek J. E. and Price J. L. (1977) The cortical projections of the mediodorsal nucleus and adjacent thalamic nuclei in the rat. *The journal of comparative neurology* 171: 157-191.
Krieg W. J. (1946) Cortical areas of the albino rat. *Archives of neurology and psychiatry* 56: 739.
Lanciego J. L. and Wouterlood F. G. (2011) A half century of experimental neuroanatomical tracing. *Journal of chemical neuroanatomy* 42: 157-183.
Linley S. B., Hoover W. B. and Vertes R. P. (2013) Pattern of distribution of serotonergic fibers to the orbitomedial and insular cortex in the rat. *Journal of chemical neuroanatomy* 48-49: 29-45.
Mascagni F., McDonald A. J. and Coleman J. R. (1993) Corticoamygdaloid and corticocortical projections of the rat temporal cortex: A *phaseolus vulgaris* leucoagglutinin study. *Neuroscience* 57: 697-715.

McNaughton B. L., Mizumori S. J., Barnes C. A., et al. (1994) Cortical representation of motion during unrestrained spatial navigation in the rat. *Cerebral cortex (New York, N.Y. : 1991)* 4: 27-39.

Mesulam M. M. (1999) Spatial attention and neglect: parietal, frontal and cingulate contributions to the mental representation and attentional targeting of salient extrapersonal events. *Philosophical transactions of the royal society B: Biological sciences* 354: 1325-1346.

Miller M. W. and Vogt B. A. (1984) Direct connections of rat visual cortex with sensory, motor, and association cortices. *The journal of comparative neurology* 226: 184-202.

Nitz D. A. (2006) Tracking route progression in the posterior parietal cortex. *Neuron* 49: 747-756.

Nitz D. A. (2012) Spaces within spaces: rat parietal cortex neurons register position across three reference frames. *Nature neuroscience* 15: 1365-1367.

O'Keefe J. and Dostrovsky J. (1971) The hippocampus as a spatial map. Preliminary evidence from unit activity in the freely-moving rat. *Brain research* 34: 171-175.

Ostlund S. B. and Balleine B. W. (2007) The contribution of orbitofrontal cortex to action selection. *Annals of the New York Academy of Sciences* 1121: 174-192.

Palomero-Gallagher N. and Zilles K. (2004) Isocortex. The Rat Nervious System, ed Paxinos G. 3 ed.: Elsevire, 729-757.

Paxinos G. and Watson C. (2007) *The rat brain in stereotaxic coordinates*: Elsevier/Academic press.

Price J. L. (2007) Definition of the Orbital Cortex in Relation to Specific Connections with Limbic and Visceral Structures and Other Cortical Regions. *Annals of the New York Academy of Sciences* 1121: 54-71.

Prinzmetal W., Zvinyatskovskiy A., Gutierrez P., et al. (2009) Voluntary and involuntary attention have different consequences: The effect of perceptual difficulty. *The quarterly journal of experimental psychology* 62: 352-369.

Raposo D., Sheppard J. P., Schrater P. R., et al. (2012) Multisensory decision-making in rats and humans. *The journal of neuroscience* 32: 3726-3735.

Ray J. P. and Price J. L. (1992) The organization of the thalamocortical connections of the mediodorsal thalamic nucleus in the rat, related to the ventral forebrain-prefrontal cortex topography. *The journal of comparative neurology* 323: 167-197.

Reep R. L., Chandler H. C., King V., et al. (1994) Rat posterior parietal cortex: topography of corticocortical and thalamic connections. *Experimental brain research* 100: 67-84.

Reep R. L., Cheatwood J. L. and Corwin J. V. (2003) The associative striatum: organization of cortical projections to the dorsocentral striatum in rats. *The journal of comparative neurology* 467: 271-292.

Reep R. L. and Corwin J. V. (2009) Posterior parietal cortex as part of a neural network for directed attention in rats. *Neurobiology of learning and memory* 91: 104-113.

Reep R. L., Corwin J. V. and King V. (1996) Neuronal connections of orbital cortex in rats: topography of cortical and thalamic afferents. *Experimental brain research* 111: 215-232.

Reep R. L., Goodwin G. S. and Corwin J. V. (1990) Topographic organization in the corticocortical connections of medial agranular cortex in rats. *The journal of comparative neurology* 294: 262-280.

Rogers J. L. and Kesner R. P. (2006) Lesions of the dorsal hippocampus or parietal cortex differentially affect spatial information processing. *Behavioral neuroscience* 120: 852-860.

Rolls E. T. (2000) The orbitofrontal cortex and reward. *Cerebral cortex (New York, N.Y. : 1991)* 10: 284-294.

Rose J. E. and Woolsey C. N. (1948) The orbitofrontal cortex and its connections with the mediodorsal nucleus in rabbit, sheep and cat. *Research publications - Association for Research in Nervous and Mental Disease* 27 (1 vol.): 210-232.

Sakshaug T. (2015) Projections of the Orbitofrontal Cortex to the Parietal Cortex in the Rat. *Department of Neuroscience.* The Norwegian University of Science and Technology (NTNU).

Save E. and Moghaddam M. (1996) Effects of lesions of the associative parietal cortex on the acquisition and use of spatial memory in egocentric and allocentric navigation tasks in the rat. *Behavioral neuroscience* 110: 74-85.

Save E. and Poucet B. (2000) Involvement of the hippocampus and associative parietal cortex in the use of proximal and distal landmarks for navigation. *Behavioural brain research* 109: 195-206.
Save E. and Poucet B. (2009) Role of the parietal cortex in long-term representation of spatial information in the rat. *Neurobiology of learning and memory* 91: 172-178.
Schoenbaum G., Chiba A. A. and Gallagher M. (1998) Orbitofrontal cortex and basolateral amygdala encode expected outcomes during learning. *Nature neuroscience* 1: 155-159.
Schoenbaum G., Nugent S. L., Saddoris M. P., et al. (2002) Orbitofrontal lesions in rats impair reversal but not acquisition of go, no-go odor discriminations. *Neuroreport* 13: 885-890.
Schoenbaum G., Saddoris M. P. and Stalnaker T. A. (2007) Reconciling the Roles of Orbitofrontal Cortex in Reversal Learning and the Encoding of Outcome Expectancies. *Annals of the New York Academy of Sciences* 1121: 320-335.
Schoenbaum G., Setlow B., Nugent S. L., et al. (2003) Lesions of orbitofrontal cortex and basolateral amygdala complex disrupt acquisition of odor-guided discriminations and reversals. *Learning & memory (Cold Spring Harbor, N.Y.)* 10: 129-140.
Shaner N. C., Steinbach P. A. and Tsien R. Y. (2005) A guide to choosing fluorescent proteins. *Nature methods* 2: 905-909.
Smith P. F., Horii A., Russell N., et al. (2005) The effects of vestibular lesions on hippocampal function in rats. *Progress in neurobiology* 75: 391-405.
Stalnaker T. A., Cooch N. K. and Schoenbaum G. (2015) What the orbitofrontal cortex does not do. *Nature neuroscience* 18: 620-627.
Thivierge J.-P. and Marcus G. F. (2007) The topographic brain: from neural connectivity to cognition. *Trends in neurosciences* 30: 251-259.
Van De Werd H. J., Rajkowska G., Evers P., et al. (2010) Cytoarchitectonic and chemoarchitectonic characterization of the prefrontal cortical areas in the mouse. *Brain structure & function* 214: 339-353.
Van De Werd H. J. and Uylings H. B. (2008) The rat orbital and agranular insular prefrontal cortical areas: a cytoarchitectonic and chemoarchitectonic study. *Brain structure & function* 212: 387-401.
Vogt B. A. and Miller M. W. (1983) Cortical connections between rat cingulate cortex and visual, motor, and postsubicular cortices. *The journal of comparative neurology* 216: 192-210.
Walker A. E. (1940) A cytoarchitectural study of the prefrontal area of the macaque monkey. *The journal of comparative neurology* 73: 59-86.
Wallis J. D. (2012) Cross-species studies of orbitofrontal cortex and value-based decision-making. *Nature neuroscience* 15: 13-19.
Whitlock J. R. (2014) Navigating actions through the rodent parietal cortex. *Frontiers in human neuroscience* 8: 293.
Whitlock J. R., Pfuhl G., Dagslott N., et al. (2012) Functional split between parietal and entorhinal cortices in the rat. *Neuron* 73: 789-802.
Whitlock J. R., Sutherland R. J., Witter M. P., et al. (2008) Navigating from hippocampus to parietal cortex. *Proceedings of the National Academy of Sciences of the United States of America* 105: 14755-14762.
Wilber A., Clark B. J., Demecha A. J., et al. (2015) Cortical Connectivity Maps Reveal Anatomically Distinct Areas in the Parietal Cortex of the Rat. *Frontiers in neural circuits* 8.
Wilber A. A., Clark B. J., Forster T. C., et al. (2014) Interaction of egocentric and world-centered reference frames in the rat posterior parietal cortex. *The journal of neuroscience* 34: 5431-5446.
Zakiewicz I. M., Bjaalie J. G. and Leergaard T. B. (2014) Brain-wide map of efferent projections from rat barrel cortex. *Frontiers in neuroinformatics* 8: 5.

Appendix A

Chemicals and suppliers

Tracer and antibodies	Manufacturer
10 KD Biotinylated dextran amine (BDA)	Vector laboratories
3,3'-Diaminobenzidin tetrahydrochloride (DAB)	Sigma-Aldrich
Donkey anti-goat	Invitrogen
Fast Blue (FB)	EMS-grivory
Fluorogold (FG)	Fluorochrome
Goat anti-PHA-L	Invitrogen
Goat Peroxidase Anti-Peroxidase (PAP)	Sigma-Aldrich
Phaseolus vulgaris-leucoagglutinin (PHA-L)	Vector laboratories
Streptavidin AX546, AX488	Invitrogen
Vector ABC-kit	Vector laboratories

Chemicals	Manufacturer
Acetic acid	VWR
Cresyl Violet	Sigma-Aldrich
Dimethyl sulfoxide (DMSO)	VWR
Entellan	Merck
Ethanol	Kemetyl Norge A/S
Gelatine	Oxoid
Glycerine	VWR
Hydrogen chloride (HCl)	Merck
Hydrogen dioxide (H_2O_2)	Sigma-Aldrich
Paraformaldehyde (PFA)	Merck
Phosphate buffer (PB)	Merck
Potassium chloride (KCl)	Merck
Sodium chloride (NaCl)	Merck
Sodium hydrogen carbonate ($NaHCO_3$)	Merck
Sucrose	VWR
Toluene	VWR
Tris(hydroxymethyl)aminomethane (Tris)	Merck
Triton-X-100	Merck
Xylene	VWR

Appendix B

Solutions

Ringer

0.85% NaCl (4.25g/500mL H_2O)
0.025% KCl (0.125g/500mL H_2O)
0.02% $NaHCO_3$ (0.1g/500mL H_2O)

Add the water in a container with a magnet and place it on a stirrer. Measure the salts, add them to the water and stir it until they are dissolved. Filtrate the solution and heat it to about 40°C before use. Set the pH to 6.9 using O_2. Fresh ringer is made before every perfusion.

Phosphate buffer (PB) 0.4M pH 7.4

A: $NaH_2PO_4H_2O$ 27.6g/500mL H_2O
B: $Na_2HPO_4H_2O$ 35.6g/500mL H_2O

Make solutions A and B (start with B as it needs longer time). Add solution A to solution B until the pH is 7.4 (= 0.4M). Store in a dark place at room temperature for up to one month.

Phosphate buffer (PB) 0.125M pH 7.4

Dilute a 0.4M PB. The solution can be stored in the fridge for up to 1 week.

100mL: 31.25mL 0.4M PB + 68.75mLH_2O
500mL: 15 mL 0.4M PB + 344mL H_2O

10% paraformaldehyde (PFA)

200mL H_2O
20g PFA
A few drops sodium hydroxide (NaOH)

Heat the water to 60°C in the microwave oven. Measure PFA and add it to the water. Add a few drops of NaOH and leave the solution on a hot stirrer until the solution is clear. Everything is carefully carried out in a ventilated hood.

Fixative 4% paraformaldehyde (PFA) 500mL

200mL 10% PFA (see above)
156mL 0.4 M PB
144mL H_2O

Add water and PB to the 10% PFA solution. Set the pH to 7.4 using HCl and filtrate the solution. Everything is carefully carried out in a ventilated hood. New fixative is made for every perfusion.

TBS buffer pH 8.0

Tris	3.03g/500mL H_2O
NaCl	4.48g/500mL H_2O

Measure the water and add Tris and NaCl. Use HCl to adjust the pH to 8.0. The solution can be stored in the fridge for up to one week.

0.5% TBS-Tx buffer pH 8.0

Tris	3.03g/500mL H_2O
NaCl	4.48g/500mL H_2O
Triton-X-100	2.5mL/500mL H_2O

Measure the water and add Tris, NaCl and Triton-X-100. Use HCl to adjust the pH to 8.0. The solution can be stored in the fridge for up to one week.

Tris-HCl pH 7.6

Tris	3.03g/500 H_2O

Measure the water and add Tris. Use HCl to adjust the pH to 7.6. The solution can be stored in the fridge for up to one week.

Gelatine

Heat Tris-HCl solution to 60°C in the microwave oven. Add 0.2g gelatine per 100mL Tris-HCl and stir the solution on stirrer until the gelatine has dissolved.

The solution can be stored in the fridge for up to one week.

Sucrose solution

Dissolve 30g sucrose in 31.25mL 0.4M PB and 68.75mL H_2O (or in 100mL 0.125M PB).

Cryoprotective solution

31.25mL 0.4 M PB
46.75mL H_2O
20mL glycerine
2mL dimethyl sulfoxide (DMSO)

Appendix C

Full surgery procedure

C.1 Surgery equipment

- Surgery table
- Stereotaxic frame with tower
- Induction chamber
- Heating pad
- Vaporiser unit for isoflurane
- Mask for isoflurane
- Electric razor
- Two tweezers
- Ear bars
- Small surgery scissor
- Clamper
- Reference scale (millimetre sheet)
- Stereomicroscope
- Tubing connecting the induction chamber or the mask with the vaporiser unit
- Drill (0.9mm burr, Foredom Micro Motor FM3545 control and MH-145 Micro Motor Handpiece)
- Iontophoresis pump (Digital Midgard Precision Current Source, Stoelting Co, USA)

C.2 Disposables

- Scalpel (blade 10)
- Isoflurane
- Sterile saline
- Q-tips
- Suture kit
- Syringes
- 27 and 25 gauge needles
- Cotton swabs (Sugi absorbent swabs, Kettenbach GmbH & Co)
- Ethanol
- Iodine
- Marcain
- Metacam
- Temgesic
- Glass capillaries
- H_2O_2

C.3 Tracers

- 10 KD Biotinylated dextran amine (BDA)
- *Phaseolus vulgaris*-leucoagglutinin (PHA-L)
- Fast Blue (FB, Blue fluorescent, 2%, diluted in 0.125M PB)
- Fluorogold (FG, Blue fluorescent, 2.5 %, diluted in H_20)

C.4 Detailed surgery procedure

Preparation

1. Coordinates for injections are calculated using the Rat Brain Atlas (Paxinos & Watson, 2007) as a reference and are further adjusted according to previous surgeries
2. Glass capillaries (Borosilicate Glass Capillaries) are pulled with single stage glass microelectrode puller (Narishige PP-830) to tips with an inner diameter of 25-30µm for anterograde tracers, 40-50µm for FG, 80-100µm for FB.
3. Disinfect the surgery table, stereotaxic tower and the microscope with ethanol (70%)
4. Place a sterile sheet of paper on the table, fill up a container with ethanol (70%) and place all the equipment in it for disinfection
5. Put cotton swabs, Q-tips, suture and the rest of the equipment on the sheet ready for use
6. Prepare small containers of H_2O_2 and saline and sterile water
7. Prepare a syringe (5mL) with sterile saline (injected subcutaneously two times during the surgery, with 2 hours in between, 2.5mL on each side of the back to prevent dehydration)
8. Prepare syringes with 25 gauge needles for Metacam (Meloxicam, 1mg/kg, Boehringer Ingelheim Vetmedica GmbH, Germany), Marcain (Bupivacaine, 1mg/kg, AstraZeneca, UK) and Temgesic (Buprenorphine, 0.05-0.1mg/kg, RB Pharmaceuticals Ltd, USA).
9. Turn on the heating pad and place a piece of paper on it
10. Fill up the vaporiser with isoflurane and make sure all the tubes are in the right place (turned to chamber when filling it up)

Surgery

1. Collect the animal from the animal room and weigh it
2. Turn on the oxygen flow (1L/min) and isoflurane (5%) and wait until the chamber is filled up (ca. 10 min)
3. Place the animal in the induction chamber and wait until it is breathing slowly and deeply
4. Place the animal in the stereotaxic frame, adjust the isoflurane flow to 3% and administer via the stereotaxic anaesthesia mask
5. Make sure the animal is fully anesthetised by checking the toe-pinch reflexes
6. Apply Simplex (Tubilux Pharma S.p.A., Italy) to prevent the animal's eyes from drying out
7. Inject Marcain subcutaneously on the head and Metacam and Temgesic subcutaneously on each side of the back
8. Fixate the skull by use of ear bars, adjust the frame, and make sure that the ear bars are on the same height
9. Reduce the isoflurane level gradually during the surgery to 1.5%, depending on the animal's breathing rate
10. Shave the head and clean it with sterile saline, ethanol (70%) and iodine
11. Check for reflexes
12. Make an incision along the midline with a scalpel and remove the periosteum on each side of the skull
13. Use two bent needles to keep the skin to each side to reveal the skull
14. Use a painted capillary to measure the height level of bregma and lambda and adjust the skull so that they align in the horizontal plane

15. Drill across to the midline, in the middle of bregma and lambda on an anterior-posterior level to expose the sagittal sinus
16. Calculate the anterior-posterior coordinate based on the position of bregma
17. Calculate the lateral coordinate
18. Drill a hole and remove the dura carefully by use of a bent, 27 gauge needle
19. Fill up a new capillary with tracer
20. Secure the capillary in the tower and prepare for injections
21. Re-calculate the coordinates
22. Lower the capillary to the surface of the brain and measure the height
23. Lower the capillary to the desired level
24. For BDA; lower the capillary and start injecting, slowly raise the capillary after the injection is completed
25. For retrograde tracers; wait for 5 min for the tissue to adapt, inject half of the volume, wait 3 min, inject the rest of the volume, wait 10 min, raise the capillary 2µm and wait for 5 min, slowly raise the capillary
26. When the capillary is out, clean the skull with sterile saline
27. Suture the wound with small stitches making sure that there are no openings between the stiches
28. Rinse with sterile saline and apply iodine on the wound to avoid infections
29. Turn off the isoflurane and remove the ear bars

Post-surgery

1. Move the animal to a heating-chamber and wait for the animal to recover from anaesthesia (15-50 min)
2. Make sure the animal is able to move around and eat
3. Return the animal to its cage and place it in the animal room
4. Check the animal after an hour to make sure it is doing well
5. Oral Metacam (1 mg/kg, Boehringer Ingelheim Vetmedica GmbH, Germany) is given the first day post-surgery to reduce potential pain
6. The overall health and weight of the animal was monitored and registered the following days

Appendix D

Histology protocols

D.1 Cresyl Violet

1) To hydrate the mounted sections, dip the sections 10 times in each container with ethanol: 50-, 70-, 80-, 90-, 100-, 100- and 100% ethanol
2) Leave the sections for two min in xylene for clearing
3) Move the sections back for rehydration. 10 dips in each container with 100-, 100-, 100-, 90-, 80-, 70- and 50% ethanol
4) Wash the sections quickly under running water
5) Let sections sit in Cresyl Violet on a shaker in dark (time depends on the age of the solution, however about three min is normally good)
6) Wash the sections under running water until all excess colour is washed away
7) Move sections into a container with ethanol + acetic acid solution for a few seconds (three dips)
8) Leave the sections under running water until all excess colour is washed away
9) Repeat point 7) and 8) until the sections have a light, purple colour. Make sure the contrast between white and grey matter is good
10) Dehydrate the sections as in step 1): dip them 10 times in each container with 50-, 70-, 80-, 90-, 100-, 100- and 100% ethanol
11) Move the sections to container of xylene for clearing; leave them for minimum two min in the first container and five (up to 60 min) for the second container
12) Use entellan/xylene solution to coverslip the sections

D.2 DAB stain for BDA

1) Rinse 3x10 min in 0.125M PB
2) Rinse 3x10 min in TBS-Tx
3) Incubate with ABC on a shaker for 90 min at room temperature or overnight at 4◦C
4) Rinse 3x10 min in TBS-Tx
5) Rinse 2x5 min in Tris-HCl
6) Incubate with DAB
7) Rinse 2x5 min in Tris-HCl
8) Mount the sections on microscope slides

ABC

ABC must be mixed well and made 30 min before use.

5mL TBS-Tx
1 drop A
1 drop B

DAB

Stir with magnet at 50°C for 2 hours (in the dark). Before use, add 12µl H_2O_2 and filtrate.

1 tablet DAB (10mg)
15mL Tris-HCl

D.3 DAB stain for PHA-L

1) Rinse 3x10 min in 125 mM PB
2) Rinse 2x10 min in H_2O_2/methanol
3) Rinse 3x10 min in 125 mM PB
4) Rinse 3x10 min in TBS-Tx
5) Incubate with superblock on a shaker for one hour at room temperature
6) Incubate with goat anti-PHA-L on a shaker 24 hours (overnight is usually sufficient) at room temperature or 48 hours at 4◦C
7) Rinse 3x10 min in TBS-Tx
8) Incubate with unconjugated donkey anti-goat on a shaker for two hours in room temperature or overnight at 4◦C
9) Rinse 3x10 min in TBS-Tx
10) Incubate with goat PAP on a shaker for 90 min in room temperature or overnight at 4◦C
11) Rinse 3x10 min in TBS-Tx
12) Rinse 2x5 min in Tris-HCl
13) Incubate with DAB
14) Rinse 2x5 min in Tris-HCl
15) Mount the sections on microscope slides

Superblock	***10mL H_2O_2/methanol***
75µl Triton X-100	1mL 30% H_2O_2
15mL Superblock	1mL 100% methanol
	8mL 125mM PB
Goat anti PHA-L (1:1000)	***Donkey anti-goat (1:100)***
12µl goat anti PHA-L	120µl donkey anti-goat
12mL TBS-Tx	11.88mL TBS-Tx
PAP (1:200)	***DAB***
60µl goat PAP	1 tablet (10mg) DAB
11.94mL TBS-Tx	15mL Tris-HCl

Stir for two hours in darkness. Add 12µl 30% H_2O_2 before use and filtrate.

D.4 Double stain BDA and PHA-L (fluorescent)

1) Rinse sections 3x10 min in 125mM PB on a shaker
2) Rinse sections 3x10 min in TBS-Tx on a shaker
3) Incubate sections in goat anti-PHA-L (1:1000) on a shaker for 24 hours at room temperature or 48 hours in the fridge
4) Rinse sections 3x10 min in TBS-Tx on a shaker
5) Incubate with streptavidin (1:200) and donkey anti-goat (1:400) on a shaker for 90-120 min at room temperature or overnight in the fridge
6) Rinse sections 1x10 min in Tris-HCl on a shaker
7) Mount the sections on slides in 0.2% gelatine/Tris-HCl
8) Coverslip the section

Anti-PHA-L

4µl goat anti-PHA-L (undiluted 2µl/vial in freezer)
4mL TBS-Tx

Streptavidin and donkey anti-goat

20µl donkey anti-goat (diluted 1:2 in glycerol, 20µl/vial in freezer)
40µl streptavidin (diluted 1:2 in glycerol, 20µl/vial in freezer)
3940µl TBS-Tx
Note: Streptavidin and donkey anti-goat need to have different fluorescent conjugates.

D.5 Fluorescent stain for BDA

1) Rinse sections 3x10 min in 0.125M PB
2) Rinse 3x10 min in TBS-Tx
3) Incubate with streptavidin (conjugated with Alexa 488, 546 or 635) for one to two hours in room temperature. Concentration: 1:200 in TBS-Tx
4) Rinse 2x5 min in Tris-HCl
5) Mount sections in gelatine and dry overnight
6) Coverslip sections with toluene and entellan

D.6 Fluorescent stain for PHA-L

1) Rinse sections 3x10 min in 0.125M PB
2) Rinse 3x10 min in TBS-Tx
3) Incubate with goat anti-PHA-L for 24 hours in room temperature or 48 hours in the fridge. Concentration: 1:1000 in TBS-Tx
4) Rinse 3x10 min in TBS-Tx
5) Incubate with Alexa 488, 546 or 645 conjugated anti-goat for one to two hours in room temperature
6) Rinse 2x5 min in Tris-HCl
7) Mount sections in gelatine and dry overnight
8) Coverslip sections with toluene and entellan

Appendix E

Supplementary figures and table of anterograde labelling

The main injection sites were delineated and presented for all cases with injections into PPC. For the injections into PtP, the main injection site was delineated for the three first cases illustrated. For the three last cases, all performed in this study, the sections directly adjacent to the core of the injection site were also delineated to illustrate the extent of the injection site.

E.1 Injections into mPPC

Case 13234P

Case 13187B

Case 14122B

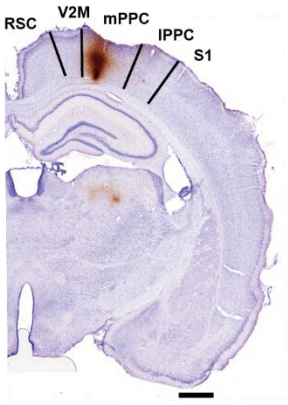

Case 13765P

Case 13236P

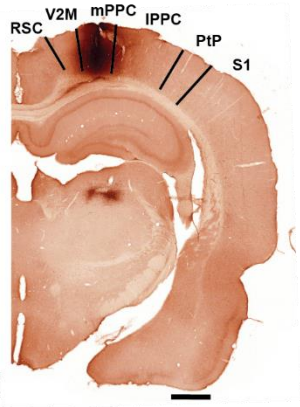

Case 13594B

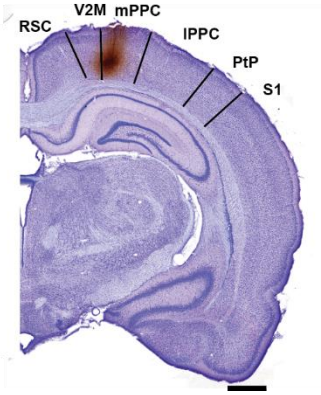

E.2 Injections into lPPC

Case 14121P

Case 13089P

Case 13234B

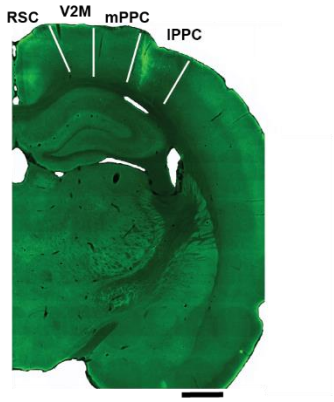

Case 14122P

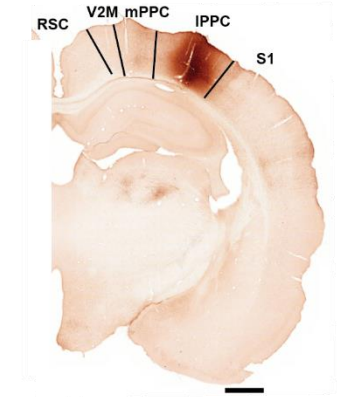

Case 13187P

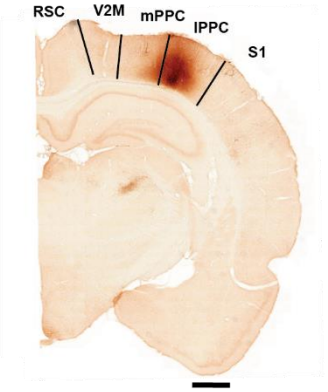

Case 13702P

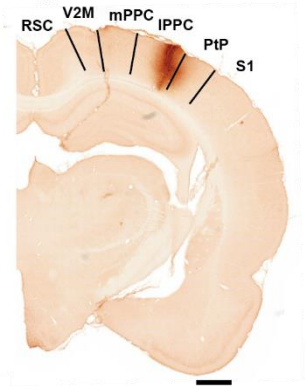

Case 13236B

Case 12948B

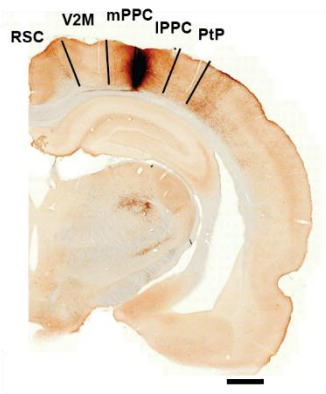

E.3 Injections into PtP

Case 12877B

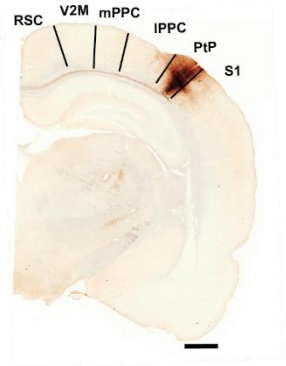

Case 12906P

Case 20420B

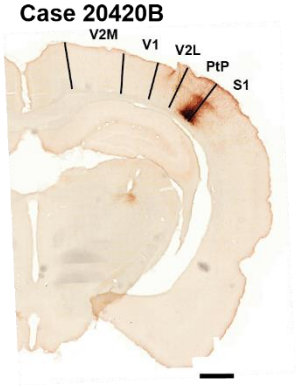

Case 20352B section 1

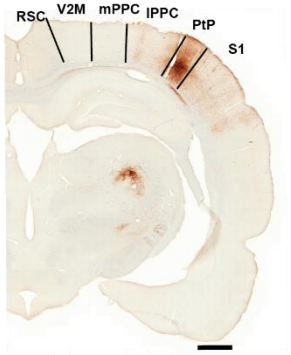

Case 20352B section 2

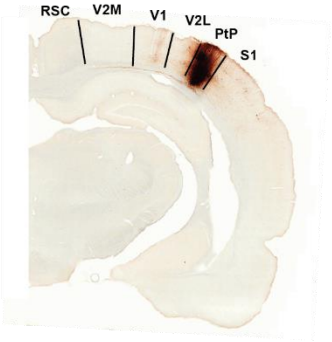

Case 20352B section 3

Case 20219B section 1

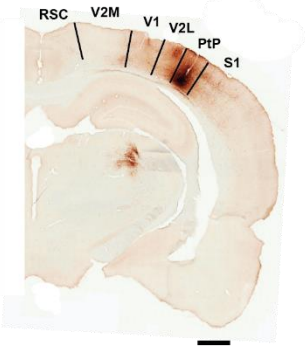

Case 20219B section 2

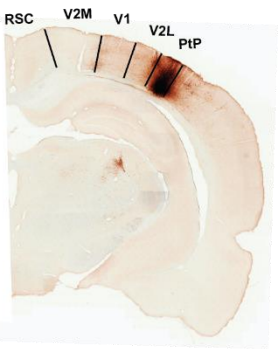

Case 20219B section 3

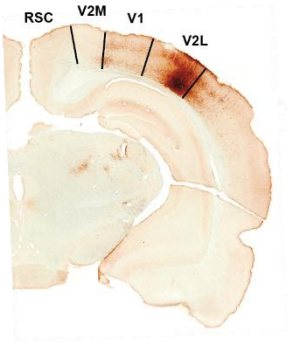

Case 20419B section 1

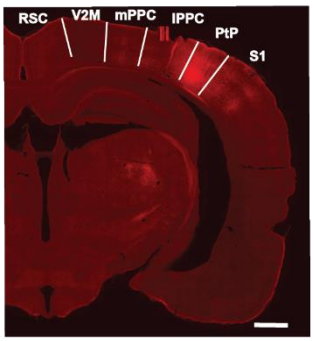

Case 20419B section 2

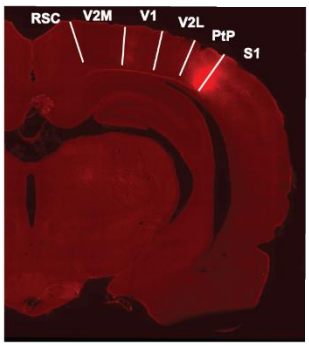

Case 20419B section 3

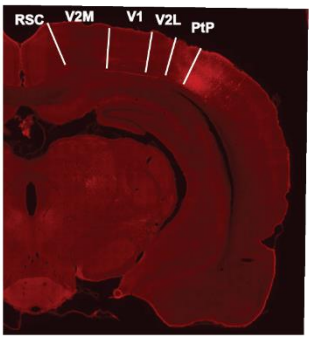

E.4 Anterograde labelling in OFC

Semiquantitative representation of the anterograde labelling in OFC in total and in the subregions MO, VO and VLO separately resulting from injections into mPPC, lPPC, PtP, V2M and V2L. The density of anterograde labelling in OFC in total is indicated by four levels: ++++, strong labelling; +++ moderate labelling; ++ weak labelling; + very weak labelling. Density within MO, VO and VLO are indicated by three levels; X strong labelling; x weak labelling; - no labelling or only a couple of fibres. Note that projections from PPC to OFC are generally not strong so that 'strong labelling' refers to the strongest labelling seen in the present study.

Animal	Tracer	Layers	Thalamus	Density in OFC	MO	VO	VLO
mPPC							
13187B	BDA	V-VI	LPmr, Po	+	-	x	x
13234P	PHA-L	I-VI	LPmr, Po, (VP)	++++	x	X	X
13236P	PHA-L	I-VI	LPmr, Po, (VP)	++++	X	X	X
13594B	BDA	I-VI	LPmr, Po, (LDl)	++	x	x	X
13765P	PHA-L	V-VI	LPmr, Po	++	-	X	X
14122B	BDA	I-VI	LPmr, Po	+	-	-	x
lPPC							
12948B	BDA	I-VI	Po, (LPmr), (LDm)	+++	-	x	X
13089P	PHA-L	I-VI	Po, LPmr, (VP)	+++	-	-	X
13187P	PHA-L	II-VI	Po, LPmr, (VP)	+++	-	x	X
13234B	BDA	I-VI	Po, LPmr	++	-	-	X
13236B	BDA	I-VI	Po, LPmr	+++	-	-	X
13702P	PHA-L	I-VI	Po, (LPmr)	++	-	-	X
14121P	PHA-L	I-VI	Po, VP	+	-	-	x
14122P	PHA-L	I-VI	Po, LPmr, LDm	++++	-	-	X
PtP							
12877B	BDA	II-VI	Po, (VPm)	++	-	-	x
12906P	PHA-L	I-VI	Po, (LPl)	+++	-	-	X
20219B	BDA	II-VI	Po, LPl	++++	-	-	X
20352B	BDA	I-VI	Po, VP	++++	-	-	X
20419B	BDA	II-VI	Po, VP	+++	-	-	X
20420B	BDA	V-VI	Po, LPl	+	-	-	x
V2							
14016P	PHA-L	I-VI	LPl, LPm, LD	++++	x	X	X
20546B	BDA	I-VI	LPl, LPm, LD	+++	-	x	X

E.5 Example of how the representative anterograde labelling figures were made

The figure below illustrates how the representative anterograde labelling figures were made in Adobe Illustrator CS6. The example is from case 13234P.

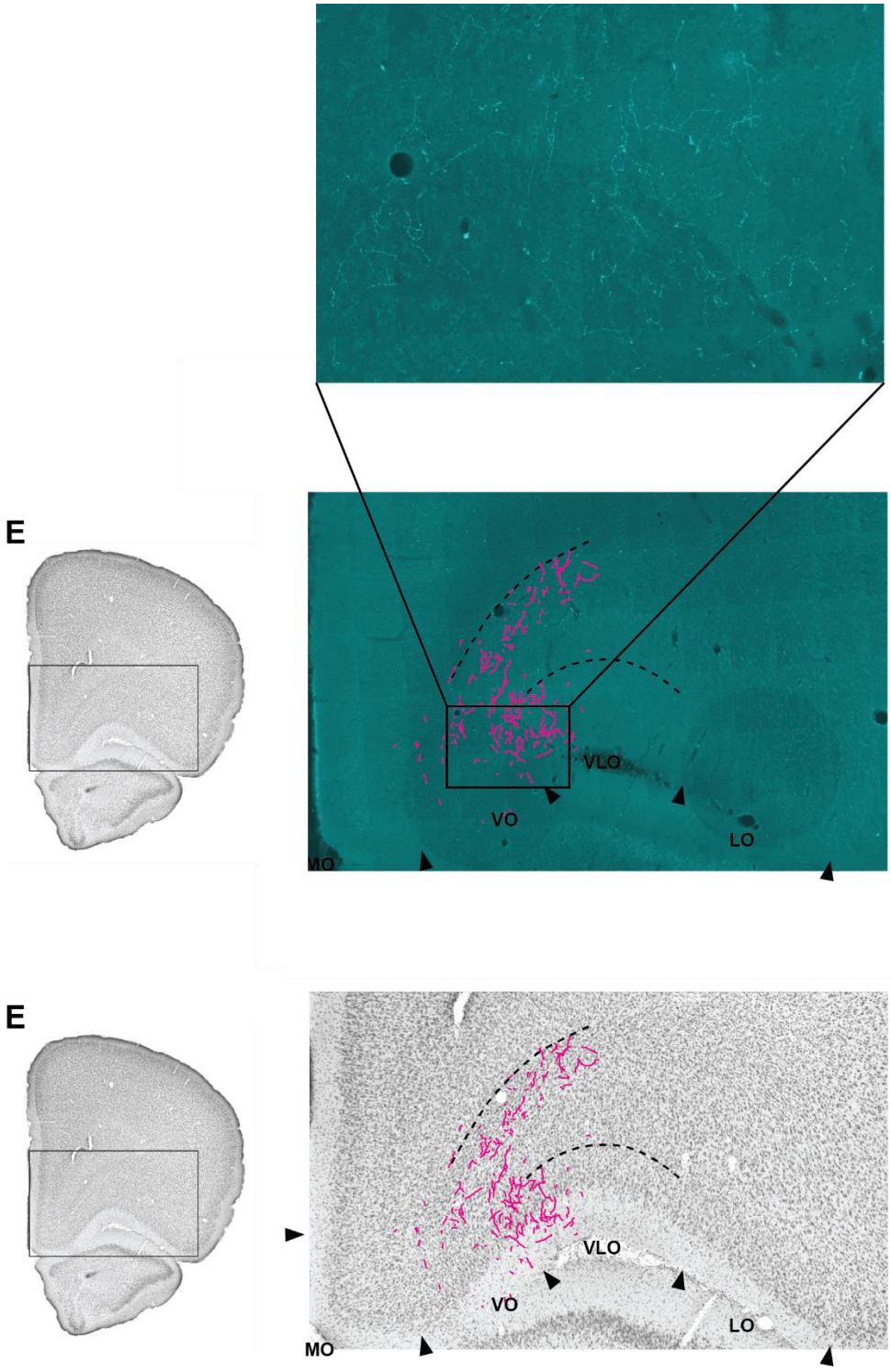

Appendix F

Supporting retrograde tracer figures

F.1 Nissl stain for the representative retrograde tracer case

Case 20461FB. Nissl stained section for the main injection site. The section is mirrored along the vertical axis.

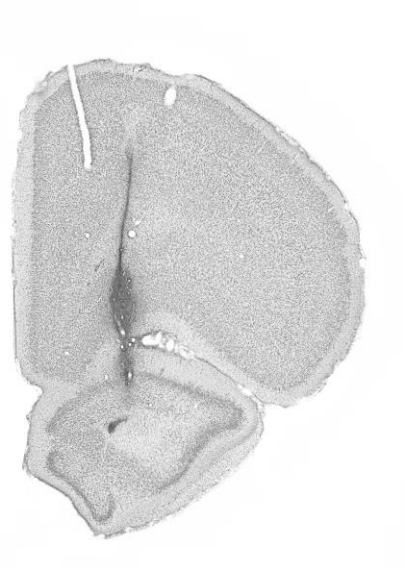

F.2 Retrograde labelling in PPC

Sections from four brains, taken at a comparable anterior-posterior level illustrating the labelling resulting from four different retrograde tracer injections into VO and VLO (Figure 10, A-D), are shown on the next page. Retrogradely labelled cells were seen in layers V and VI in mPPC, lPPC and PtP for all cases. Arrows indicate the position of cells. A) Case 20705FG, B) case 20545FB, C) case 20560FB, D) case 20705FB. Scale bar 1000 µm.

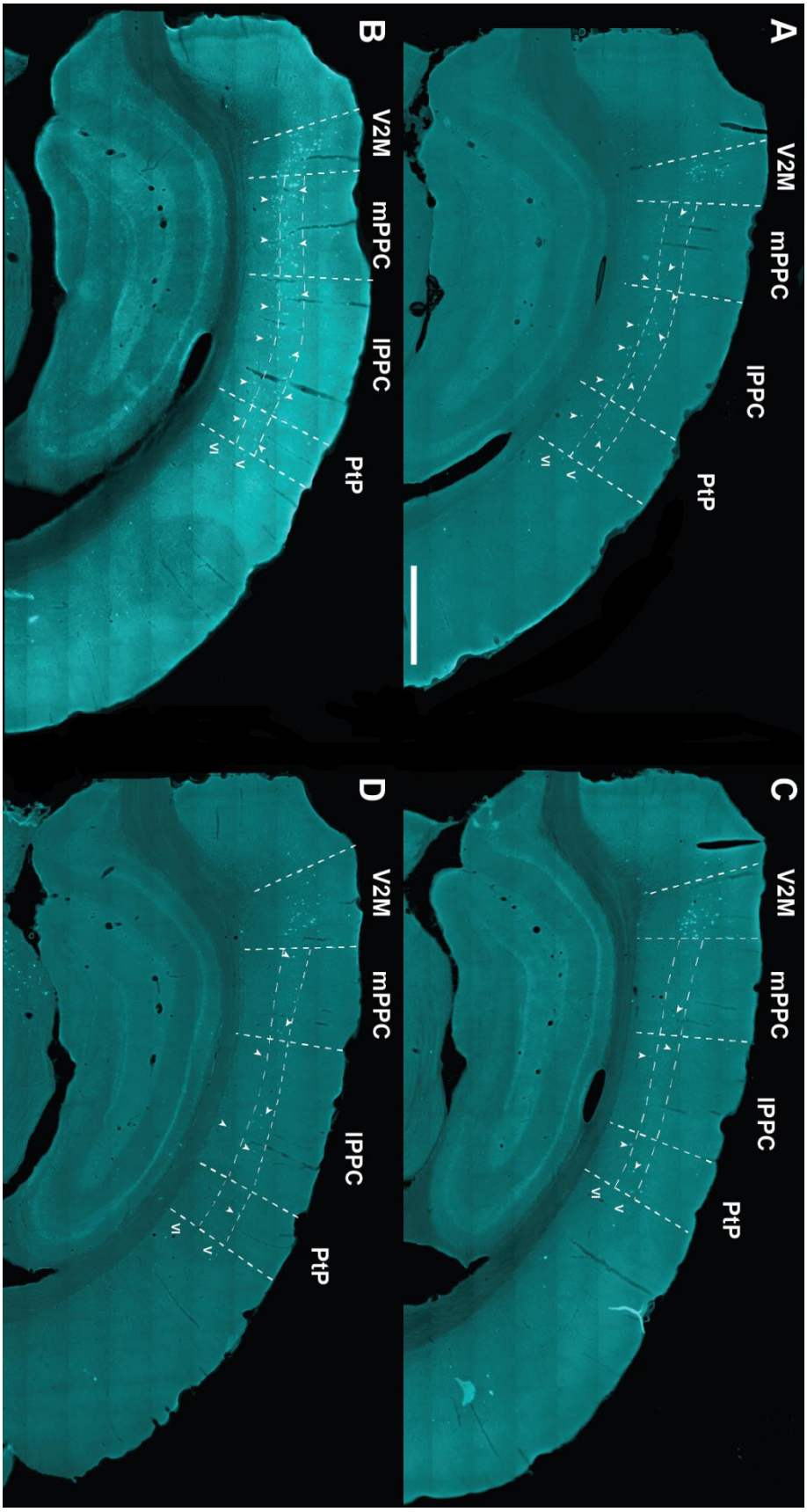
A
V2M
mPPC
lPPC
PtP
VI
V
B
V2M
mPPC
lPPC
PtP
VI
V
C
V2M
mPPC
lPPC
PtP
VI
V
D
V2M
mPPC
lPPC
PtP
VI
V

Appendix G

Comparison of delineations of OFC

The figure below shows one anterior (left panel) and one posterior (right panel) level of OFC with delineations from the present study (A), Van De Werd and Uylings (2008) (B), Kondo and Witter (2014) (C) and Linley et al. (2013) (D) as described in the result section. The figure shows that differences in delineation of OFC are mainly in the posterior sections. Other adjacent areas are not discussed in this thesis.

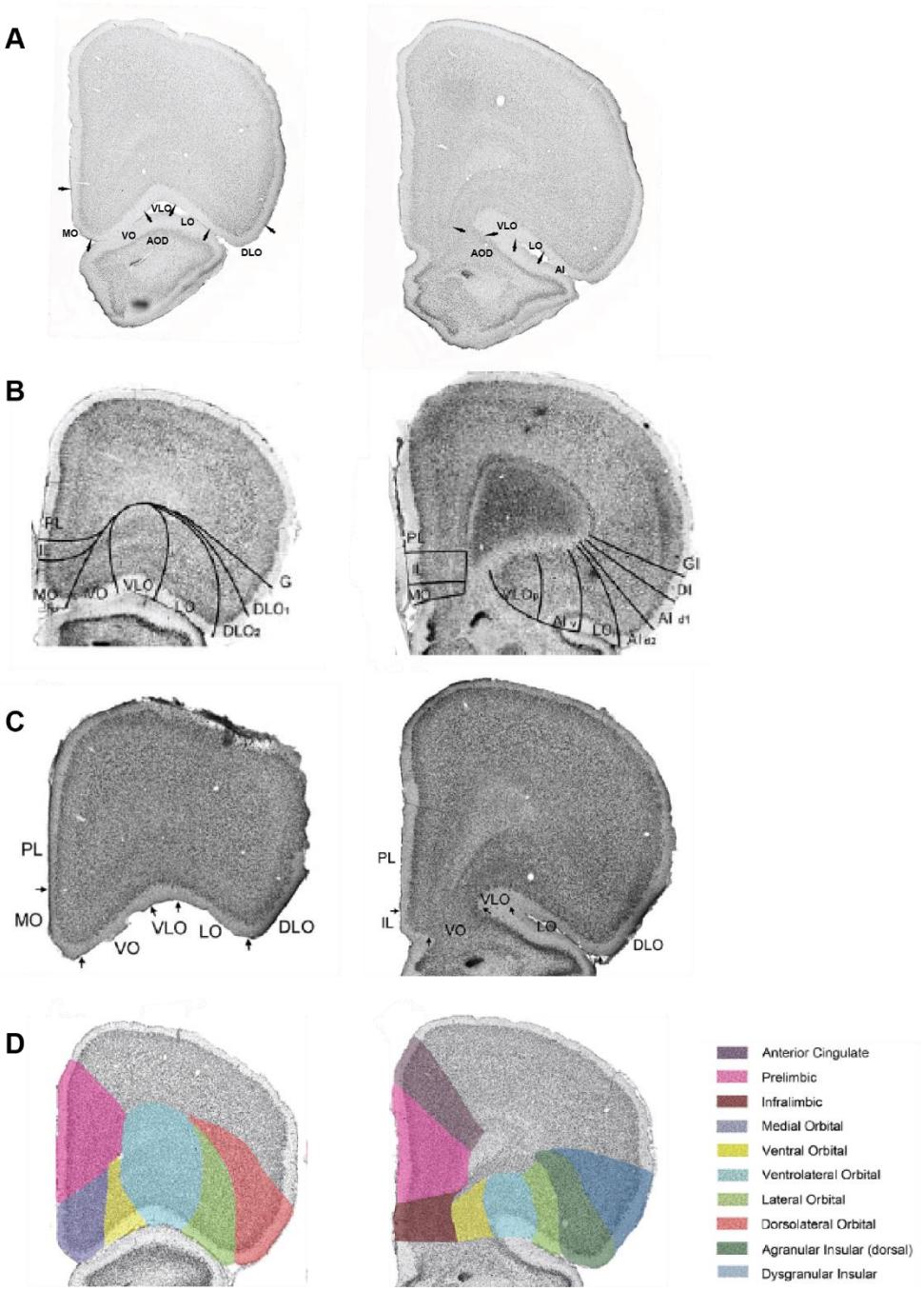

The figure below shows the cytoarchitecture of the five subregions of OFC where the black arrows point at the approximate borders used in this thesis.